

RELEASED
2007/12/20

PC-000550
Revision 0

ADVANCED GAS REACTOR FUEL DEVELOPMENT AND QUALIFICATION PROGRAM

TEST PLAN FOR CHARACTERIZING TRITIUM TRANSPORT IN A VHTR

Prepared under
Idaho Operations Office
Contract No. DE-AC07-03ID14488
for the U.S. Department of Energy

General Atomics Project 30192



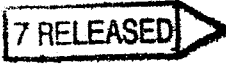
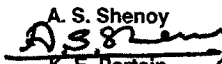
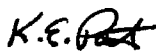


GA 2175 (1199E)

PROJECT CONTROL ISSUE SUMMARY

DOC. CODE	PROJECT	DOCUMENT NO.	REV.
TPN	30192	PC-000550	0

TITLE: Test Plan for Characterizing Tritium Transport in a VHTR

CM APPROVAL/ DATE	REV.	PREPARED BY	APPROVALS		REVISION DESCRIPTION/ W.O. NO.
			RESOURCE/ SUPPORT	PROJECT	
 DEC 20 2007	0	D. L. Hanson 	A. S. Shenoy  K. E. Partain 	J. J. Saurwein 	Initial Issue A30192 0210

* SEE LIST OF EFFECTIVE PAGES

GA PROPRIETARY INFORMATION

THIS DOCUMENT IS THE PROPERTY OF GENERAL ATOMICS. ANY TRANSMITTAL OF THIS DOCUMENT OUTSIDE GA WILL BE IN CONFIDENCE. EXCEPT WITH THE WRITTEN CONSENT OF GA, (1) THIS DOCUMENT MAY NOT BE COPIED IN WHOLE OR IN PART AND WILL BE RETURNED UPON REQUEST OR WHEN NO LONGER NEEDED BY RECIPIENT AND (2) INFORMATION CONTAINED HEREIN MAY NOT BE COMMUNICATED TO OTHERS AND MAY BE USED BY RECIPIENT ONLY FOR THE PURPOSE FOR WHICH IT WAS TRANSMITTED.

NO GA PROPRIETARY INFORMATION

LIST OF EFFECTIVE PAGES

<u>Page Number</u>	<u>Page Count</u>	<u>Revision</u>
Cover page	1	0
ii through ix	8	0
1 through	81	0
Back page	1	0
Total Pages	91	

TABLE OF CONTENTS

ACRONYMS AND ABBREVIATIONS.....viii

1 SUMMARY..... 1

2 INTRODUCTION AND BACKGROUND..... 5

2.1 Purpose.....5

2.2 Tritium Fundamentals5

2.3 VHTR Conceptual Designs for Hydrogen Production6

2.4 Significance of Tritium in a VHTR.....7

2.5 Tritium Transport Design Data Needs8

2.6 Proposed Experimental Program..... 11

3 TRITIUM BEHAVIOR IN AN HTGR..... 12

3.1 Sources of Tritium in an HTGR..... 12

3.1.1 Ternary Fission 12

3.1.2 Neutron Activation of Lithium 13

3.1.3 Neutron Activation of He-3 13

3.1.4 Neutron Capture Reactions in Control Materials..... 13

3.2 H-3 Transport in an HTGR..... 14

3.2.1 Tritium Release into Primary Coolant 14

3.2.2 Tritium Removal from Primary Coolant..... 21

4 DESIGN METHODS FOR PREDICTING H-3 TRANSPORT..... 42

4.1 Computer Codes..... 42

4.2 H-3 Transport Models 44

4.2.1 H-3 from Fuel Particles 44

4.2.2 H-3 Release from B₄C Pellets..... 46

4.2.3 H-3 Sorption on Graphite 47

4.2.4 H-3 Permeation through Metals 50

4.3 Material Property Data 52

5 TEST REQUIREMENTS 53

5.1 H-3 Release from TRISO Particles 53

5.1.1 Test Articles 53

5.1.2 Measurement Technique 53

5.1.3 Required Data 54

5.1.4 Instrumentation 54

5.1.5 Pre-test Characterization 54

5.1.6 Test Conditions 54

5.1.7 Posttest Examination 55

5.2 H-3 Sorption on Core Graphite 55

5.2.1 Test Articles 55

5.2.2 Measurement Technique 55

5.2.3 Sorptivities to be Determined 55

5.2.4 Instrumentation 56

5.2.5 Pre-test Characterization 56

5.2.6 Test Conditions 56

5.2.7 Posttest Examination 56

5.3 H-3 Release from B₄C Pellets..... 57

5.3.1 Test Articles 57

5.3.2 Measurement Technique 57

5.3.3 Required Test Data 57

5.3.4	Instrumentation	57
5.3.5	Pre-test Characterization	58
5.3.6	Test Conditions	58
5.3.7	Posttest Examination	58
5.4	H-3 Permeation through Heat Exchanger Metals	58
5.4.1	Measurement Technique	58
5.4.2	Permeabilities to be Determined	58
5.4.3	Instrumentation	59
5.4.4	Pre-test Characterization	59
5.4.5	Test Conditions	59
5.4.6	Posttest Examination	60
6	QUALITY ASSURANCE REQUIREMENTS	61
7	DESCRIPTION OF PLANNED TESTS	62
7.1	H-3 Release from TRISO Particles	64
7.1.1	Subtask 3.5.14.1.1. Prepare Test Specification	64
7.1.2	Subtask 3.5.14.1.2. Select Measurement Technique	64
7.1.3	Subtask 3.5.14.1.3. Construct/Commission Test Facility	65
7.1.4	Subtask 3.5.14.1.4. Perform H-3 Release Measurements	65
7.2	H-3 Sorptivities of Core Graphites	65
7.2.1	Subtask 3.5.14.2.1. Prepare Test Specification	66
7.2.2	Subtask 3.5.14.2.2. Select Measurement Technique	66
7.2.3	Subtask 3.5.14.2.3. Construct/Commission Test Facility	67
7.2.4	Subtask 3.5.14.2.4. Measure H-3 Sorptivity of Replaceable Core Graphite	67
7.2.5	Subtask 3.5.14.2.5. Measure H-3 sorptivity of Permanent Core Graphite	67
7.2.6	Subtask 3.5.14.2.6. Measure H-3 Sorptivity of Compact Matrix	67
7.3	H-3 Release from B ₄ C Pellets	67
7.3.1	Subtask 3.5.14.3.1. Prepare Test Specification	68
7.3.2	Subtask 3.5.14.3.2. Fabricate Test Articles	69
7.3.3	Subtask 3.5.14.3.3. Select Measurement Technique	69
7.3.4	Subtask 3.5.14.3.4. Construct/commission Test Facility	69
7.3.5	Subtask 3.5.14.3.5. Perform H-3 Release Measurements	69
7.4	H-3 Permeabilities of HX Metals	69
7.4.1	Subtask 3.5.14.4.1. Prepare Test Specification	70
7.4.2	Subtask 3.5.14.4.2. Select Measurement Technique(s)	70
7.4.3	Subtask 3.5.14.4.3. Construct/Commission Test Facility	70
7.4.4	Subtask 3.5.14.4.4. Measure H-3 Permeability of IN 617	71
7.4.5	Subtask 3.5.14.4.5. Measure H-3 Permeability of Hastelloy XR	71
7.4.6	Subtask 3.5.14.4.6. Measure H-3 Permeability of Alloy 800H	71
7.4.7	Subtask 3.5.14.4.7. Measure H-3 Permeability of T22	71
8	COST AND SCHEDULE	72
8.1	Schedule Estimate	72
8.2	Cost Estimate	73
9	DELIVERABLES	76
10	REFERENCES	79

LIST OF FIGURES

Figure 1-1. Summary Schedule and Cost Estimate for H-3 Program	4
Figure 2-1 H-3 Permeabilities of Various Materials	6
Figure 3-1. H-3 Distribution in an HTGR (Steam-Cycle Plant).....	14
Figure 3-2. H-3 Release from Intact TRISO Fuel Particles	16
Figure 3-3. Tritium Release Isotherms from Annealed/Irradiated Graphite Probes	18
Figure 3-4. H-3 Release from Graphite during Postirradiation Heating	19
Figure 3-5. Tritium Retained in Boron Carbide	20
Figure 3-6. Temperature Dependence of H-3 Retention in B ₄ C Pellets.....	20
Figure 3-7. Hydrogen Sorption on TSP Nuclear Graphite	22
Figure 3-8. Hydrogen Permeation through Incoloy 800	26
Figure 3-9. Effect of Oxide Films on Permeation Pressure Dependence	29
Figure 3-10. Effect of Steam Oxidation on H-3 Permeation through I-800	30
Figure 3-11. Apparatus for D ₂ Permeation Measurements	32
Figure 3-12. Effect of Progressive Oxidation on D ₂ Permeation through I-800.....	34
Figure 3-13. Apparatus for PB H-3 Permeation Measurements	35
Figure 3-14. H-3 Permeabilities of PB Steam Generator Tubes	36
Figure 3-15. JAERI Apparatus for H/D Permeation Measurements.....	39
Figure 3-16. H/D Permeation Measurements for Hastelloy XR	40
Figure 4-1. TRITGO Code Data Management.....	43
Figure 4-2. H-3 Release from Intact TRISO Particles	45
Figure 4-3. H-3 Release from B ₄ C Granules.....	47
Figure 4-4. Myers Isotherm for H-3 Sorption on Graphite.....	49
Figure 4-5. H-3 Permeation in Alloy 800H and T22	51
Figure 8-1. Schedule for H-3 Characterization Program.....	74

LIST OF TABLES

Table 2-1. Workscope for Tritium Transport DDNs..... 10

Table 3-1. Sources of H-3 Production in HTGRs..... 12

Table 3-2. Permeabilities for Hydrogen Permeation of Metals 27

Table 3-3. Hydrogen Permeabilities for High-Temperature Alloys..... 41

Table 4-1. H-3 Permeation Constants for TRISO Particles 44

Table 4-2. H-3 Release Constants for B₄C Pellets 46

Table 4-3. Coefficients for H-3 Permeation Correlations 50

Table 7-1. Experimental Tasks to Satisfy H-3 Transport DDNs..... 63

Table 8-1. Cost Estimate for H-3 Characterization Program 75

Table 9-1. Major Deliverables 77

ACRONYMS AND ABBREVIATIONS

AGR	Advanced Gas Reactor
AVR	Arbeitsgemeinschaft Versuchsreaktor [German pebble-bed HTR]
BET	Brunauer, Emmett and Teller [a standard analytical technique for measuring the internal surface area of a porous solid]
BISO	Coated-fuel particle design with two materials in coating system [low-density PyC and high-density PyC]
CCCTF	Core Conduction Cooldown Test Facility
CFR	Code of Federal Regulations
DOE	[US] Department of Energy
DV&S	design verification and support
EFPD	effective full power days
EOL	end-of-life
EC	economizer [section of steam generator]; elsewhere: European Commission
EV	evaporator [section of steam generator]
FP	fission product
FSV	Fort St. Vrain [HTGR]
FZJ	Forschungszentrum – Juelich [formerly Kernforschungsanlage - Juelich, KFA]
GA	General Atomics
GT-MHR	[commercial] Gas Turbine-Modular Helium Reactor
HEU	high-enriched uranium [~93% U-235]
HPS	helium purification system
HTGR	High Temperature Gas-cooled Reactor ¹
HTR	High Temperature Reactor [pebble-bed HTGR]
HTTR	[Japanese] High Temperature Test Reactor
IHX	intermediate heat exchanger
INL	Idaho National Laboratory
JAEA	Japanese Atomic Energy Agency
JAERI	Japanese Atomic Energy Research Institute
KFA	Kernforschungsanlage - Juelich [now renamed FZJ]
LEU	low-enriched uranium [$\leq 19.9\%$ U-235]
MHR	Modular Helium Reactor
MHTGR	Modular High Temperature Gas-cooled Reactor [steam cycle]

¹ In this report, "HTGR" is used generically to represent all high temperature, helium-cooled reactors with coated-particle fuel, regardless of core configuration, fuel-element type, or power conversion cycle; in contrast, "HTR" refers specifically to HTGRs with pebble-bed cores.

MW _e	megawatt (electrical)
MW _t	megawatt (thermal)
NGNP	Next Generation Nuclear Plant
NPR	New Production Reactor
NTP	normal temperature and pressure [20 °C (293 K) and 1 atm]
ORNL	Oak Ridge National Laboratory
PB	Peach Bottom 1[HTGR]
PCDSR	Pre-Conceptual Design Studies Report
PCHE	printed circuit heat exchanger
PyC	pyrolytic carbon
QA	quality assurance
RGA	residual gas analyzer
RN	radionuclide
SH	superheater [section of steam generator]
SI	sulfur-iodine
SiC	silicon carbide
SG	steam generator
STP	standard temperature and pressure [0 °C (273 K) and 1 atm]
T	tritium [also designated as H-3, ${}^3_1\text{H}$]
TBD	to be determined
TRISO	Coated-fuel particle design with three materials in coating system [low-density PyC, high-density PyC, and SiC]
UCNI	Unclassified Controlled Nuclear Information
UCO	uranium oxycarbide [an admixture of UC ₂ and UO ₂ in various proportions]
VHTR	Very High Temperature Reactor
WBS	work breakdown structure

1 SUMMARY

A test plan is proposed herein to characterize tritium transport behavior in He-cooled, Very High Temperature Reactors (VHTRs). It is anticipated that this tritium characterization plan will be incorporated into the on-going, Advanced Gas Reactor (AGR) fuel development and qualification program. In addition to qualifying fuel for the Next Generation Nuclear Plant (NGNP) Project, the AGR program is also responsible for providing validated radionuclide source terms for NGNP design and licensing, and tritium is expected to be a key radionuclide, especially for a hydrogen-producing VHTR (referred to herein as an H₂-MHR).

The tritium transport issues addressed in this test plan are generic to all HTGRs, but the test program priorities and test articles are design specific. The NGNP is still in the preconceptual design phase at this writing; consequently, this test plan will need to be reviewed and revised as appropriate when the conceptual design of the NGNP is finalized. In particular, the inclusion of a steam generator in the primary coolant circuit of the NGNP would increase the priority of the tests to determine the effects of water on tritium transport behavior.

Tritium will be produced in a VHTR by various nuclear reactions. Given its high mobility, especially at high temperatures, some tritium will permeate through the intermediate heat exchanger (IHX) and hydrogen process heat exchangers, contaminating the product hydrogen. This tritium contamination will contribute to public and occupational radiation exposures; consequently, stringent limits on tritium contamination in the product hydrogen are anticipated to be imposed by regulatory authorities. Tritium will also contaminate the process steam in a VHTR supplying steam for chemical processing. The issue of tritium transport and product contamination will have to be addressed for the NGNP design and licensing as well as for future commercial VHTRs. Design options are available to control tritium, but they can be expensive so an optimal combination of mitigating features must be implemented in the design. Some technology development will be necessary to assure that these design features will be effective in controlling tritium contamination to acceptable levels. This test plan describes a tritium characterization program to provide the requisite technology.

The following sources of tritium production have been identified, primarily from early surveillance programs at operating HTGRs (steam-cycle plants): (1) ternary fission, (2) neutron activation of lithium impurities in fuel-compact matrix and core graphite, (3) neutron capture reactions in boron used in control materials, and (4) neutron activation of He-3 in the primary He coolant. These sources can be reasonably well quantified for a VHTR. Ternary fission will be the dominant source of tritium production, but this tritium is expected to be largely retained in the TRISO-coated fuel particles. The tritium produced by activation of Li impurities and by capture reactions in boron is also expected to be largely contained in solid core materials. He-3 activation will generate a relatively modest fraction of the total tritium produced in the reactor; however, since it is born in the

primary coolant, it will likely be the dominant source of tritium in the primary helium and, hence, the dominant source of product contamination as well.

The following sinks will serve to remove tritium from the primary coolant: (1) recoil into solids, (2) chemisorption on core graphite, (3) the helium purification system, and (4) permeation through metals. Based upon operating HTGR experience, chemisorption on graphite is a more effective sink than the He purification system; however, tritium rapidly desorbs from the graphite if water is introduced into the primary coolant. Removal by permeation through the heat exchangers and process piping is obviously undesirable since it can lead to product contamination. Surface films will play a critically important role in establishing the in-reactor, tritium permeation rates. Oxide films can reduce H-3 permeability by orders of magnitude; however, normal plant operating transients (e.g., startup/shutdown, etc.) may compromise film integrity, resulting in increased H-3 permeation rates.

Design methods are available to estimate H-3 production, distribution, and release, but they are rather rudimentary and characterized by large uncertainties. Nevertheless, the current design methods appear adequate for conceptual design, but they will need to be upgraded for preliminary design and independently validated prior to completion of final design. Some technology development will be necessary to provide the bases for these design methods improvements and validation. Four Design Data Needs (DDNs) related to tritium behavior have been identified at this writing (more may be identified as the NGNP design matures): (1) measurement of H-3 release from irradiated, failed and intact TRISO particles, (2) measurement of the H-3 sorptivities of irradiated core graphites, (3) measurement of H-3 release from irradiated, bare and coated² B₄C granules, and (4) measurement of H-3 permeation rates through candidate IHX and steam generator metals. Of these DDNs, H-3 metal permeabilities and H-3 release from TRISO particles are the highest priorities, and H-3 release from B₄C is the lowest. The priority of the latter DDN would increase if the plant design includes a steam generator in the primary circuit because water ingress can lead to hydrolysis and subsequent boron migration as well as to enhanced H-3 release.

To satisfy these tritium DDNs, a series of single-effects tests to provide the experimental bases for deriving improved component models and material property correlations are proposed. The experimental techniques are reasonably well established based upon previous work performed to characterize tritium behavior in steam-cycle HTGRs and in fusion systems, especially in lithium blankets designed to breed tritium. The greatest experimental challenge will be to obtain on a timely basis the required irradiated test articles: TRISO particles, core graphite specimens, and bare and coated B₄C. In contrast, metal specimens for permeation testing are readily available, and these tests could begin as soon as funds are available. Measuring the tritium permeability of IN 617, the leading candidate IHX material, is judged the highest priority task. These measurements

² B₄C granules can be coated with pyrocarbon and/or SiC to improve their resistance to hydrolysis and to increase tritium retention.

could be performed in the tritium laboratory at the Idaho National Laboratory where the tritium permeabilities of other metals have been measured.

To minimize cost, this plan assumes that irradiated TRISO particles can be obtained from the ongoing, fuel irradiation test AGR-1 and that irradiated core graphites can be obtained from the planned, graphite irradiation test AGC-1. Obtaining irradiated B₄C test specimens is more problematic. Coated B₄C granules will first have to be fabricated in a laboratory-scale coater. It is assumed here that the B₄C test specimens can be irradiated as piggyback samples in the planned AGR-3/-4 tests (fission product transport tests that are part of the AGR fuel program). The alternative is to irradiate the B₄C test specimens in a non-instrumented drop-in capsule in ATR or HFIR. While feasible, drop-in capsules would be much more expensive than piggyback samples.

A preliminary schedule and rough order-of-magnitude cost estimate were developed for the proposed H-3 characterization program; the results are summarized Figure 1-1. This schedule assumes that funding will be available to initiate the H-3 program at the beginning of FY2009 (the metal permeation tests would be first), and the program would be completed in six years. The tritium program schedule is compared with the current NGNP design schedule since the H-3 program is intended to support NGNP design and licensing. The schedules for fuel tests AGR-1/-3/-4 and for graphite test AGC-1 were also considered since these irradiation tests are assumed to provide test articles for the tritium characterization tests. The cost of the program was estimated from the workscopes and previous experience; assuming an average labor rate of \$30K/man-month, the estimated total cost is \$3.9M. The cost for each of the four test programs is approximately \$1M. The costs would increase substantially if drop-in capsules were required.

If the requisite funds are made available and the irradiated test articles become available as currently planned, the proposed test programs could be completed by early FY2014 which is the scheduled end of the NGNP final design phase. The highest priority tests – H-3 release from TRISO particles and H-3 permeation through heat-exchanger metals – would be completed approximately two years prior to the end of final design. The program could be accelerated by constructing multiple test facilities and performing tests in parallel rather than in series; however, this approach would increase the program costs.

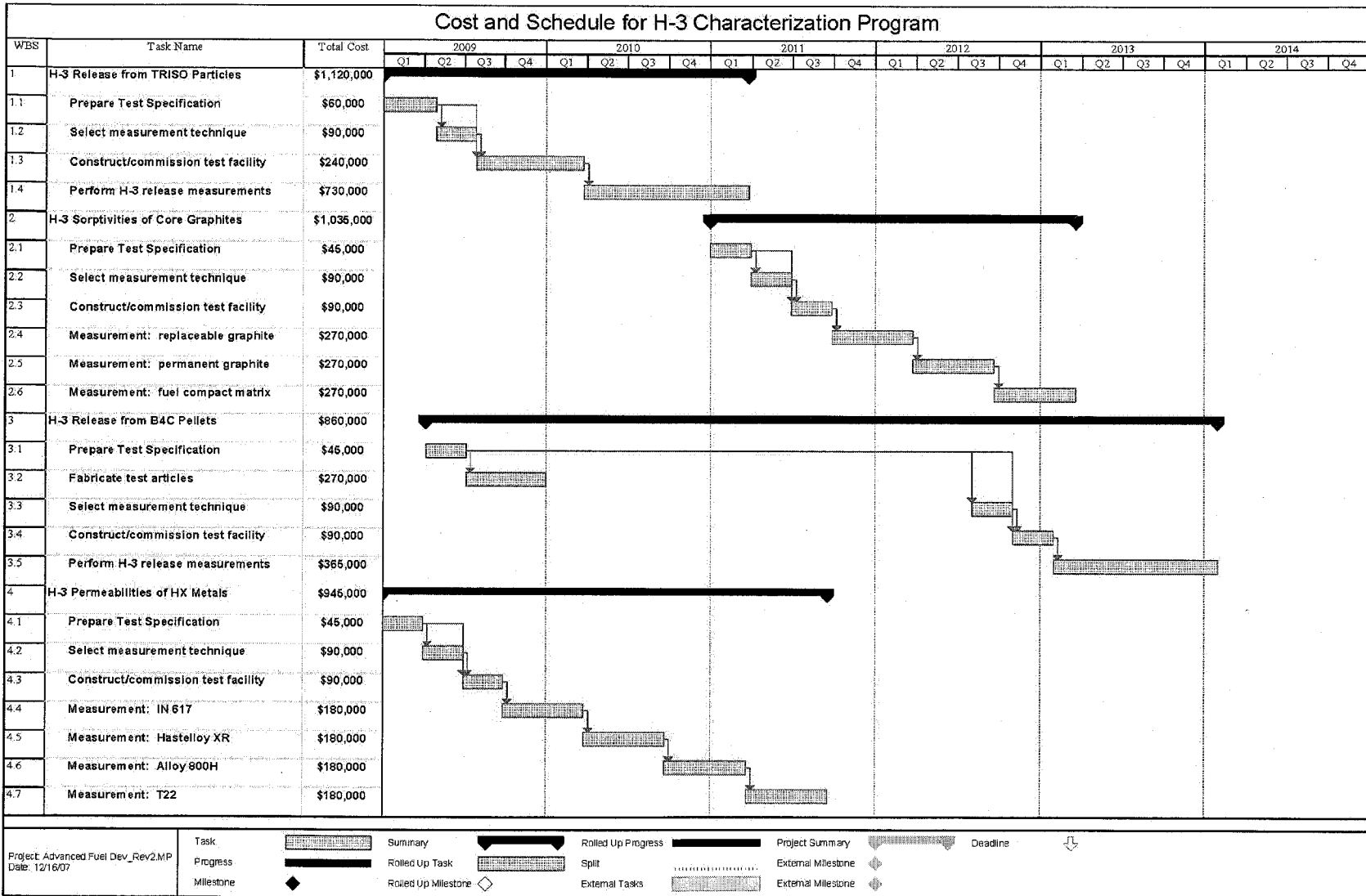


Figure 1-1. Summary Schedule and Cost Estimate for H-3 Program

2 INTRODUCTION AND BACKGROUND

The US Department of Energy (DOE) has chosen the Very High Temperature Reactor (VHTR) for the Next Generation Nuclear Plant (NGNP) Project [PPMP 2006]. The reactor design will be a helium-cooled, graphite-moderated thermal reactor that will be designed to produce electricity and hydrogen as required by the Energy Policy Act of 2005.

A radionuclide containment issue of special interest for the NGNP is the containment of tritium. Tritium will be produced in a VHTR by various nuclear reactions. Given its high mobility, especially at high temperatures, some tritium will permeate through the primary circuit heat exchangers and hydrogen plant process heat exchangers, contaminating the product hydrogen [Hanson 2006b, NGNP TDP 2007]. This tritium contamination will contribute to public and occupational radiation exposures; consequently, stringent limits on tritium contamination in the product hydrogen are anticipated to be imposed by regulatory authorities. Design methods are available to estimate tritium transport in a VHTR [e.g., Hanson 2006a]. However, these design methods are characterized by large uncertainties, and additional experimental data will be required to improve their predictive accuracies for NGNP design and licensing.

The DOE AGR Fuel Development and Qualification Program [AGR Plan/1 2005], which is now part of the NGNP Project, has the mission to develop and qualify fuel for the NGNP. Validation of radionuclide source terms is also within the scope of the AGR Program. The current AGR/1 Plan does not address tritium transport issues. This test plan describes a series of tasks to better characterize tritium retention in a VHTR core and tritium permeation through heat exchanger materials that should be added to the AGR Program in order to satisfy anticipated NGNP Design Data Needs (DDNs) related to tritium transport behavior.

2.1 Purpose

As indicated above, the purpose of this test plan is to describe an experimental program to better characterize tritium retention in the core and tritium permeation through heat exchanger materials in a VHTR designed to provide high-temperature process heat for hydrogen production and/or other process applications. It is anticipated that this workscope would be incorporated into the next issue of the AGR Fuel Plan.

2.2 Tritium Fundamentals

Tritium ($H-3$, 3_1H , T) is a radioactive isotope of hydrogen with a nucleus composed of one proton and two neutrons. It has a radioactive half life of 12.3 yr (such that 5.6%/yr decays); it is a pure beta emitter ($E = 0.0186$ Mev) with a single decay mode to stable He-3 [e.g., Lederer 1978]. Tritium is produced in all fission reactors via ternary fission and from neutron activation of various tritium-forming materials; the H-3 producing, neutron activation reactions of importance in HTGRs are described in Section 3. Tritium is a significant internal radiological hazard with inhalation and

ingestion being the dominant pathways [ISU 2006]. The effectivity of tritiated water (HTO or T₂O) is 20,000 times the effectivity of elemental tritium (HT or T₂).

Tritium is extremely mobile, especially at high temperature. It permeates and/or diffuses through most solid materials, including ceramics and metals. While tritium does permeate through most solid materials, the permeation rates can vary by many orders of magnitude as illustrated in Figure 2-1.

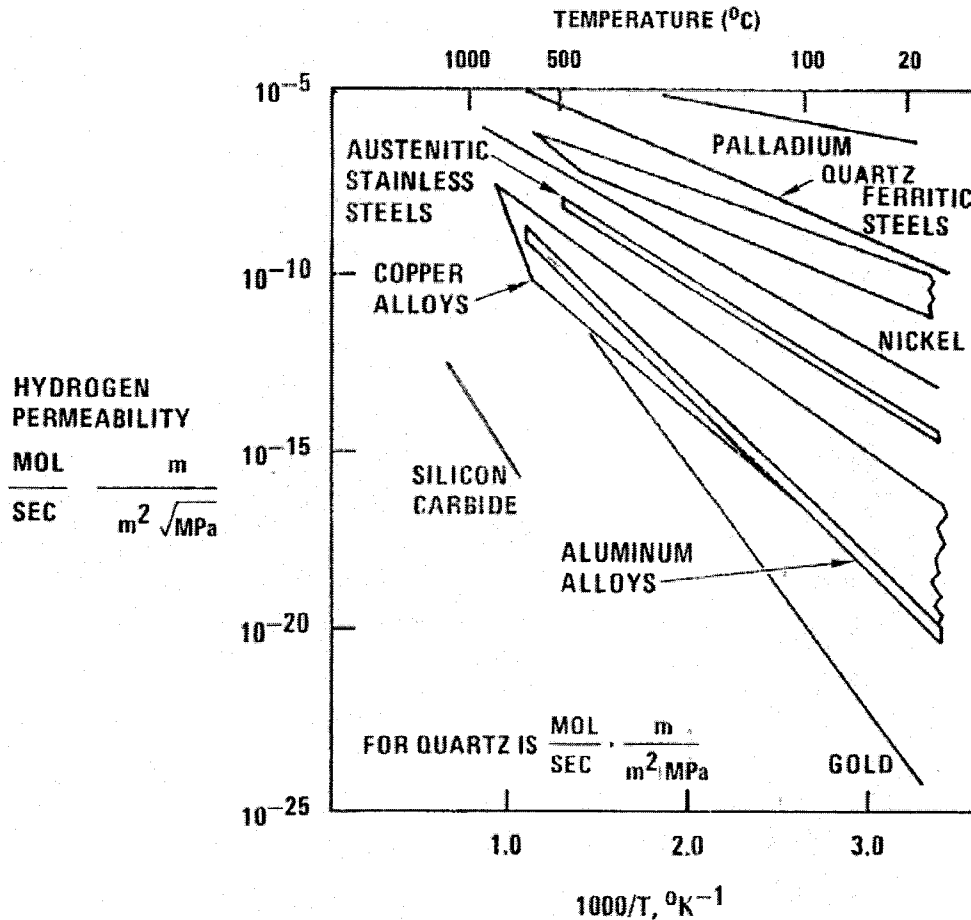


Figure 2-1 H-3 Permeabilities of Various Materials

2.3 VHTR Conceptual Designs for Hydrogen Production

There is a growing interest throughout the industrialized world in using nuclear energy to produce hydrogen. Of the advanced reactor concepts, the VHTR is especially well suited for producing hydrogen because of its high-temperature capability, advanced stage of development relative to other high-temperature reactor concepts, and passive-safety features. The VHTR can provide the high-temperature process heat to produce hydrogen by either thermochemical water splitting or by high temperature electrolysis [e.g., Richards 2004]. A leading conceptual design for nuclear hydrogen production is a Modular Helium Reactor (MHR) coupled via an intermediate heat

exchanger³ (IHX) to a hydrogen production plant using the sulfur-iodine (SI) process or high temperature electrolysis (HTE); this plant concept is referred to as the H2-MHR in this test plan.

The configurations of the primary and secondary heat-transport systems can strongly influence the dominant tritium transport pathways. Pre-conceptual designs have been developed for an H2-MHR based upon the SI process and for an H2-MHR based upon HTE under Nuclear Energy Research Initiative (NERI) contracts to General Atomics (GA), Idaho National Laboratory (INL), and Texas A&M University [Richards 2006a and Richards 2006b, respectively]. Both designs have a 600 MW(t) MHR operating with a core outlet temperature of 950 °C to provide the process heat for hydrogen production. The SI-based design has a large IHX in the primary circuit which transfers all of the reactor thermal energy to the SI plant. The HTE-based design has a smaller IHX which transfers ~10% of the heat to the HTE plant and a direct-cycle, gas-turbine power conversion system (PCS) in the primary circuit to provide the electricity required for the HTE process. A number of different plant configurations are under consideration for H2-MHRs (e.g., the SI-based plant could also contain a PCS in the primary circuit to generate the considerable house electrical load required for the SI plant).

The specific design of the NGNP has not yet been determined [PPMP 2006]. Presumably, the NGNP should serve as a prototype for a commercial H2-MHR; as such, it will be designed to produce both electricity and hydrogen. Consequently, the GA NGNP team proposed a pre-conceptual design that included a small IHX and a direct-cycle, gas turbine PCS in the primary circuit [GA PCDSR 2007]. The NGNP Project has rejected the inclusion of a direct-cycle PCS in the NGNP conceptual design and mandated the inclusion of a steam generator (SG) in either the primary- or secondary heat transport system [NGNP PCD 2007]. Once the conceptual design of the NGNP is finalized, this test plan will need to be reviewed and revised as necessary.

2.4 Significance of Tritium in a VHTR

Given the properties of tritium and its observed behavior in operating HTGRs, tritium will be produced in an H2-MHR and will migrate, to some degree, throughout the plant; consequently, the primary helium coolant and the process streams, including the hydrogen product stream, will likely contain measurable quantities of tritium. The tritium production rates and its transport behavior in the primary coolant circuit of an H2-MHR can be conservatively estimated, given the available design methods for predicting tritium transport (summarized in Section 4) and its observed behavior in operating HTGRs.

In addition to contaminating the product hydrogen stream, tritium will likely be present at some concentration in the gaseous and liquid effluent streams released from the plant into the surrounding environment. While compliance with the various national regulations on public

³ The IHX design for the NGNP may be either a conventional helical-coil design or more developmental compact heat exchanger designs, such as a printed circuit heat exchanger (PCHE) design.

radiation exposure from nuclear plants (e.g., 10CFR50, Appendix I, in the USA) was not a problem, tritium was nevertheless the dominant contributor to offsite doses during normal operation for previous steam-cycle HTGRs [Hanson 2006b]. Moreover, for those operating HTGRs that solidified the tritiated water removed by their helium purification systems, tritium was a major contributor to the total radionuclide inventories disposed of as solid waste as well.

In contrast, tritium has consistently been predicted to be an insignificant dose contributor for postulated accidents for operating HTGRs and for proposed advanced MHR designs. For postulated accidents in advanced MHR designs, including core heatup events, the dominant offsite dose contributors are consistently predicted to be the radioiodines, especially I-131 [e.g., PSID 1992]. The H-3 inventories in an HTGR are too small to be significant compared to the radioiodines and noble gases (the exception being the tritium-producing New Production Reactor). It is anticipated that the same results will be obtained when dose assessments for normal plant operation and postulated accidents are made for a commercial H₂-MHR and for the NGNP.

2.5 Tritium Transport Design Data Needs

During the design of systems, components, and processes, the designers identify engineering development data that are needed to confirm the design (i.e., to validate assumptions made in the design process). In cases where this information cannot be obtained through the normally accepted level of engineering analysis, the designer prepares a Design Data Need [DDN Procedure 1986]. Although certain DDNs are generic to most advanced MHR designs (e.g., the material properties of SiC coatings, etc.), many DDNs are design specific, especially those related to design verification and support (DV&S) issues.

Since the NGNP is still in pre-conceptual design, the Design Data Needs for the NGNP have not yet been finalized.⁴ However, a provisional set of fuel/fission product DDNs for a generic VHTR, including tritium transport DDNs, has been identified as a prerequisite for preparing a Development Plan for Advanced High Temperature Coated-Particle Fuels [Hanson 2003]. The source materials for developing the VHTR DDNs were those DDNs and development plans prepared by GA, INL and ORNL for earlier modular HTGR designs, including the direct-cycle GT-MHR [DOE-GT-MHR-100217 1996] and the steam-cycle MHTGR [DOE-HTGR-86025 1989]. From these previous DDN compilations, one can reasonably determine the tritium transport DDNs for a commercial H₂-MHR and for the NGNP.

⁴ A complete set of DDNs was identified in [NGNP TDP 2007] for the NGNP preconceptual design recommended by the GA NGNP team which included a direct-cycle, gas-turbine, power conversion system [GA PCDSR 2007]. However, as indicated above, the NGNP Project has rejected the inclusion of a direct-cycle PCS in the NGNP conceptual design and mandated the inclusion of a steam generator in either the primary- or secondary heat transport system [NGNP PCD 2007]. Consequently, the issue of NGNP DDNs will need to be revisited once the conceptual design is determined. The DDNs related to radionuclide transport, including tritium transport, are anticipated to be largely unaffected since they are mostly generic.

Each of the DDN compilations for modular MHRs include a DDN related to H-3 permeation through heat exchanger tubes and another DDN related to H-3 transport in core materials. The scope of the latter DDN varies from one compilation to the other. For the steam-cycle MHTGR [DOE-HTGR-86025 1989], the DDN includes H-3 release from intact TRISO particles and H-3 sorption on core graphite. The DDN for the direct-cycle GT-MHR [DOE-GT-MHR-100217 1996] includes only H-3 sorption on core graphite along with the statement that the data on H-3 diffusive release from TRISO-coated LiAl_3O_7 target particles might be used to predict H-3 release from intact TRISO fuel particles. The latter assertion appears to be highly speculative and would require experimental confirmation in any case since the partial pressure of H-3 in a target particle is many orders of magnitude higher than in a fuel particle, the fast fluences are higher in a fuel particle, and the fuel particles, especially in a VHTR, operate at much higher temperatures than target particles in a steam-cycle NP-MHTGR. Neither the MHTGR nor the GT-MHR DDN addresses H-3 release from control materials which could be significant, especially with the higher operating temperatures in a VHTR (to the first approximation, the difference in core inlet temperatures is an indication of the difference in operating temperatures for the control rods located in the inner and outer side reflectors).

The NGNP DDNs identified in [NGNP TDP 2007] used the commercial GT-MHR DDNs as the point of departure since these DDNs (i.e., DDNs designated "DDN C.XX.YY.ZZ") are largely applicable to the NGNP (e.g., fuel and fission product DDNs, etc.). Following the conventions established in [NGNP TDP 2007], the commercial GT-MHR DDNs are again used as the point of departure here, and new DDNs are defined for H-3 release from intact TRISO particles and for H-3 release from control materials (i.e., designated "DDN N.XX.YY.ZZ" where the prefix "N" signifies "NGNP"). The worksopes for the resulting H-3 transport DDNs are summarized in Table 2-1.⁵ These DDNs apply to both prismatic- and pebble-bed core designs although some of the test articles would be core design specific (e.g., different core graphites are used in prismatic and pebble-bed cores).

The DDN priorities assigned in the table reflect engineering judgment based upon previous assessments of H-3 transport in steam-cycle HTGRs; they are subject to reassessment once a conceptual design is established for the NGNP, and a tritium mass balance has been calculated for that design to determine the dominant H-3 sources and sinks for that specific design. If a steam generator is included in the primary circuit of the NGNP, the priority of those subtasks to determine the effect of water on H-3 transport will obviously increase.

⁵ Clearly, these H-3 transport DDNs could be organized differently, but this definition seems logical (e.g., it will allow prioritization by core material: fuel particles, graphite, and control material).

Table 2-1. Workscope for Tritium Transport DDNs

DDN No.	DDN Title	Workscope	Priority
C.07.03.05	Tritium Permeation in Heat Exchanger Tubes	Data are needed describing the permeation of tritium through heat exchanger material(s) used the intermediate heat exchanger and steam generator as function of temperature, H-3 partial pressure, system pressure, coolant impurity concentrations and tube surface oxidation state. The effects of thermal cycling, which would occur as a result of reactor startup, shutdown, and load changes, needs to be determined. Sufficient data are needed to develop and refine H-3 permeation models with uncertainties [$<10x$] ⁶ at 95% confidence.	High
C.07.03.06	Tritium Transport in Core Materials	Data are needed to determine sorptivities of tritium on core structural graphites as a function of temperature, tritium partial pressure, fluence, and coolant impurity concentrations, especially H ₂ O and H ₂ , during normal and accident conditions. Sufficient data are needed to develop and refine H-3 transport models with uncertainties [$<10x$] ⁷ at 95% confidence.	High/Medium ⁸
N.07.03.23	Tritium Release from TRISO Particles	Data are needed to determine H-3 release rates from failed and intact, reference TRISO particles as a function of temperature and burnup (H-3 release from intact particles is more important since the H-3 fractional release from failed particles is expected to approach 100%). Sufficient data are needed to develop and refine H-3 release models with uncertainties [$<10x$] at 95% confidence.	High
N.07.03.24	Tritium Release from Control Materials	Data are needed to determine H-3 retention by boron-based control materials. H-3 release rates need to be measured as a function of temperature, fast fluence, and water partial pressure. The need for applying pyrocarbon and/or SiC coatings to the B ₄ C granules (expected to be used in the control materials) should be determined. Sufficient data are needed to develop and refine H-3 transport models with uncertainties [$<10x$] at 95% confidence.	Medium/Low ⁸

⁶ Numerical values given in [square brackets] are tentative values subject to change when test specifications are written.

⁷ Numerical values given in [square brackets] are tentative values subject to change when test specifications are written.

⁸ Priority increases if a steam generator is included in the primary coolant circuit.

2.6 Proposed Experimental Program

Upon consideration of the H-3 transport DDNs described above and previous experimental investigations in this area, a test program is proposed herein that is comprised of four elements: (1) measurement of H-3 release from irradiated TRISO particles, (2) measurement of H-3 sorptivities of irradiated core graphites, (3) measurement of H-3 release from irradiated B₄C granules, and (4) measurement of H-3 permeation rates through candidate IHX and SG metals. The current data base for describing H-3 transport behavior is described in Section 3, and the attendant design methods for predicting H-3 transport are described in Section 4. The test requirements are given in Section 5, and the Quality Assurance requirements are given in Section 6. The proposed test program is described in Section 7, and cost and schedule estimates are given in Section 8. Major deliverables are listed in Section 9.

3 TRITIUM BEHAVIOR IN AN HTGR

The tritium sources and its transport behavior in an HTGR are summarized in this section. There is an extensive literature on this topic [e.g., Gainey 1976, Hanson 2006b], and many of the key references are cited below.

3.1 Sources of Tritium in an HTGR

There are multiple sources of H-3 production in an HTGR, including ternary fission and a variety of neutron capture reactions [Gainey 1976]. Even if the nuclear properties (thermal and fast neutron fluxes, cross sections, etc.) are well known, a reliable knowledge of the tritium-forming impurities present in the reactor is also required. Of greatest importance is the Li-6 content of core materials, including fuel element graphite, fuel particles, fuel-compact matrix, reflector graphite, control materials, and core insulation.

As shown in Table 3-1, ternary fission is typically the dominant source of H-3 production in an HTGR (results are for a steam-cycle HTGR). However, of greater importance is the dominant source(s) of H-3 release into the primary coolant.

Table 3-1. Sources of H-3 Production in HTGRs

H-3 source	% total ⁹	Release potential
Ternary Fission	62	Time at temperature
He-3 Activation	18	Produced in He coolant
Li-6 Activation		Partly retained in graphite; released during H ₂ O ingress
Core graphite	2	
Core matrix	10	
Reflector (replaceable)	<1	
Reflector (permanent)	<1	
B Capture Reactions		Apparently retained at source
Control rods	7	
Burnable poison	1	
Reflector	<1	

3.1.1 Ternary Fission

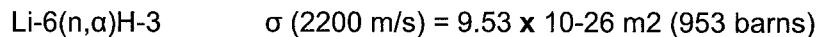
Tritium is formed by ternary fission in an HTGR core with the reported yields typically ranging from about 0.8 to 2.3 x 10⁻⁴ atoms/fission, depending on the nuclide undergoing fissioning and the

⁹ Typical values; results strongly dependent upon the Li impurity content of core materials.

neutron flux spectrum [Gainey 1976]. The H-3 yields from thermal fissioning of U-235 and Pu-239 are reasonably well known. However, the H-3 yields from fast fissioning are not well known; reported H-3 yields from fast fissioning of U-238 are an order of magnitude greater than from the thermal fissioning of U-235 and Pu-239 and from fast fissioning of U-235. Since about 10% of total fissioning in an HTGR core is from fast fissioning, this uncertainty in the fast fission H-3 yields introduces a nontrivial uncertainty in the total core production of H-3 from ternary fission. A core average H-3 yield of 1.0×10^{-4} atoms/fission has been traditionally assumed at GA for reactor design and safety analysis.

3.1.2 Neutron Activation of Lithium

As stated above, lithium is present as a trace impurity in many core materials, including fuel element graphite, fuel particles, fuel-compact matrix, reflector graphite, control materials, and core insulation. Li-6 with a natural abundance of 7.5% has a significant neutron capture cross section and transmutes to H-3:



In general, the total lithium content of the core materials is extremely low, often bordering on the detection limits for most analytical methods for Li measurement.

3.1.3 Neutron Activation of He-3

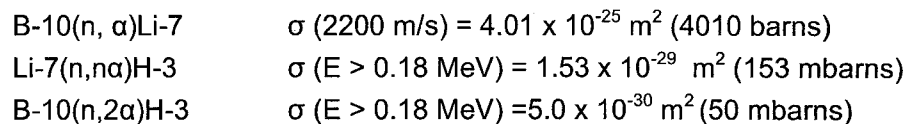
The trace He-3 content of the primary He has a large cross section and will readily activate to H-3 under irradiation:



The He-3 content of the helium (atom ratio He-3/He-4) ranges from about 2×10^{-7} for He obtained from natural gas wells (the normal source of He coolant for HTGRs) to an order of magnitude higher for He obtained from the atmosphere [Wichner 1979].

3.1.4 Neutron Capture Reactions in Control Materials

Boron-10 is used as a neutron absorber in control rods, in burnable poison in fuel elements, and often in the permanent reflectors and core support structure to reduce neutron damage. Several neutron capture reactions with these B-10 control materials in the core will produce tritium. The dominant reactions are:



In summary, the mechanisms by which H-3 is produced in an HTGR are well established (i.e., ternary fission and various neutron capture reactions with Li-6, He-3 and B-10). However, the

uncertainties in the total in-reactor H-3 production rates are nontrivial because of the uncertainties in the ternary fission yields, especially for fast fissioning, and because of the uncertainties in the concentrations of H-3 generating trace impurities, especially Li-6.

3.2 H-3 Transport in an HTGR

The various H-3 transport pathways in an HTGR (steam-cycle plant) are shown schematically in Figure 3-1. The transport behavior of H-3 in HTGRs has been reviewed previously [e.g., Gainey 1976, Hanson 2006b].

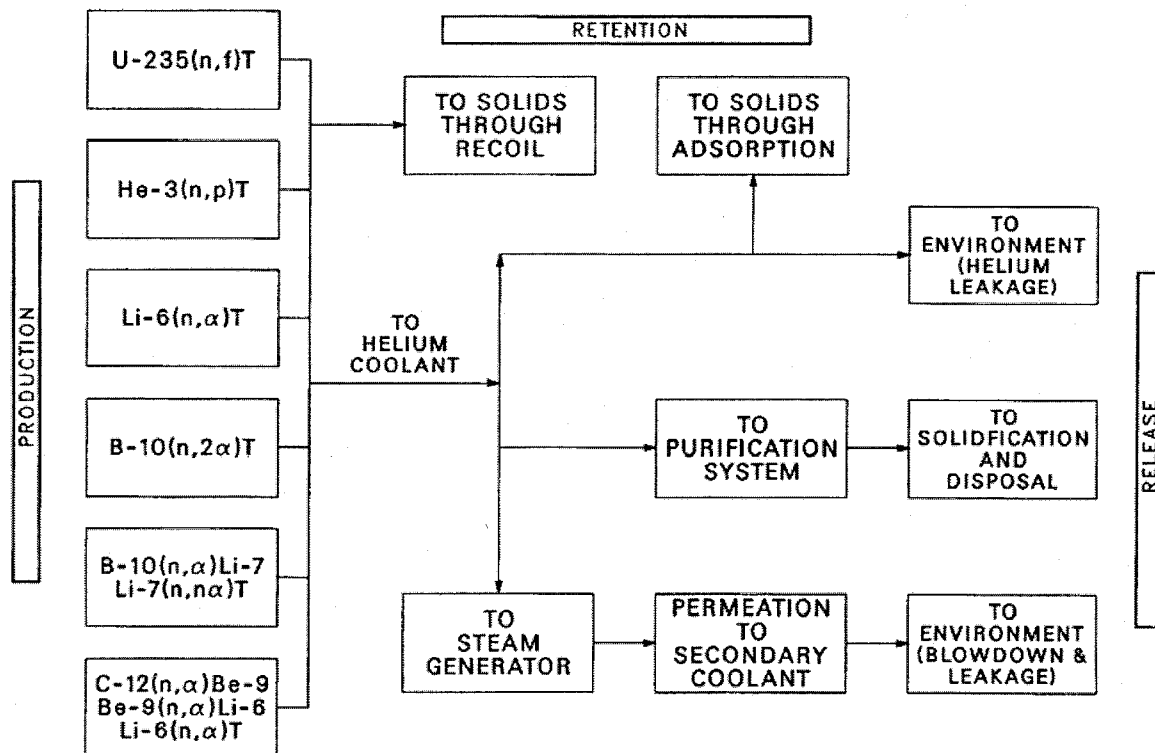


Figure 3-1. H-3 Distribution in an HTGR (Steam-Cycle Plant)

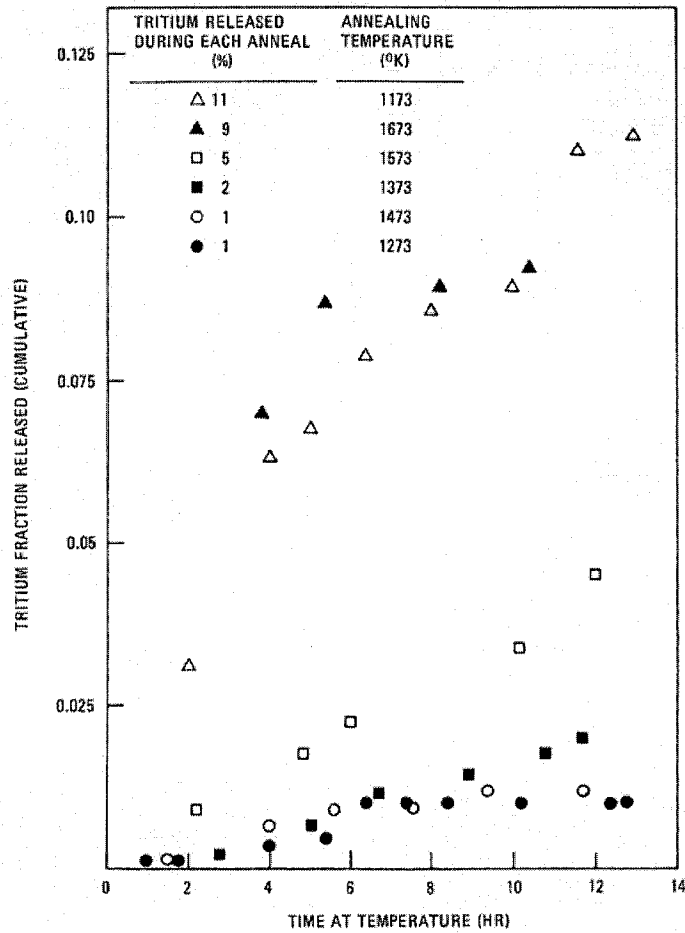
The information about H-3 transport in HTGRs can be organized in a number of ways. The tritium in the primary coolant is of greatest importance in the present context since it is most readily available for transport into the secondary heat transport system and beyond to contaminate the product hydrogen or end products of other process-heat applications. Consequently, this subsection is organized by sources of H-3 release into the primary coolant and by sinks for H-3 removal from the primary coolant.

3.2.1 Tritium Release into Primary Coolant

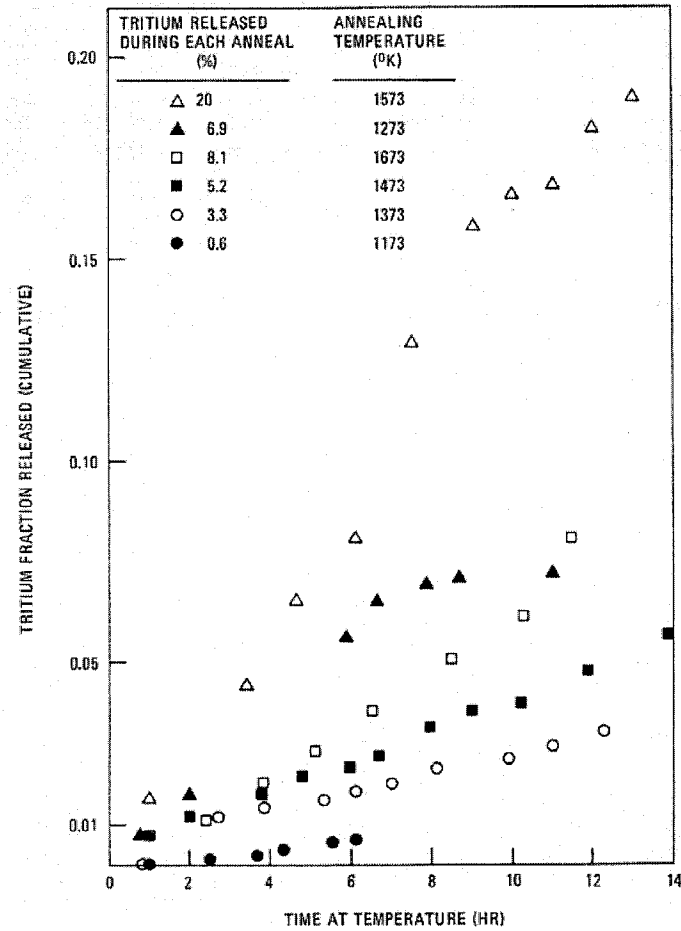
The most readily available source of H-3 in the primary He is obviously the neutron activation of He-3 directly in the primary coolant. The other potential sources are H-3 inventories produced by neutron capture reactions in various core materials.

3.2.1.1 H-3 Release from Coated Fuel Particles

As stated previously, the largest source of H-3 production in an HTGR is typically ternary fission; hence, the largest H-3 inventory is contained within the coated fuel particles. Before this tritium can be released into the primary coolant, it must be released from the fuel kernels and permeate through the pyrocarbon (PyC) and SiC coatings of intact TRISO fuel particles. The available data on tritium retention in early high enriched uranium (HEU) TRISO particles at the end of irradiation is summarized in [General Atomic 1972]. Figure 3-2 shows the tritium release from intact UO_2 and UC_2 particles during postirradiation heating tests. In general, tritium retention decreases with higher irradiation and heating temperatures and with higher burnups, although quantitative models are difficult to derive because of the limited data available. There is also considerable uncertainty regarding possible SiC defects in the test particles. Undetected SiC defects would serve to give an artificially high apparent SiC permeability for tritium.



H-3 Release from Intact UO₂ TRISO Particles



H-3 Release from Intact UC₂ TRISO Particles

Figure 3-2. H-3 Release from Intact TRISO Fuel Particles

A review of both the internal GA data base and the external HTGR literature did not produce any significant information about measured H-3 release rates from modern, low enriched uranium (LEU) TRISO fuel particles. However, there is another large data base regarding H-3 release from TRISO-coated particles. TRISO-coated target particles have been investigated for the production of H-3 for nuclear weapons and for future fusion reactors. Typically, these target particles have a kernel composed of a lithium aluminum oxide compound with a conventional TRISO coating system. The critical performance parameter for these target particles is the H-3 permeation rate in the TRISO coating system, especially in the SiC coating; consequently, H-3 permeabilities through TRISO coatings, especially SiC, have been investigated as part of target development programs in the USA and Japan.

There was a major target development program in the USA in the late 1980s and early 1990s to develop TRISO-coated lithium aluminate particles for use in the New Production Reactor (NPR) [Thomas 1989]. Extensive data on H-3 release from target particles under irradiation and during postirradiation heating tests were developed as a result. While there are few open-literature publications, the data are documented in technical reports that are "Unclassified Controlled Nuclear Information" (UCNI) and, thus, not publicly available. Presumably, most of these data could be reclassified following established DOE procedures and made available to the NGNP Project.

3.2.1.2 H-3 Release from Matrix and Core Graphite

As introduced previously, tritium is produced within the graphite moderator, reflector blocks, and the compact matrix material from neutron activation of Li-6 and B-10 impurities. It appears that some tritium produced in this way is retained at its place of birth (i.e., by recoil into solid matter), and some would be capable of migrating out into the helium coolant [Gainey 1976]. Tritium retention by recoil into structural solids is described in Section 3.2.2.1. Because of these recoil effects, tritium born in solid graphitic structures in the core, principally the fuel and reflector graphite, may well behave differently (i.e., be more effectively retained) than tritium that is adsorbed from the coolant on to these graphitic structures; tritium chemisorption on graphitic structures is described in Section 3.2.2.2.

Elleman's results, cited in [Gainey 1976], indicate that ~20% of the tritium produced could be permanently held in the graphite structure. Figure 3-3 shows the results of studies of tritium release at different temperatures from graphite containing 0.1 ppm Li irradiated at high neutron flux [Walter 1973]. The results imply that tritium release from graphite is a diffusion-limited process since the fractional release is proportional to the square root of time.

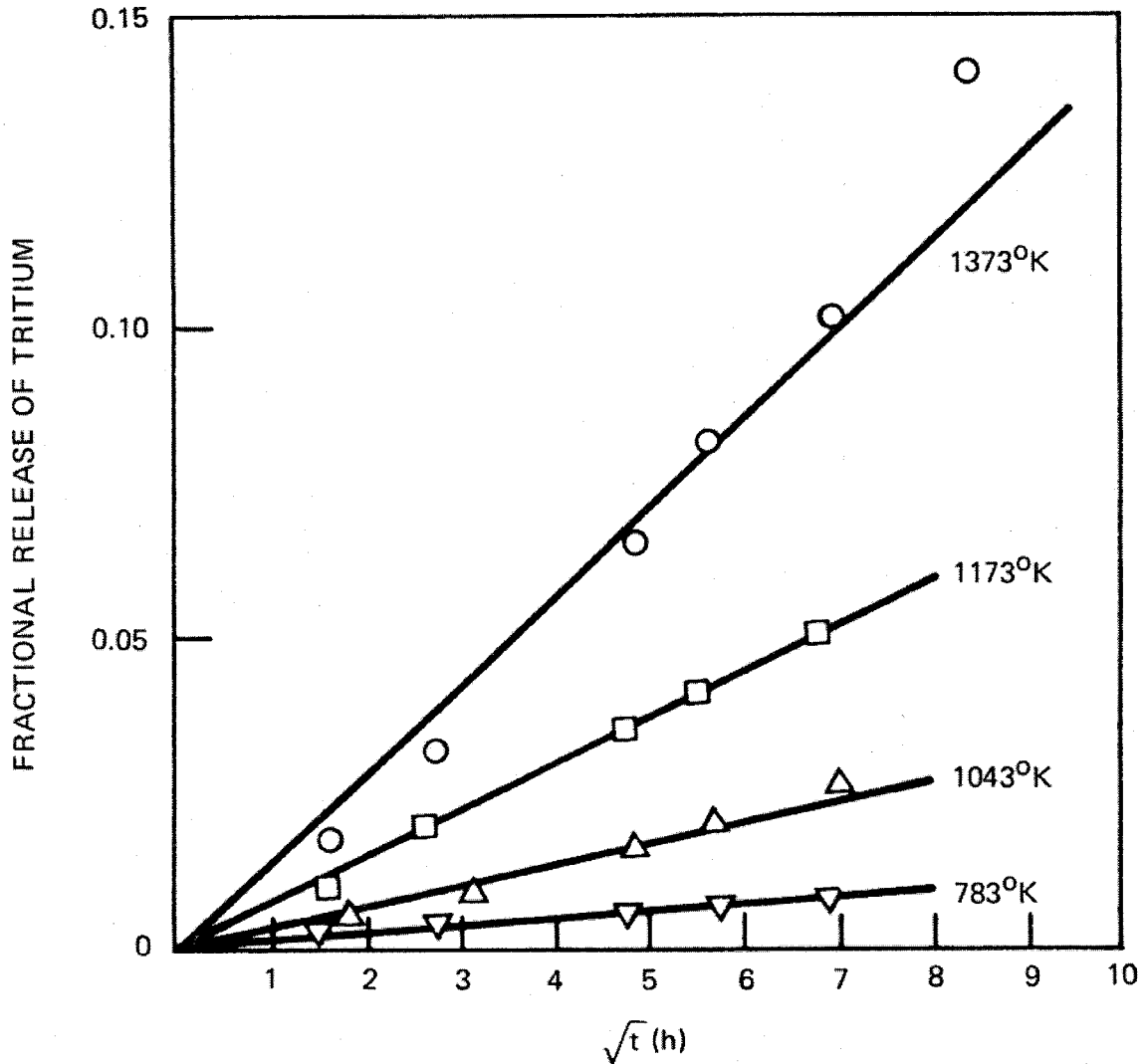


Figure 3-3. Tritium Release Isotherms from Annealed/Irradiated Graphite Probes

The results of postirradiation heating tests on irradiated graphite performed at KFA Juelich are shown in Figure 3-4 [Fischer 1974]. Although the heating times are short (a few hours), the data imply that H-3 would be very strongly retained at normal operating temperatures. KFA explained their results by assuming that a combined diffusion/desorption mechanism was responsible for the release. They considered chemisorption and molecular dissociation at the graphite surface and absorption and diffusion into the graphite bulk. Data are also available for hydrogen (protium) desorption from several graphites, including TSP nuclear graphite [e.g., Bansal 1971].

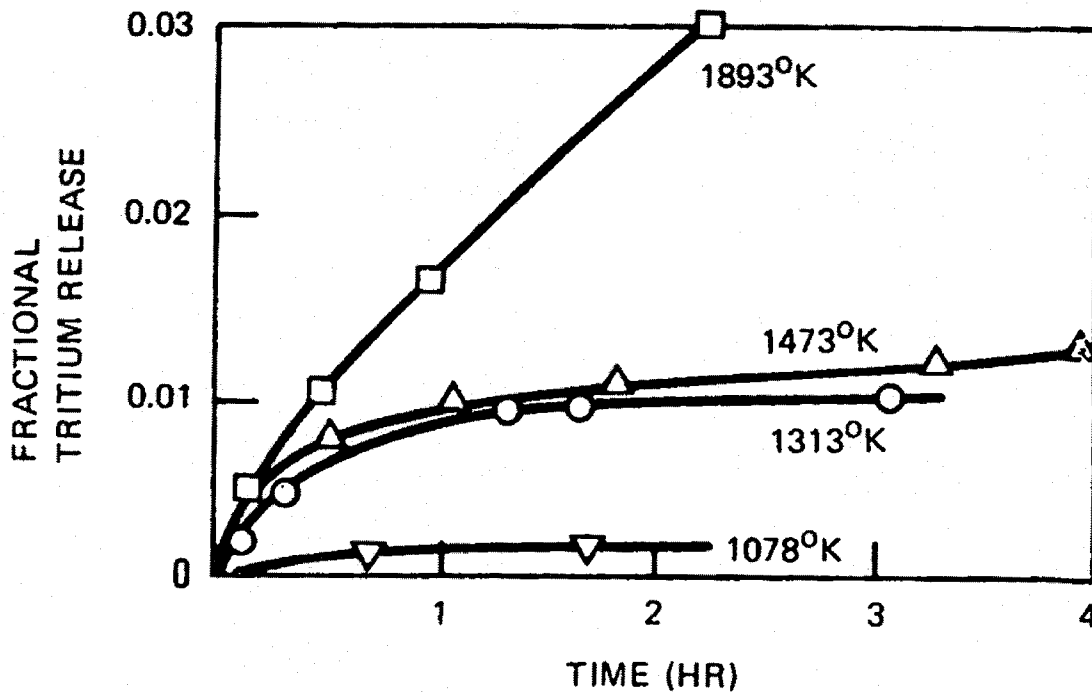


Figure 3-4. H-3 Release from Graphite during Postirradiation Heating

The TRITGO manual¹⁰ (Hanson 2006a) recommends a graphite retention factor of 0.99 for H-3 born in core graphite; given the data in Figures 3-3 and 3-4 that assumption seems rather optimistic for a VHTR core. Isotherms for H-3 chemisorption on graphite are described in Section 4.2.2.

3.2.1.3 H-3 Release from Control Materials

Boron-10 is used as a neutron absorber in control rods, in burnable poison in fuel elements, and often in the permanent reflectors and core support structures to reduce neutron damage. Several neutron capture reactions with these B-10 control materials in the core will produce tritium (Section 3.1.4). The boron is typically present as B₄C granules which have been pressed into pellets with a carbonaceous binder.

There are limited data available on H-3 release from B₄C pellets. Data presented by [Gainey 1976] for tritium release from B₄C pellets shows a minimum fractional release of about 20% at approximately 760 °C, with increasing release fractions at hotter and colder temperatures. Tritium release fractions between 80 and 85% were measured at temperatures of 593 and 871 °C. These H-3 release data were obtained from [Pitner 1973]; the results are shown in Figures 3-5 and 3-6. Little information was provided about the physical characteristics of the B₄C pellets used in these experiments so it is not clear how representative the samples were of the B₄C used in HTGRs. These results show the H-3 fractional release to be a complex function of irradiation temperature

¹⁰ TRITGO is a computer code for predicting an overall plant mass balance for tritium; see Section 4 for description,

but not of the burnup level. This behavior was thought to be due to the way in which tritium combined chemically with the B_4C . Annealing at temperatures well above the irradiation temperature was necessary to release tritium from the pellets.

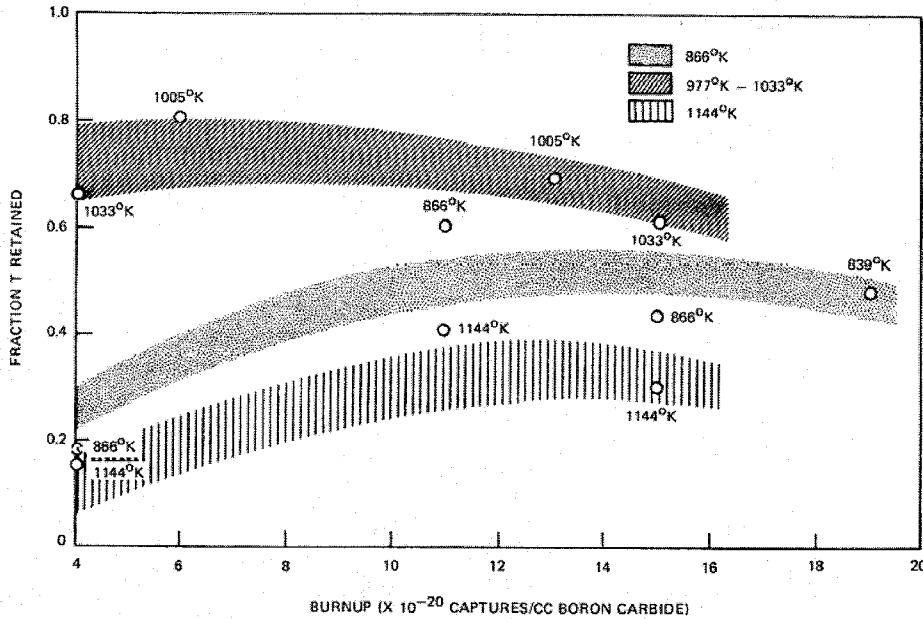


Figure 3-5. Tritium Retained in Boron Carbide

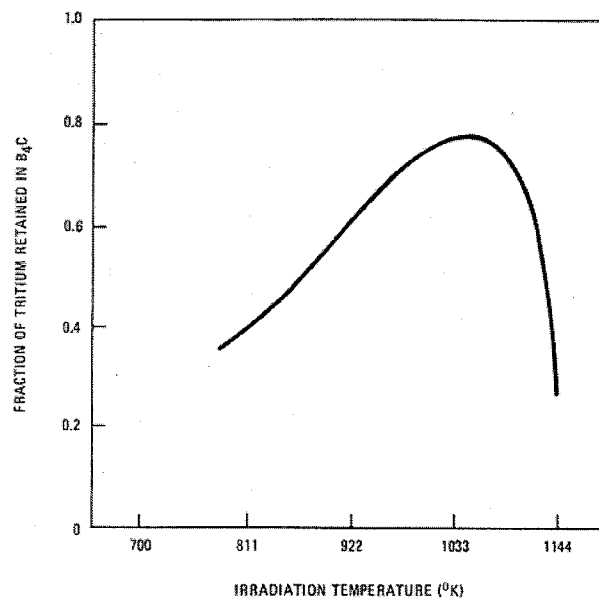


Figure 3-6. Temperature Dependence of H-3 Retention in B_4C Pellets

One of the design issues associated with the use of B_4C as a control material in HTGR cores is that it can hydrolyze if exposed to water, forming volatile boric acid which leads to the potential for migration of neutron poison within the core. In fact, hydrolysis of the B_4C in the reserve shutdown pellets with the attendant formation of boric acid did occur in Fort St. Vrain as a result of chronic

water ingress; although this occurrence presented no safety issue for FSV operation, it was nevertheless an undesirable operational event.

One design option for mitigating the potential for B4C hydrolysis is to apply a protective coating to the B4C granules prior to pressing them into pellets. Such protective coatings should also increase the tritium retention. Specimens of B4C granules coated with dense PyC and other specimens coated with PyC+SiC¹¹ were prepared and irradiated as piggyback samples in fuel irradiation capsule HRB-21 [Heffernan 1991]. Unfortunately, only the structural integrity of the coated B4C particles was examined visually during the postirradiation examination (PIE), and no quantitative results were reported [Acharya 1995]. The tritium retention characteristics were not determined.

3.2.2 Tritium Removal from Primary Coolant

The various sinks which can remove H-3 from the primary coolant are described below. With the exception of the helium purification system, the effectiveness of these various removal mechanisms is not well quantified.

3.2.2.1 Removal by Recoil

In neutron activation reactions, tritium is generated as a triton, which is the tritium nucleus without an orbiting electron (i.e., a positively charged tritium ion); tritons are highly reactive. Tritons produced by neutron activation reactions in solids, such as graphite, could energetically recoil into graphite crystallites where they could displace a hydrogen atom in a C-H bond or carbon atom in a C-C bond. This recoil action might also produce additional active sites upon which further chemisorption could occur. It is not known what fraction of tritium trapped by recoil is held irreversibly; the estimates range from a high of 99% [Compere 1974] to ~20% [Gainey 1976]. Tritons produced by neutron capture reactions in boron control materials may also react chemically with the carbon in the B4C [Gainey 1976].

Tritons from He-3 activation in the primary coolant in the core will come to rest in solids in fractions which vary from region to region because of the varying proportion of space associated with coolant channels and fabricated holes, clearance annuli, and pores. The recoil energy of a triton is about 0.2 MeV leading to an estimated range of 0.05 cm (500 μm) in helium at 47.6 atm and 600 °C. Because graphite pores generally are smaller than 0.05 cm, the fraction of tritons bound is generally assumed to be unity [Compere 1974].

3.2.2.2 Removal by Chemisorption on Graphite

All isotopes of hydrogen chemisorb on graphite, especially at high temperatures. Tritium entering the primary coolant becomes equilibrated with the relatively much larger concentration of ordinary

¹¹ Both coating designs had low density buffer layers; i.e., one coating design was equivalent to a BISO fuel coating system, and the other was equivalent to a TRISO coating system without the outer PyC.

hydrogen (i.e., protium) which is present in the primary coolant (~10 ppmv H₂ is a typical value for steam-cycle HTGRs), and its chemical behavior then becomes indistinguishable from that of ordinary hydrogen.

There are a limited number of old (pre-1980) measurements of hydrogen sorption on nuclear graphite. An example of these old data is the measurement of hydrogen sorption on TSP nuclear graphite shown in Figure 3-7. Note that the sorptivity increases with increasing temperature up to about 1100 °C (which is well above the peak temperatures experienced by much of the core reflector graphite).

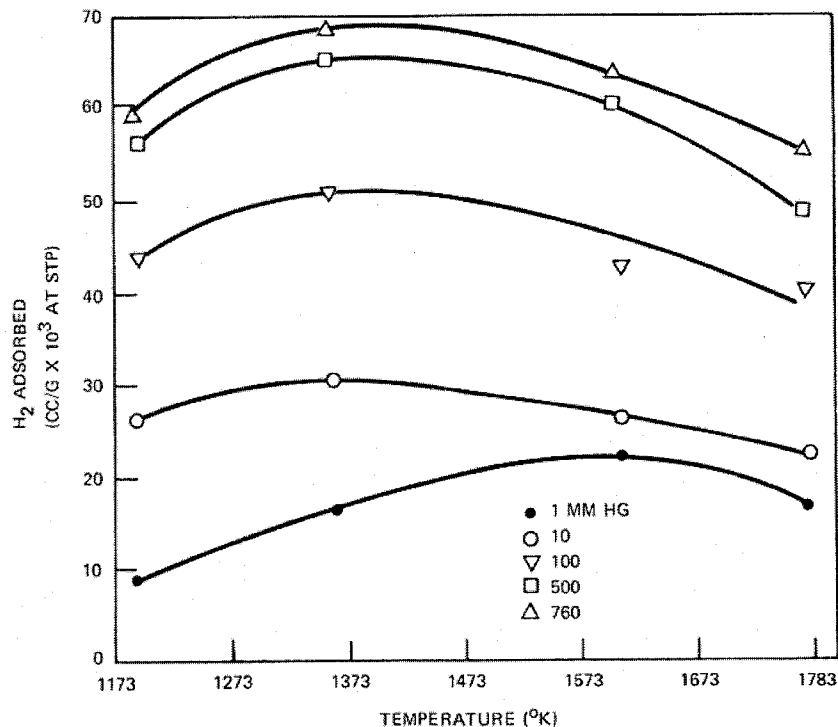


Figure 3-7. Hydrogen Sorption on TSP Nuclear Graphite

In the mid-1980s Strehlow [1985] at ORNL measured the sorptivities of several nuclear graphite, including H-327 and POCO, for tritium gas and tritium oxide at temperatures ranging from 175 to 750 °C.¹² Higher temperatures were found to result in tritium sorption at concentrations as high as 2.1×10^{13} a/cm². Sorbed quantities at lower temperatures after exposure to either tritium oxide or tritium gas were found to be in the range of 1×10^8 a/cm², some five orders of magnitude lower. Oxidized specimens showed the expected profile effects of greater penetration of the tritium into the specimens. The relationship of the BET surface area to the amount adsorbed appeared to be linear for oxidized specimens; however, the amount of tritium sorbed by unoxidized specimens could not be simply related to the BET surface area.

¹² These results are reported in a brief journal article [Strehlow 1985]. Surprisingly, no detailed technical report could be located in the ORNL library.

High-purity graphite is also a candidate material for various applications in magnetic confinement fusion reactors, including for the first wall. Consequently, tritium sorption on graphite has also been investigated by fusion researchers [e.g., Causey 1989, etc.]. In general, the experimental conditions investigated are not representative of the conditions in an HTGR primary circuit. Typically, hydrogen and tritium sorption on graphite is correlated using a Temkin isotherm.¹³

During and after water ingress, the loss of tritium from the graphite by isotopic exchange with the hydrogen in the water becomes significant [Myers 1986]. It has been reported that exchange occurs at low temperatures although experiments have been conducted in which no significant amount of tritiated water has been detected below 400 °C. In FSV, water ingress occurring during startup and shutdown led to large increases in the tritium concentration in the primary coolant.

3.2.2.3 Removal by the Helium Purification System

In order to avoid deleterious effects on structural materials, undesirable chemical impurities present in the primary coolant must be controlled; consequently, all HTGR designs, including modern VHTR designs, include a helium purification system (HPS). Principally, the chemical impurities are:

1. H₂O, N₂, and O₂ from graphite outgassing;
2. H₂O, CO, CH₄, CO₂ and H₂ from water ingress and its subsequent reaction with graphite;
3. H₂ and CH₄ from reaction of oil contaminants with graphite;
4. N₂ and O₂ from air ingress during maintenance and venting operations.

Source #2 will be of much less importance for direct-cycle GT-MHRs and for hydrogen-producing VHTRs with an intermediate heat exchanger because of the absence of a steam-generator in the primary circuit which is typically the primary source of water ingress for a steam-cycle HTGR (FSV with its water-bearing circulators was an exception). Source #3 has been practically eliminated for modern MHR designs wherein magnetic bearings have replaced oil-lubricated bearings.

While the primary purpose of the HPS is to control chemical impurities, it also serves to remove radionuclides in the circulating helium coolant, including noble gases and tritium. The HPS also removes condensable radionuclides, including iodine isotopes and volatile fission metals (Ag, Cs, Sr, etc.), but these condensable radionuclides typically deposit, or "plate out," on the He-wetted surfaces in the primary coolant circuit much more rapidly than they are removed by the HPS.

¹³ With a Temkin isotherm, the heat of adsorption decreases as a linear function of increasing fractional surface coverage. In contrast, the heat of adsorption is constant with a Langmuir isotherm and decreases as an exponential function of increasing fractional surface coverage with a Freundlich isotherm.

3.2.2.4 Sorption on Metal Surfaces

Hydrogen, and by inference tritium as well, chemisorbs on metals, especially noble metals and high-nickel alloys. Tests in Sweden [Gainey 1976] have also shown that tritium will sorb on metal oxide films that are in contact with tritiated water. However, the amount of metal surface area in the primary circuit of a VHTR is small compared to the huge BET surface area of the graphite structures in the reactor system. Hence, sorption on metal surfaces, especially at the high service temperatures in the primary coolant loop of a VHTR, is considered to be insignificant compared to the sorption on the core graphite.

3.2.2.5 H-3 Permeation through Metals

As previously discussed, tritium is of concern for hydrogen-producing VHTRs because the isotopes of hydrogen, including tritium, can permeate through most solid materials, including those metals comprising heat exchangers, and contaminate the product hydrogen. The permeation of hydrogen isotopes through metals and ceramics has been investigated for many decades. There is a vast literature on the topic and on-going research, especially in the fusion community; however, the data are limited for the specific combination of materials of construction, service temperatures, tritium and hydrogen concentrations, and oxidation potentials that are postulated for the IHX and the H₂ process plant of an H₂-MHR.

The available data indicate that each of the aforementioned variables can be important. As shown in Figure 2-1, the measured permeabilities of hydrogen isotopes in metals and ceramics span many orders of magnitude. A key factor, which is discussed in more detail below, is that the hydrogen permeability of most metals is strongly influenced by the oxidation potential and the attendant surface oxide layers that are typically present on both sides of the wall material in a heat exchanger, such as the steam generator in a steam-cycle HTGR or the IHX in an H₂-MHR. In general, the presence of a coherent oxide layer can reduce the effective hydrogen permeability by orders of magnitude.

While these oxide-permeation barrier phenomena could, in principle, be very beneficial in an operating H₂-MHR, they are also a major complication: (1) modeling of H-3 permeation behavior must account for the effect of the oxide layers; (2) accurate prediction of H-3 behavior, including product contamination, in an H₂-MHR must address the effects of coolant chemistry and oxide-layer formation; (3) extrapolation of existing hydrogen permeation data to H₂-MHR service conditions becomes more uncertain; and (4) any experimental measurements of H-3 permeation rates through candidate materials of construction for the IHX should include representative coolant chemistries and surface layers on both sides of the material. At this stage of development of a first-of-a-kind facility, it is practically impossible to predict with high confidence the coolant chemistries, hence characteristic surface oxidation states, in the primary and secondary circuits of an H₂-MHR.

The general approach that has been taken in modeling the permeation of hydrogen isotopes through metals and in correlating experimental permeation data is summarized below.

3.2.2.5.1 Permeation Models and Data Correlation

In the first approximation, the permeation of gases, including tritium, through metals is usually described in terms of Fick's first law of diffusion; in one dimension, the flux is proportional to the concentration gradient (after [Gainey 1976]):

$$J = -D_g \frac{dC}{dx} \quad (3-1)$$

where: J = permeation flux (atom/cm²-sec),
 D_g = gaseous diffusion coefficient (cm²/sec),
 C = concentration in the metal (atom/cm³),
 x = distance (cm).

Sievert's law states that the equilibrium concentration of a diatomic gas dissolved in a metal is given by (i.e., the gas has dissociated and is migrating in atomic form):

$$C = K_s p^{1/2} \quad (3-2)$$

where: K_s = Sievert's law constant [cm³(STP)-mm/cm²-torr^{1/2}],
 p = pressure (torr),

Combining Fick's law with Sievert's law (for a small wall thickness) gives

$$J = \frac{K_p}{x} (p_1^{1/2} - p_2^{1/2}) \quad (3-3)$$

where K_p includes both the diffusion coefficient and Sievert's law constant and is called a permeability coefficient [cm³(STP)-mm/cm²-sec-torr^{1/2}]. The subscript 1 refers to upstream pressure while subscript 2 refers to downstream pressure. When the downstream pressure is low,

$$J \approx \frac{K_p}{x} (p_1^{1/2}) \quad (3-4)$$

The square-root of pressure dependence of J assumes that the diatomic gas dissociates and permeates through the metal lattice in the atomic state.

K_p may be written in the form of an Arrhenius relation:

$$K_p = K_o \exp(-Q/RT) \quad (3-5)$$

where K_o = preexponential factor [cm³(STP)-mm/cm²-sec-torr^{1/2}],
 Q = activation energy for gas permeation (J/mol),
 R = gas constant,

T = absolute temperature (K)

As postulated above, measured hydrogen isotope permeabilities in metals generally show exponential temperature dependence as illustrated in Figure 3-8 for Incoloy 800 [Gainey 1976]; as shown in Table 3-2, the measured activation energies are generally less than 20,000 cal/mol and are occasionally quite small (e.g., 3430 cal/mol for niobium).

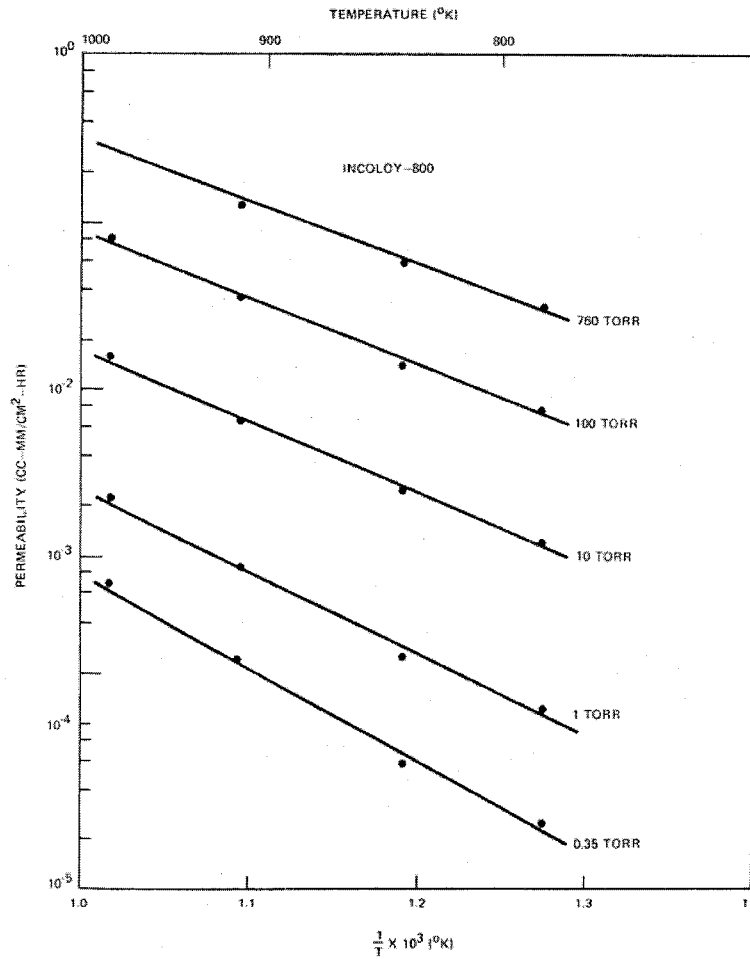


Figure 3-8. Hydrogen Permeation through Incoloy 800

Table 3-2. Permeabilities for Hydrogen Permeation of Metals

Metal	Q (cal/mol)	K_o $\frac{cm^3(STP)mm}{sec-cm^2-torr^{1/2}}$
Hastelloy N	13,800	1.9×10^{-3}
Hastelloy B	16,675	1.82×10^{-2}
Nickel	13,400	1.00×10^{-2}
Iron	9100	1.45×10^{-3}
304 SS	16,100	8.56×10^{-3}
316 SS	16,075	1.54×10^{-2}
321 SS	16,075	1.54×10^{-2}
430 SS	11,200	3.62×10^{-3}
PH15-7Mo SS	20,000	7.86×10^{-2}
Haynes 25	15,100	3.29×10^{-3}
Molybdenum	20,100	9.57×10^{-3}
Tungsten	29,340	1.85×10^{-2}
Niobium	3,430	1.05×10^{-2}
Platinum	18,600	1.85×10^{-2}
Palladium	4,500	6.15×10^{-2}
Vanadium	14,200	5.4
Copper	18,560	1.11×10^{-2}

However, the observed dependence of the permeation rate on hydrogen partial pressure is often different from the square-root dependence predicted by Eqns (3-4) and (3-5), especially if the experimental data span a large partial pressure range. In fact, the data often show a square root of pressure dependence at high partial pressures; a pressure dependence between square root and linear at intermediate partial pressures; and a square root dependence again at very low partial pressures [Gainey 1976]. The first two observations are easily rationalized: diatomic gases are assumed to dissociate and permeate through metal lattices in the atomic state (square-root pressure dependence; see above), but they are assumed to permeate through oxides in the molecular state (linear pressure dependence). Since it is difficult to prevent at least a partial oxide layer from forming on most metals (exceptions being the noble metals, nickel, etc.), pressure dependence between square root and linear suggests the presence of an oxide layer which represents a resistance to permeation of the same order of magnitude as that of the base metal.

The observation that the pressure dependence again becomes square root at very low partial pressures is more difficult to rationalize. Strehlow and Savage [1974] suggested that defects or cracks in the oxide layer could be responsible for this behavior. The expected behavior for the permeation of hydrogen through a metal coated with an oxide containing no holes or other gross imperfections is illustrated in the upper diagram of Figure 3-9. Permeation through a metal with an oxide film that contains cracks, holes, or other porosity would be expected to lead to a different asymptote when the permeation rate is low. Defects in the film constitute a path for permeation which is parallel to that through the crystalline portion of the oxide but which is in series with the path through the metal. The flux through the defects would add to that through the crystalline oxide, with the net flux expected to depend on the half power of driving pressure according to Strehlow and Savage (the basis for this conclusion is the citation of unpublished ORNL-4881). The general behavior expected for permeation through a metal with a defective oxide film is illustrated in the lower diagram of Figure 3-9.

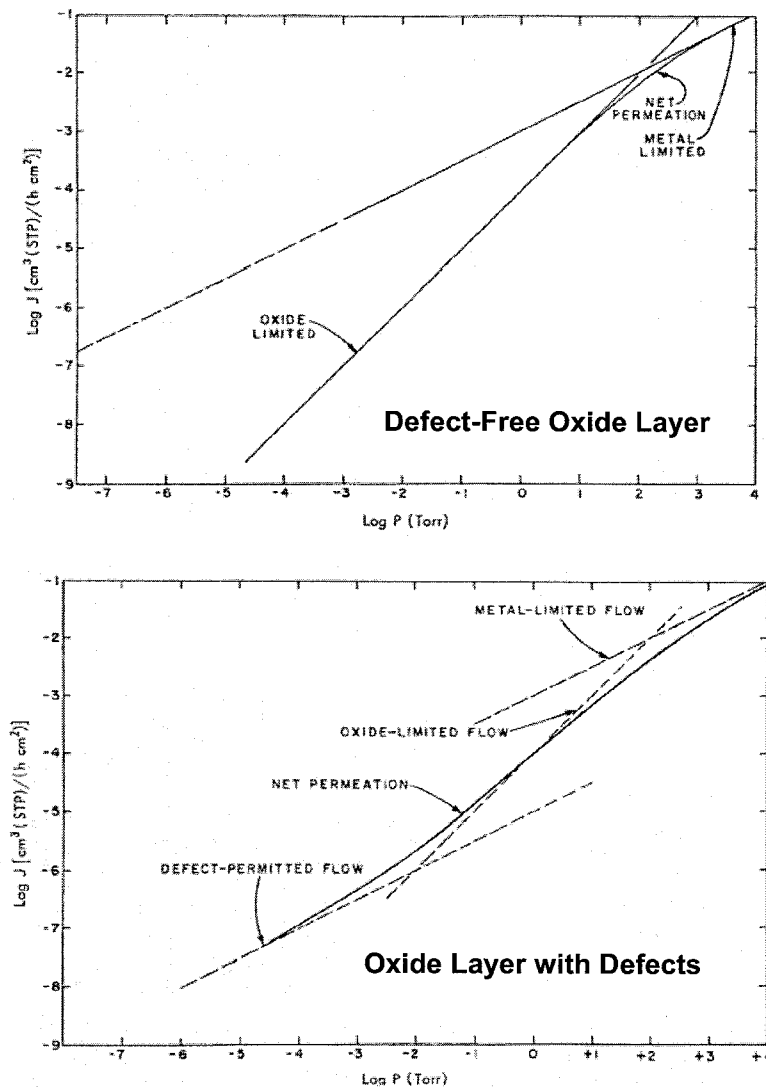


Figure 3-9. Effect of Oxide Films on Permeation Pressure Dependence

A recurring theme in the hydrogen permeation literature is that the oxidation effects must be considered in modeling and data correlation. A dramatic illustration of the effect of oxidation is given in Figure 3-10. Workers at ORNL [Bell 1975] used a mixed isotope technique to measure the permeability of tritium through Incoloy 800 with a controlled steam atmosphere on the inside of the tube. Hence, the influence of surface oxidation on tritium permeation was determined. A long-term experiment (>2000 hr) was conducted with Incoloy 800 at 930 K with the inside of the tube continuously purged with a sweep gas of Ar/H₂O with a H₂O partial pressure of 0.3 MPa. The tritium permeability of the metal dropped continuously with time (a factor of 160 in 84 days, which was attributed to the progressive oxidation of the metal to form a protective oxide coating). The permeability rapidly decreased for the first 36 hr, and then linearly decreased at a much slower rate as a function of the square root of time, suggesting that diffusion through a growing oxide layer was the rate limiting step.

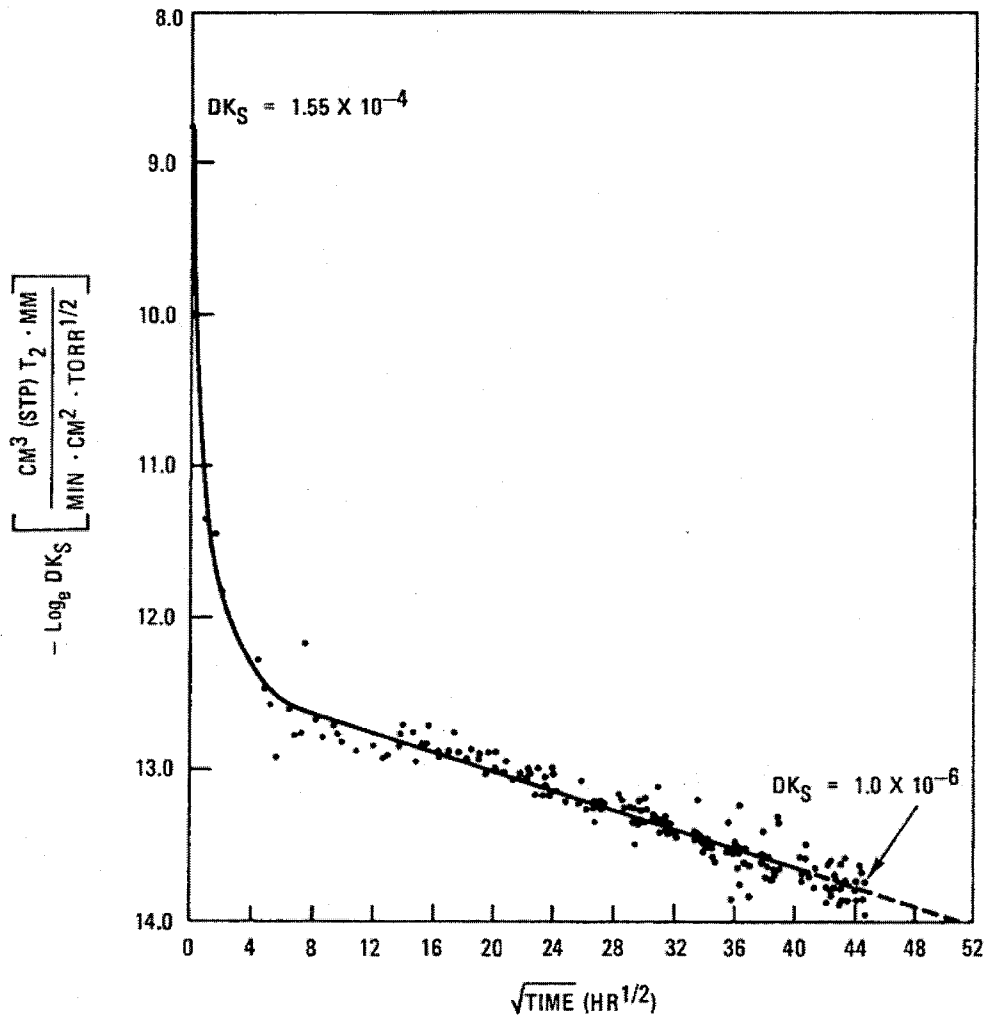


Figure 3-10. Effect of Steam Oxidation on H-3 Permeation through I-800

Given such results, it is important that the surface oxidation state be considered when developing H-3 permeation models and when performing H-3 permeation measurements. The first step in this regard is to determine the oxidation potential which can be related to oxygen partial pressure through the following relationship [Perdijk 1971]:

$$\log P_{O_2} = 5.73 - \frac{25750}{T} - \log \frac{P_{H_2}^2}{P_{H_2O}^2} \tag{3-6}$$

and/or the oxidation potential can be related to the CO/CO₂ ratio by the following relationship:

$$\log \frac{P_{H_2}}{P_{H_2O}} = 1.67 - \frac{1900}{T} + \log \left(\frac{P_{CO}}{P_{CO_2}} \right) \tag{3-7}$$

Of course, the nature of the surface oxide produced by a given oxidation potential will depend upon the metal alloy involved. For instance, ferritic low-alloy steels are more readily oxidized than are the high-nickel alloys, such as IN 617, that are the leading candidates for use in the H2-MHR IHX.

More sophisticated models for hydrogen permeation through metals have been proposed than the simple models described here. Andrew and Haasz [1992] provide a history of these various permeation models and conclude that the dissociative chemisorption model with saturation effects is sufficient to describe the bulk of the available data; although their paper is a good historical summary, it is largely an academic exercise that does not address the effects of surface oxidation, which is usually the dominant effect.

3.2.2.5.2 H-3 Permeation Measurement Techniques

Conceptually, the experimental techniques for measuring the permeation rates of hydrogen isotopes through metals are rather simple. For the determination of tritium permeation rates, there are two basic approaches: (1) experiments utilizing tritium directly where the H-3 quantitative analysis is performed by beta counting; and (2) experiments utilizing protium and/or deuterium surrogates where the quantitative analysis for protium and/or deuterium is by mass spectroscopy. Technically, the direct use of tritium is preferred because the detection limits for tritium by beta counting are generally lower than the detection limits for hydrogen or deuterium by mass spectroscopy. In the latter case, deuterium is generally preferred to protium because of a better signal-to-noise ratio. The disadvantage with tritium, of course, is that it poses a radiation hazard that many researchers would prefer to avoid. Deuterium also poses a minor, but easily managed, occupational hazard.

For either approach, the experimental apparatus is generally quite simple which can be illustrated by the apparatus used by Strehlow [1974] at ORNL for measuring deuterium permeation through a variety of metals (see below). In addition, several other experimental programs are described to illustrate the standard measurement techniques and the experimental challenges encountered.

3.2.2.5.2.1 ORNL Measurements of D₂ Permeation through Incoloy 800

As shown schematically in Figure 3-11, the chief feature of the apparatus used by Strehlow [1974] at ORNL was a jacketed permeation tube fabricated of the metal or alloy of interest, whose temperature during testing was maintained and controlled by an electrically heated tube furnace. The tube specimens were generally about 1.27 cm in outer diameter and 18 to 36 cm long, with wall thicknesses ranging between 0.9 and 1.65 mm.

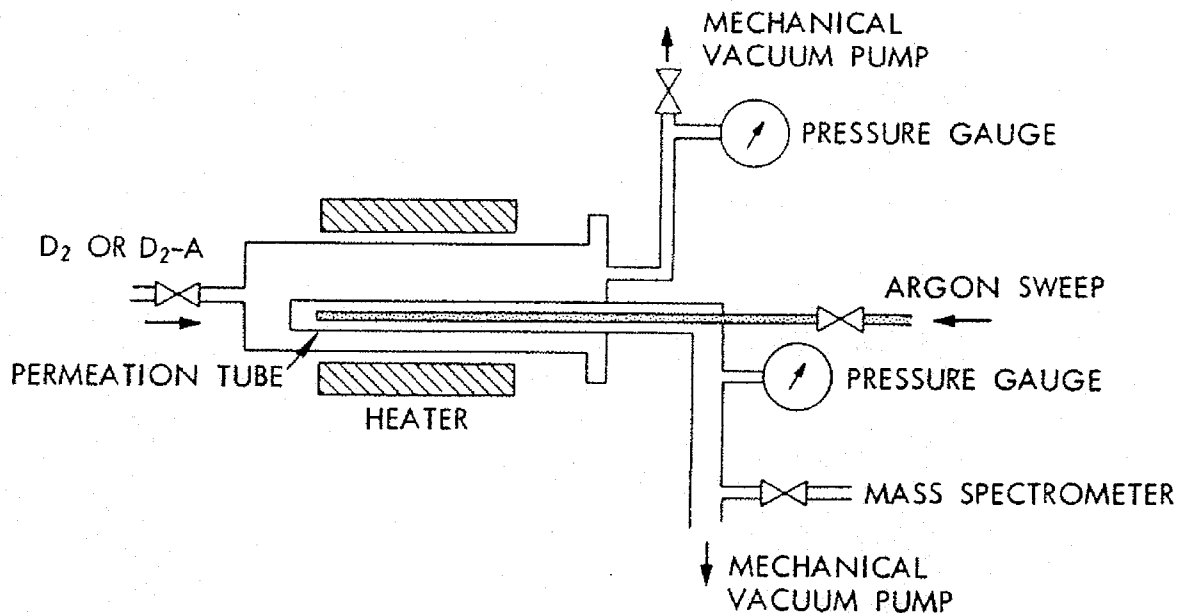


Figure 3-11. Apparatus for D_2 Permeation Measurements

Deuterium gas or a mixture of deuterium gas in argon (or helium) was maintained at pressures from 760 Torr down to <1Torr at the tube outlet. The deuterium permeating through the tube mixed and flowed with argon sweeping the inside of the tube. The argon was continuously sampled and analyzed for deuterium content with a quadrupole mass spectrometer. Two absolute pressure gauges, with ranges from 0 to 800 and 0 to 20 Torr, were used to measure the pressure of the permeating deuterium or deuterium-argon mixture on the outside of the tube. From this pressure and the measured deuterium concentration of the sweep gas, an accurate determination of the deuterium back pressure inside the tube could be made. The flow rate of the argon sweep gas, measured by a calibrated rotometer, was used in combination with the measured composition to determine the permeation rate of deuterium.

While the test apparatus was indeed physically simple, these permeation tests proved to be complex because of the effects of surface oxide films that would form during the experiments. In fact, even the sequence of changing the test conditions affected the measured permeation rates as demonstrated in Figure 3-12; these deuterium permeation data for Incoloy 800 indicate that the permeation rate and the pressure dependence of permeation depended strongly on the conditions under which the oxide film was formed [Strehlow 1974].

In Figure 3-12, the numbers associated with the curves indicate the sequence of conditions in a series of tests with a single specimen of Incoloy 800. Curves 1, 2, and 3 show the behavior prior to intentional oxidation of the specimen. The permeation rates decreased slightly, and the pressure dependence increased slightly after a 12-hr measurement period at 649 °C. This initial effect was probably due to inadvertent oxidation of the specimen by contaminants in the deuterium and/or

argon. This oxide film presumably was highly defective because the permeation rates increased about as expected when the temperature was raised to 744 °C (Figure 3-12, Curve 3). In addition there was no substantial change in the pressure dependence. The permeation rate at 1 Torr was reduced by a factor of 50 after intentional oxidation of the Incoloy 800 with D₂-2.6% D₂O at 649°C (Figure 8-5, Curve 4). Formation of an oxide film by this treatment yielded a pressure dependence of permeation that was nearly first power, suggesting a coherent oxide film had formed.

After obtaining Curve 4, the temperature of the specimen was increased to 744 °C; the specimen was continuously being oxidized by the D₂-D₂O mixture during the temperature change. Tests at 744 °C (Figure 3-12, curve 5) showed that, despite the ~100°C temperature increase, the permeation rates and pressure dependence had not changed markedly from those obtained in the previous tests at 649°C (curve 4). Finally, the temperature was returned to 649°C, with the specimen continuously being subjected to the D₂-D₂O mixture. Tests at this temperature (curve 6) showed that the permeation rates had decreased significantly and that the pressure dependence was still nearly first power. The whole sequence of tests illustrates that highly effective films can be applied to metals by controlled oxidation and that rates of permeation through metal-oxide composites formed in this manner can be reduced by several orders of magnitude.

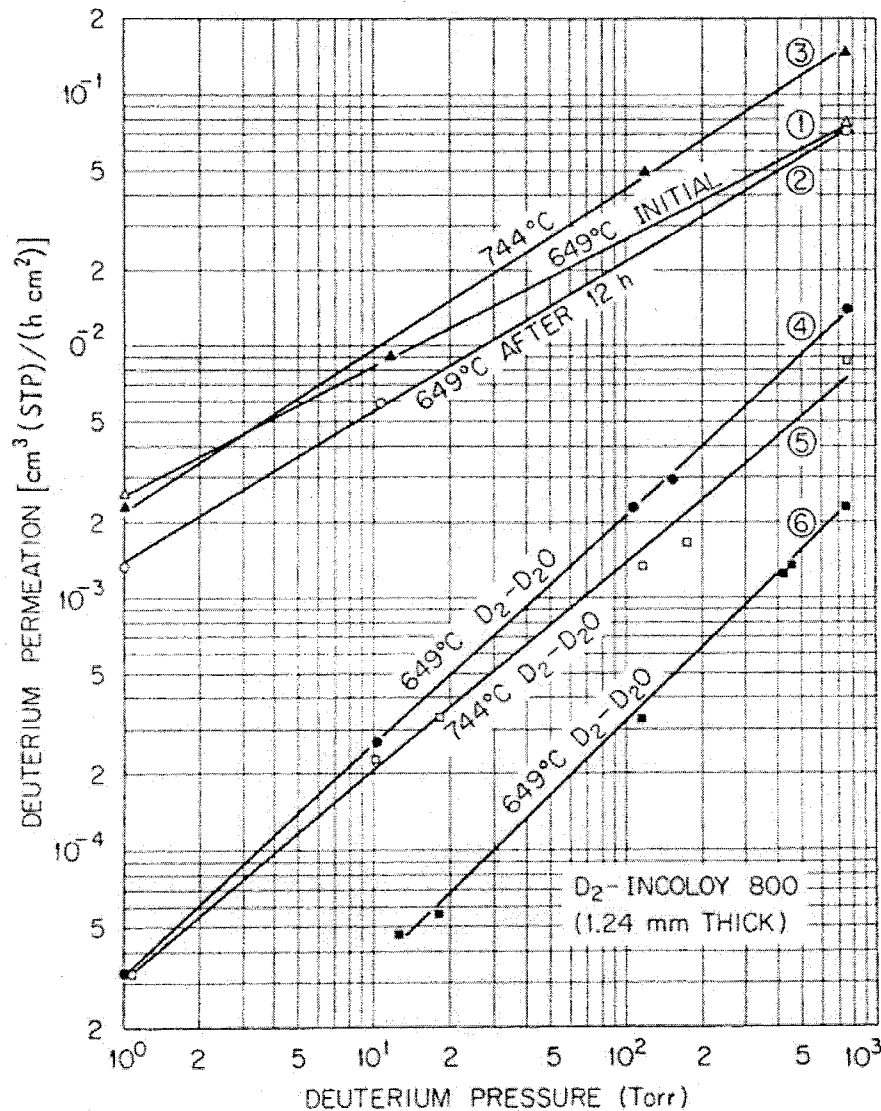


Figure 3-12. Effect of Progressive Oxidation on D₂ Permeation through I-800

3.2.2.5.2.2 GA Measurements of H-3 Permeation through PB SG Tubes

An extensive end-of-life R&D program was conducted for the Peach Bottom (PB) HTGR which included removal of steam-generator tube specimens; the PB steam generator had Incoloy 800 superheater (SH) tubes, and carbon steel evaporator (EV) and economizer (EC) tubes [Steward 1978]. In addition to metallurgical and radiochemical examinations, a number of H-3 permeation experiments were performed at GA on selected PB SG tube specimens [Yang 1977].

The He-side of the Peach Bottom SG tubes were covered with a carbonaceous deposit produced by cracking of lubricating oil that leaked periodically from a purified helium transfer compressor into the primary circuit. This soot-like deposit was tightly bound to the tube surfaces; in fact, the circulating quantities of dust in the Peach Bottom primary coolant were quite low [Dyer 1977].

A schematic of the experimental apparatus used to make the permeation measurements is shown in Figure 3-13. For the present purpose, the most important feature of the apparatus is that the coolant chemistry could be controlled on both the outside (He side) and inside (steam side) of the tube specimens. On the outside of the tube (He side), both the measured Peach Bottom primary coolant chemistry and the predicted coolant chemistry for the large HTGR¹⁴ were simulated during the permeation tests. On the inside of the tube (steam side), the purge gas for recovering the H-3 that permeated through the tube wall could be either pure dry helium or a helium/steam mixture.

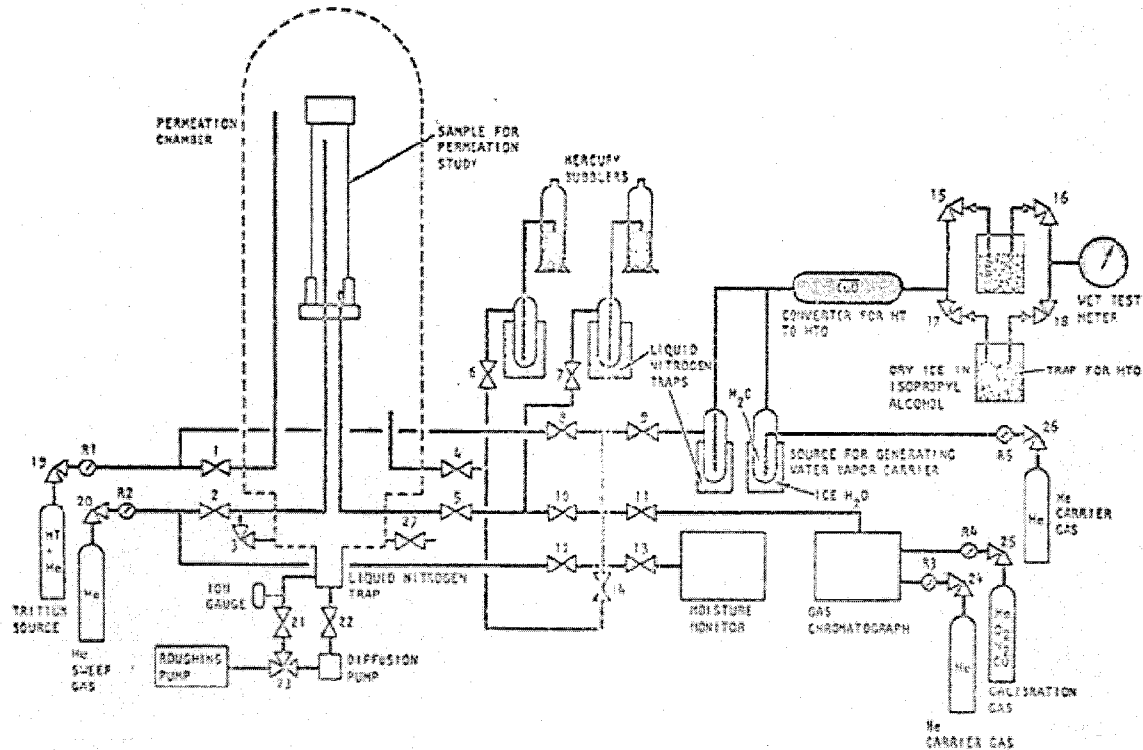
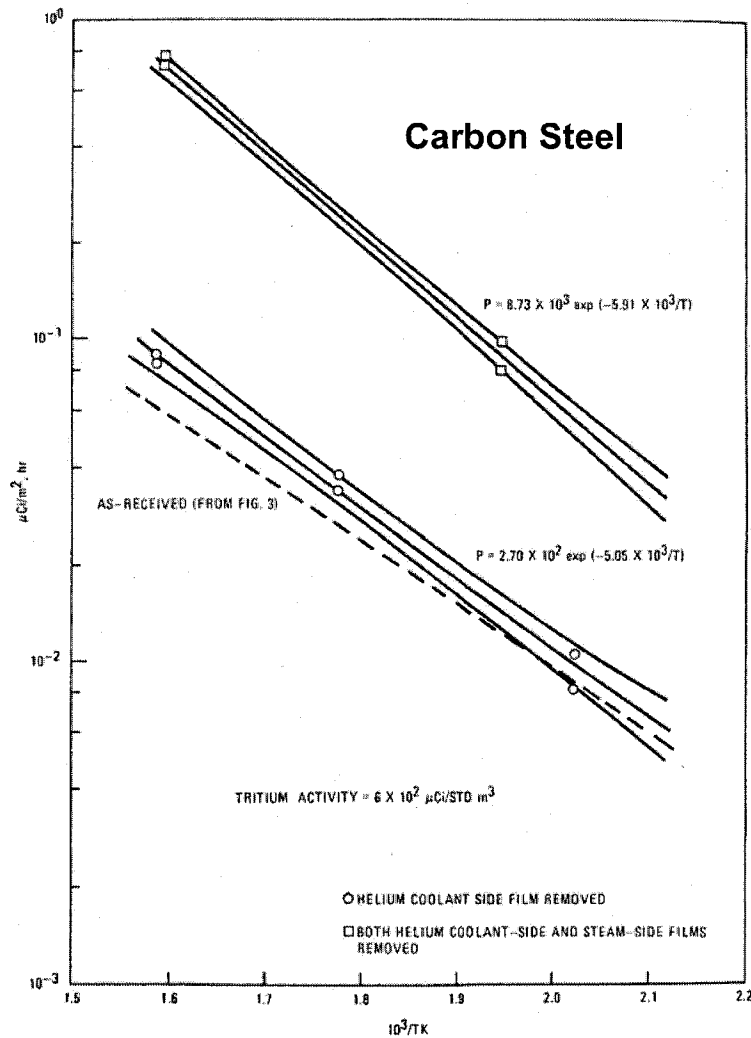


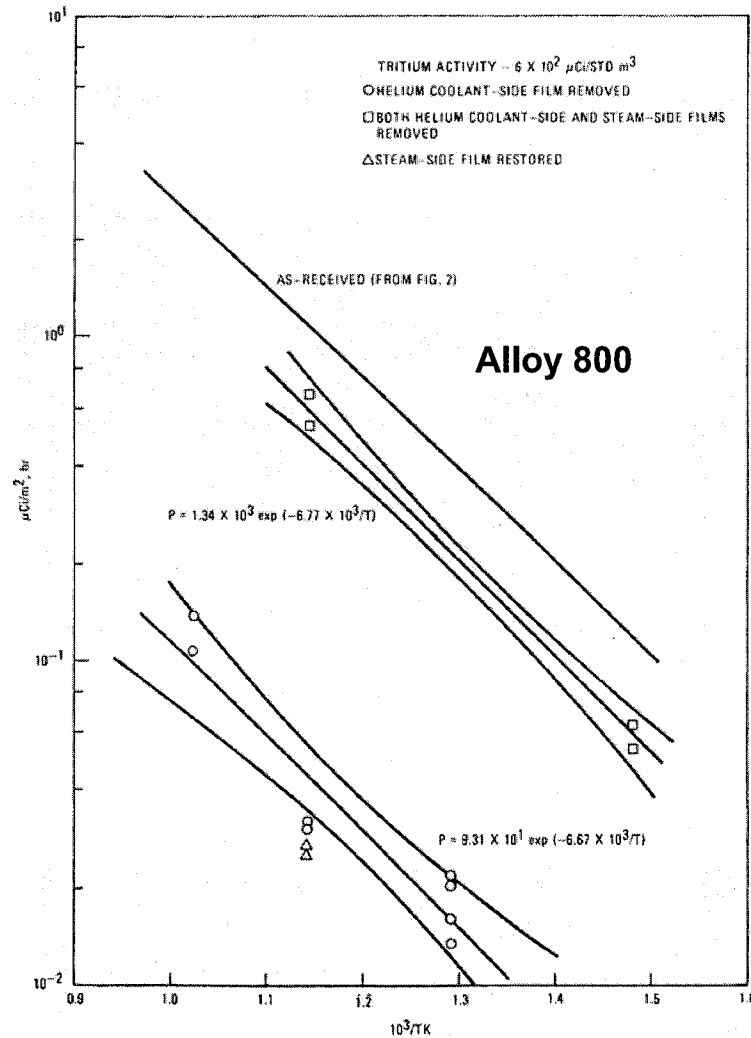
Figure 3-13. Apparatus for PB H-3 Permeation Measurements

The tritium permeation rates observed for the two Incoloy-800 superheater samples were in good agreement even though they had operated at different temperatures in the Peach Bottom steam generator. The same was true for the two low-carbon steel economizer samples. As shown in Figure 3-13, removal of the surface film that had formed on the helium-coolant side of the economizer tubes during reactor operation had no appreciable effect on the tritium permeation rate. Removal of the surface film that formed on the helium-coolant side of the evaporator or the superheater, however, lowered the tritium permeation rate (lower curves in Figure 3-14 compared to the "as-received" curve). It appears that the removal of these films allowed the formation of protective layers having low tritium permeabilities by a reaction between the impurities in the tritium source and Incoloy-800 or carbon steel during the permeation test.

¹⁴ The "large" HTGR was the generic term for a generation of 2000 – 4000 MW_t HTGRs under design at GA at the time these H-3 permeation measurements were made.



PB Economizer Tube Specimen



PB Superheater Tube Specimen

Figure 3-14. H-3 Permeabilities of PB Steam Generator Tubes

For all three types of samples studied, the surface films on the steam side lowered the tritium permeation rates significantly. For the two Incoloy-800 superheater samples, the increase of the tritium permeation rates with tritium concentration in the tritium source obeyed neither the linear nor the square root relationship, suggesting that both the surface film and the base metal contributed to the overall permeation resistance (Section 3.2.2.5.1). For an increase of tritium concentration from 600 to 10,000 $\mu\text{Ci}/\text{m}^3$ (STP), the tritium permeation rate increased by a factor of about six when the sample had the surface film in the as-received state, and by a factor of about ten after the removal of the as-received surface film.

Using the measured H-3 permeation rates for the as-received tube samples and the surface areas and of the operating temperature ranges of the steam generators, the tritium transfer rate from the primary helium to the secondary steam in the Peach Bottom reactor was calculated to be 1.3 Ci per year. Yang [1977] reported that this was in good agreement with the observed value of about 1 Ci per year. It should be noted that Wichner [1979] estimated the actual H-3 permeation rate to be about four times lower than the estimate by Yang.

The results of these H-3 permeation measurements with Peach Bottom SG tube specimens showed that the H-3 permeation rate is strongly dependent upon the surface conditions of the SG tubes and that the change of H-3 permeation rate with tritium concentration in the source does not obey a simple relationship.

3.2.2.5.2.3 JAERI Measurements of D/H Permeation through Hastelloy XR

JAERI (now part of JAEA) has measured the permeation rates of hydrogen and deuterium through Hastelloy XR in support of their earlier plans to couple a steam reformer for hydrogen production to the HTTR via the existing intermediate heat exchanger [Takeda 1999]. More recently, JAERI has decided to forego plans for the steam reformer and to couple a SI pilot plant to the HTTR instead. Hastelloy XR and Inconel 617 are also leading candidate metals for the IHX in the H₂-MHR, and so the JAERI permeation data are of direct interest for that application as well.

The hydrogen and deuterium permeabilities of Hastelloy XR were measured in an experimental apparatus shown schematically in Figure 3-15. The deuterium and hydrogen concentrations in the He carrier gas were measured using a quadrupole mass spectrometer with detection limit of about 1 ppm. Measurements were made over a temperature range of 600 - 850 °C (900 °C maximum with this apparatus). Hydrogen partial pressures of 100 Pa, 1 kPa, and 4 kPa were investigated. Significantly, the coolant chemistry was unspecified and apparently uncontrolled [Takeda 1999].

As shown in Figure 3-16, the measured H₂ permeabilities in Hastelloy XR were in good agreement with literature values for Hastelloy X, an alloy with a very similar composition (Hastelloy XR is a low Co-content variant of Hastelloy X). After 140 hours of operation, the measured permeability had decreased by about a factor of three, and the activation energy had increased from 67.2 to

70.2 kJ/mol. Evidently, an oxide film(s) was progressively forming during the test. The surface films were not characterized before or after the permeation testing.

While the observed factor-of-three decrease in permeability in 140 hours is not particularly dramatic, this result should be evaluated in the context of the long-term test data for I-800 shown in Figure 3-10. In these earlier ORNL tests investigating the effects of steam oxidation, the H-3 permeation rate decreased rapidly during the first 36 hours and then continued to decrease over the next 84 days for a total reduction factor of 160. Depending upon the actual coolant chemistry in the reactor, the long-term H-3 permeation rates through the IHX may be significantly higher if the chemistry is reducing or significantly lower if the chemistry strongly oxidizing for Hastelloy XR.

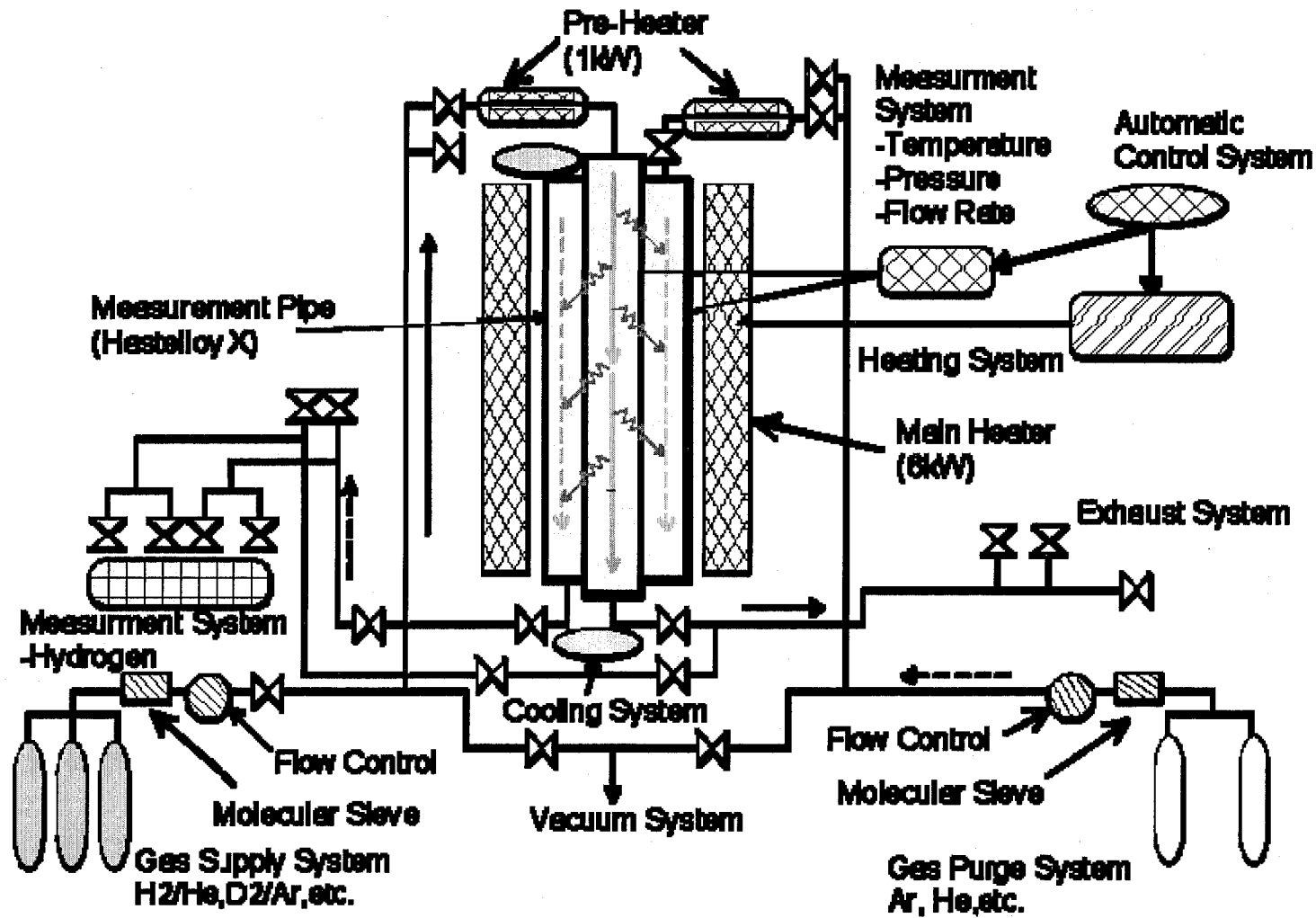
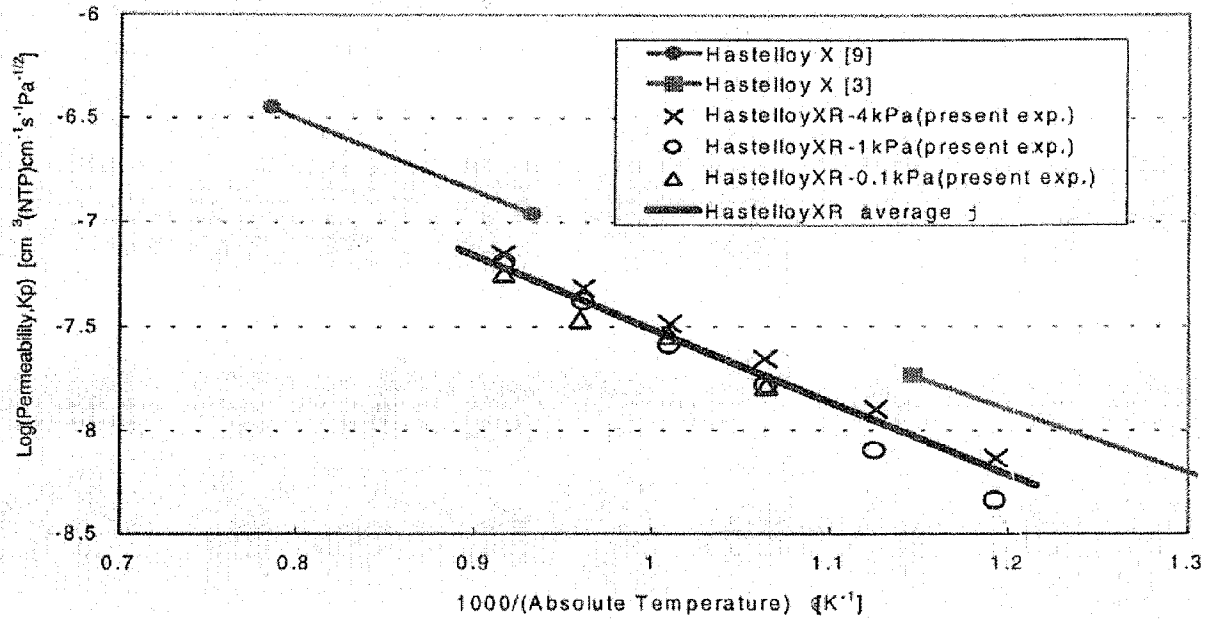


Figure 3-15. JAERI Apparatus for H/D Permeation Measurements



Permeability : $K_p = F_0 \exp(-E_0 / RT)$

	Temperature [°C]	Partial pressure of H2 [Pa]	E_0 [kJ/mol]	F_0 [cm³(NTP)(cm·s·Pa ^{1/2})]
Hydrogen	570 ~ 820	1.06×10 ² ~ 3.95×10 ³	67.2 ± 1.2	(1.0 ± 0.2)×10 ⁻⁴
Deuterium	670 ~ 820	9.89×10 ² ~ 4.04×10 ³	76.6 ± 0.5	(2.5 ± 0.3)×10 ⁻⁴

Figure 3-16. H/D Permeation Measurements for Hastelloy XR

3.2.2.5.3 H-3 Permeation Data

There is a large and growing literature regarding the permeabilities of hydrogen isotopes through a variety of metals and ceramics.¹⁵ The topic is being actively investigated by the fusion community because possible tritium release from breeding blankets will be a design and safety issue for fusion power plants. Despite this large literature, relatively little H-3 permeation data have been identified for the exact service conditions anticipated for the IHX in an H2-MHR. Takeda [1999] has assembled the relevant hydrogen permeation data for high-temperature alloys relevant for the IHX in an H2-MHR; his efforts are summarized in Table 3-3. The greatest weakness of these data is that the coolant chemistry was often unspecified and uncontrolled in the subject tests.

Table 3-3. Hydrogen Permeabilities for High-Temperature Alloys

Alloy	Pre-exponential factor K_0 [$\text{cm}^3(\text{NTP})\text{-cm}^{-1}\text{-s}^{-1}\text{-Pa}^{-0.5}$]	Activation energy E_0 [kJ.mol ⁻¹]	Temperature T [°C]
Nickel	7.73×10^{-5}	54.84	-
Inconel-600	2.22×10^{-4}	66.14	800 - 1000
Inconel-625	1.37×10^{-4}	62.12	800 - 1000
Incoloy-600*	1.00×10^{-4}	64.05	700 - 950
Incoloy-800	2.13×10^{-4}	69.07	800 - 1000
Incoloy-800*	5.45×10^{-4}	64.05	700 - 950
Incoloy-800	2.31×10^{-4}	74.1	600 - 950
Incoloy-800**	9.77×10^{-5}	74.1	649
Incoloy-807	2.96×10^{-4}	73.18	800 - 1000
Hastelloy-N**	2.59×10^{-4}	77.99	605
Hastelloy-X	2.00×10^{-4}	66.98	800 - 1000
Hastelloy-XR	1.0×10^{-4}	67.2	570 - 820
Hastelloy-XR*	4.7×10^{-5}	70.2	800
Hastelloy-XR**	2.5×10^{-4}	76.6	670 - 820

*Some oxidation of test specimen. **Deuterium data.

In fact, one of the greatest challenges when predicting the extent of product contamination in a H2-MHR is that the primary and secondary coolant chemistries in such a first-of-a-kind plant cannot be predicted with high confidence. As a practical matter, these uncertainties will remain until there are actual operating data from an operating H2-MHR. As mentioned previously, the first data could be available shortly after 2010 if the plans to couple a SI pilot plant to the HTTR come to fruition.

¹⁵ For example, a Google search in April, 2006, resulted in ~313,000 hits for "hydrogen permeation metals;" ~26,000 hits for "tritium permeation metals;" and ~400 hits for "hydrogen permeation Inconel 625."

4 DESIGN METHODS FOR PREDICTING H-3 TRANSPORT

The design methods used at GA to predict H-3 transport in HTGRs are summarized in this section.

4.1 Computer Codes

The TRITGO code was originally developed at ORNL to assess tritium production and distribution in HTGRs [Compere 1974]. TRITGO was slightly modified and used in the 1980s at GA to predict the tritium production and distribution within a steam-cycle MHTGR. It was further modified in the early 1990s for use in predicting H-3 source terms for the NPR program. The most significant modification for the NPR application was the addition of H-3 producing Li targets to the code; that version of the code is Unclassified Controlled Nuclear Information and is not generally available. More recently, the target-related information has been removed, and a non-UCNI version of the TRITGO user's manual has been prepared [Hanson 2006a].

The basic computational model in TRITGO was also adopted for analysis of pebble-bed HTRs by Cordewiner [1979] at KFA Juelich. TRITGO was originally developed for the analysis of HTGRs with prismatic (block) cores; consequently the core model in the code had to be modified extensively to account for the spherical fuel elements and, in particular, for the recirculation of the fuel spheres.

For a typical application of TRITGO, the reactor is divided into a number of tritium source regions such as the active core, the inner reflector, the outer reflector, the top reflector, the bottom reflector, and the control rods. The user inputs characteristic parameters for each region, including the average neutron flux, average temperature, impurity concentrations, and total mass. As illustrated in Figure 4-1, TRITGO determines the amount of tritium present in each region due to ternary fission, neutron reactions with graphite impurities, neutron capture in boron control materials, and He-3 activation in the coolant. The TRITGO output includes the amount of tritium bound in solids, adsorbed on graphite surfaces, in the primary coolant, in the HPS, in the steam generator (SG), and lost to the environment through blowdown or steam generator leakage.

TRITGO would need further modification for rigorous application to an H2-MHR with a secondary heat transport loop since the code as written models H-3 transport from a primary- to a secondary coolant loop, and H2-MHR has three loops (primary, secondary, and H₂ process). Rather than adding a third loop to the code, it may be sufficient to slightly modify the code such that the H2-MHR is modeled in two sequential runs: (1) the H-3 transport from the primary to secondary loop is first calculated; and (2) the H-3 transport from the secondary loop to the process loop is calculated using the H-3 concentration in the secondary coolant from the first run as the source term.

Alternatively, it may prove more efficient to write a new three-loop code for H2-MHR applications using essentially the same component models that are used in TRITGO. The TRITGO code makes a number of simplifying assumptions such that a system of coupled, linear, first-order ordinary differential equations can be solved analytically. Undoubtedly, in any new code, would be solved numerically and would include modern user friendly features, such as a graphical user interface.

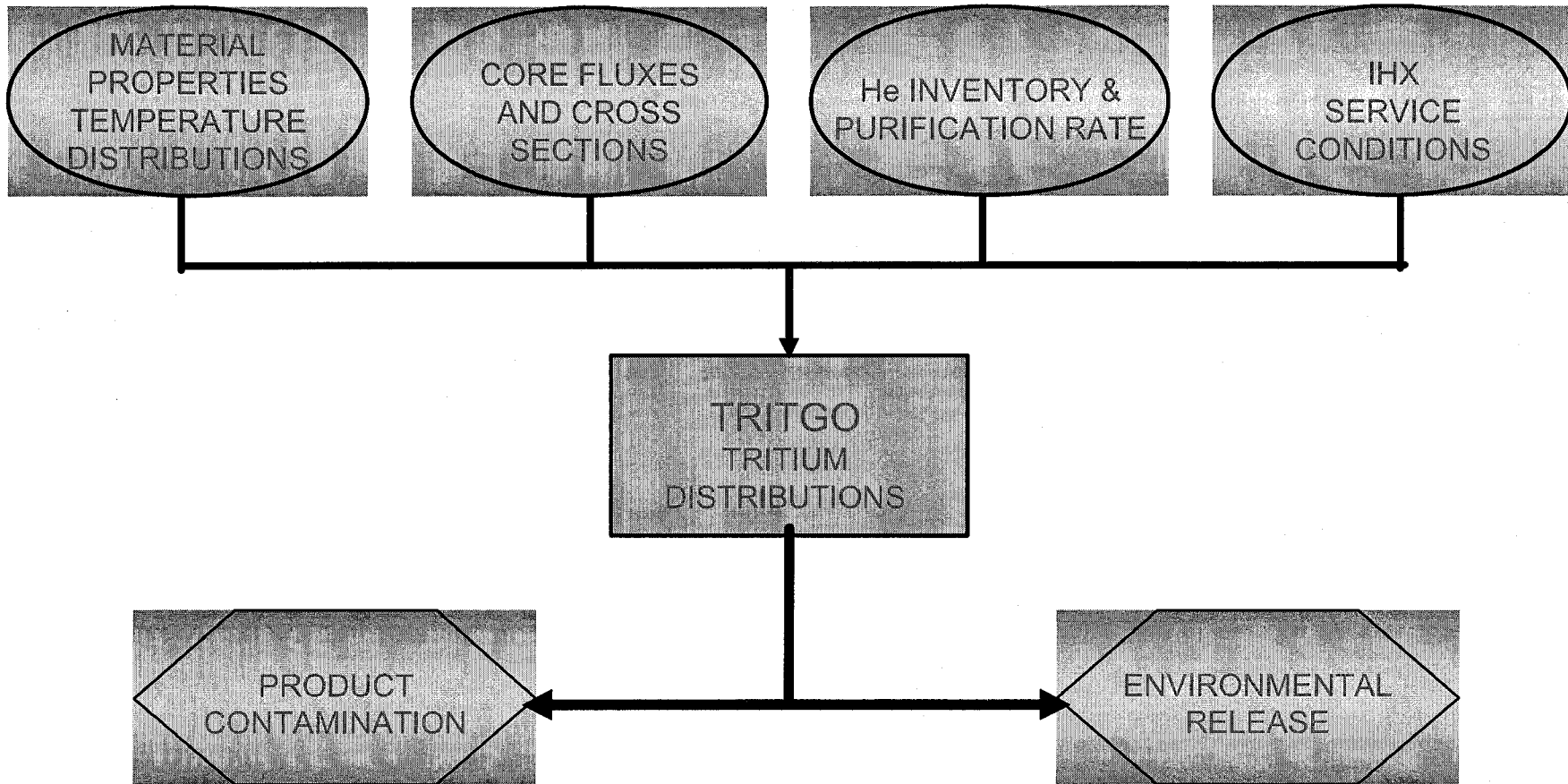


Figure 4-1. TRITGO Code Data Management

4.2 H-3 Transport Models

The H-3 transport models currently in use at GA are described in this section. Some of these component models have not yet been incorporated into the TRITGO code described above. It is anticipated that they would be incorporated into a modified version of TRITGO or into a new code written for H2-MHR applications.

4.2.1 H-3 from Fuel Particles

Using the available information on H-3 release rates from TRISO-coated particles, especially target particles (Section 3.2.1.1), models were developed at GA for predicting H-3 release from failed and intact TRISO fuel particles [Martin 1993]. The transport of tritium in the kernel and coating layers of intact, TRISO-coated fuel particles is calculated with an effective permeation coefficient given by

$$K = K_o \exp(-Q/RT) \tag{4-1}$$

where K = effective permeation coefficient (m²/sec),

K_o = preexponential constant (m²/sec),

Q = activation energy (J/mol)

T = absolute temperature (K)

R = gas constant = 8.314 J/mol-K.

The effective permeation coefficient K may be used in place of the diffusion coefficient in codes such as TRAFIC [Tzung 1992] which use solutions of the classical diffusion equation to calculate radionuclide transport in HTGR prismatic cores. The constants for Eqn (4-1) are given in Table 4-1, and the predicted fractional release of tritium from intact TRISO-coated particles as a function of temperature for selected times is shown in Figure 4-2.

Table 4-1. H-3 Permeation Constants for TRISO Particles

Particle Component	K _o (m ² /sec)	Q (J/mol)
Kernel	1.0 x 10 ⁻⁶	0.0
Buffer	1.0 x 10 ⁻⁶	0.0
IPyC	1.0 x 10 ⁻⁶	0.0
SiC	4.7 x 10 ⁻¹⁵	76,500
OPyC	1.0 x 10 ⁻⁶	0.0

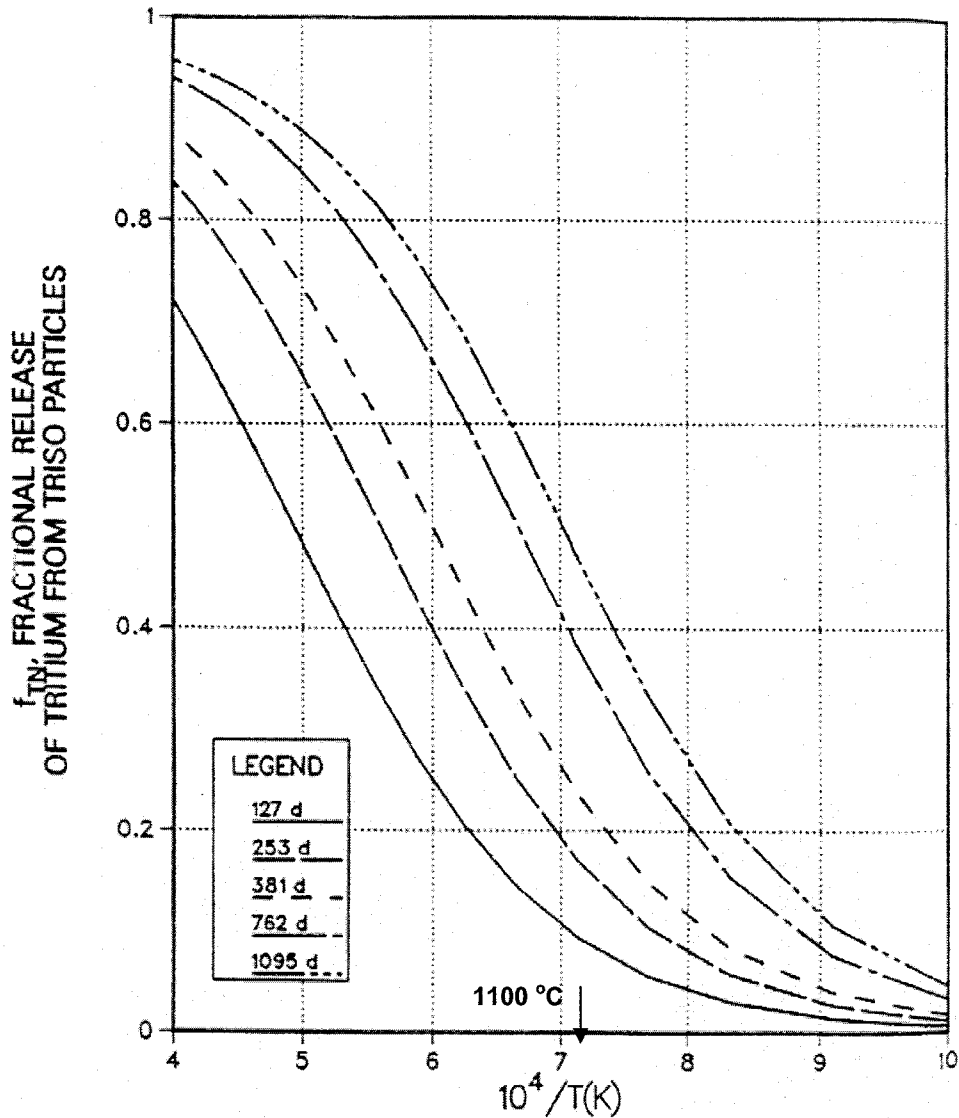


Figure 4-2. H-3 Release from Intact TRISO Particles

The release of tritium from failed particles, defined in this case as particles with failed SiC layers, is assumed to be complete and time independent [Martin 1993]. This assumption may be conservative by a factor of two or three, based upon the data for release from failed UO₂ and UC₂ fuel particles [Gainey 1976]. However, for modern MHR core designs with high-quality TRISO fuel particles, the typical core-average failure fraction is 10^{-4}; consequently, this degree of conservatism is of little consequence compared to the predicted H-3 release from intact TRISO particles (Figure 4-2). Note also from Table 4-1 that no hold up by the pyrocarbon layers is assumed; this assumption is clearly conservative based upon measured H-3 retention by BISO particles. However, for the reason noted above, this conservatism is of little consequence.

This H-3 release model for intact TRISO particles has not been incorporated into the TRITGO code as of this writing

4.2.2 H-3 Release from B₄C Pellets

Using the limited data available (Section 3.2.1.3), a model was developed for H-3 release from B₄C pellets (Martin 1993).

$$f = 1 - \frac{1}{g_1 g_2} \quad (4-2)$$

$$g_i = 1 + \exp \left[a_i \left(\frac{10^4}{T} - \frac{10^4}{T_{oi}} \right) \right], \quad i = 1, 2 \quad (4-3)$$

where: f = fractional release of tritium from B₄C,

g_i = curve-fitting parameters, $i = 1, 2$ (dimensionless)

a_i = constant (K⁻¹),

T = absolute temperature (K),

T_{oi} = reference temperature, $i = 1, 2$ (K).

The values for the constants are given in Table 4-2, and the resulting correlation is shown in Figure 4-3. This H-3 release model for B₄C pellets has not been incorporated into the TRITGO as of this writing.

Table 4-2. H-3 Release Constants for B₄C Pellets

Parameter	Units	Value
a_1	1/K	0.65
$10^4/T_{o1}$	K	11.6
a_2	1/K	-6.26
$10^4/T_{o2}$	K	8.87

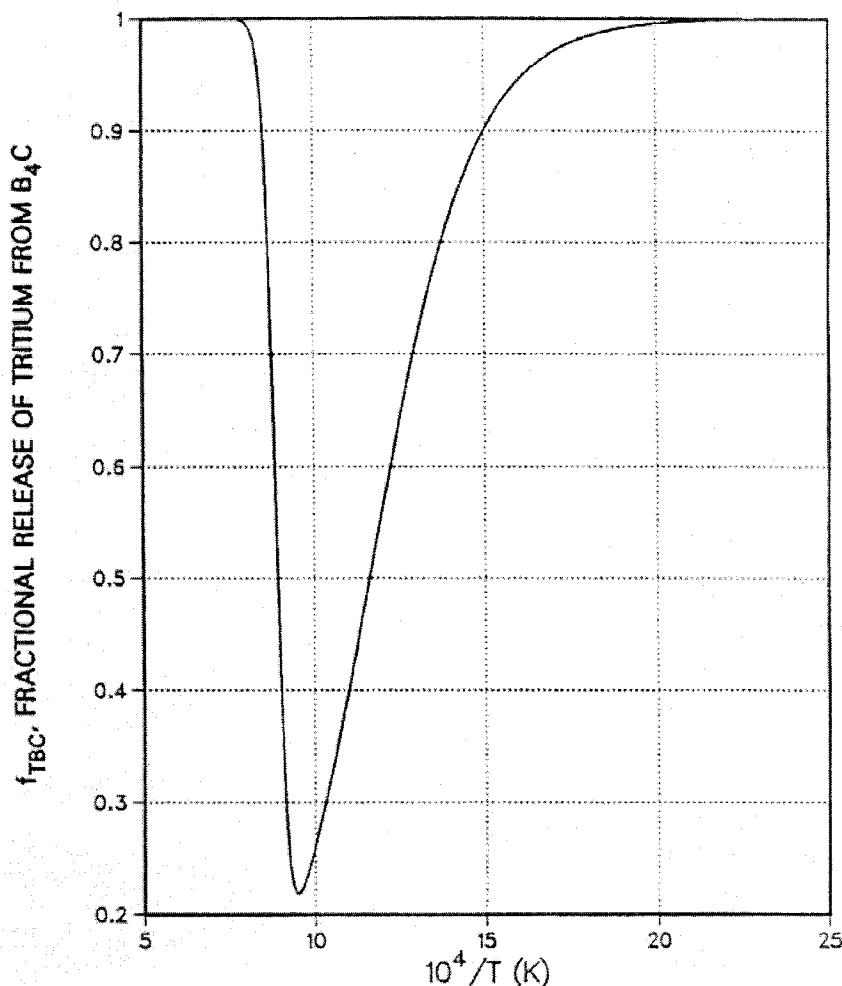


Figure 4-3. H-3 Release from B₄C Granules

4.2.3 H-3 Sorption on Graphite

When the TRITGO code was first developed at ORNL [Compere 1974], an isotherm for H-3 sorption on graphite was derived by fitting the sparse experimental data then available to a Temkin isotherm . They concluded that their isotherm fit the literature data well with respect to the pressure dependence, but it did not include a temperature dependence which was clearly incorrect, at least over a broad temperature range considering the data now available [e.g., Strehlow 1985]. The ORNL isotherm was written in a form that had to be solved iteratively:

$$A = A_m / B_1 \ln[B_2 P_{H_2} (A_m - A) / A] \tag{4-4}$$

where: A = tritium sorbed on graphite per BET surface area [cm²(STP)/m²],

A_m = monolayer saturation value [0.2 cm²(STP)/m²]¹⁶,

¹⁶ Typical value for H-327 graphite which was used for the fuel elements in the FSV initial core and the first reload; fuel blocks for subsequent reloads were made from more dimensionally stable H-451 graphite.

- $B_1 = \text{constant (17.97)},$
 $B_2 = \text{constant (16.54 mm Hg}^{-1}\text{)},$
 $P_{H_2} = \text{hydrogen partial pressure (mm Hg}^{-1}\text{)}.$

Later, Myers [1986] derived a new isotherm which includes crude temperature dependence, and this new isotherm has also been added as an option in the TRITGO code [Hanson 2006a]. The new isotherm is also based upon very limited experimental data. It assumes no H-3 sorption at temperatures below 650 °C. For temperatures between 650 °C and 1250 °C, the sorptivity of H-3 is assumed to be a function of the hydrogen partial pressure and fast fluence but independent of temperature. Above 1250 °C, tritium begins to have a significant desorption pressure, and effective sorptivity decreases with increasing temperature. The Myers isotherm has the following form:

$$A = 0, T < 650 \text{ }^\circ\text{C} \quad (4-5)$$

$$A = C_1(1 + fC_2C_H)P_{H_2} / \{1 + \exp[C_3(T - T_o)]\}, T > 650 \text{ }^\circ\text{C} \quad (4-6)$$

and: $C_H = \{1 + \exp[C_3(T - 1423)]\}^{-1} \quad (4-7)$

where: $C_1 = \text{constant } [[1.38 \times 10^3 \text{ cm}^3(\text{STP})/\text{m}^2\text{-mmHg}],$

$C_2 = \text{constant } (2.6 \times 10^{-25} \text{ m}^2/\text{n}),$

$C_3 = \text{constant } (0.0439 \text{ K}^{-1}),$

$P_{H_2} = \text{partial pressure of hydrogen (Pa)},$

$f = \text{fast fluence (n/m}^2\text{)},$ ¹⁷

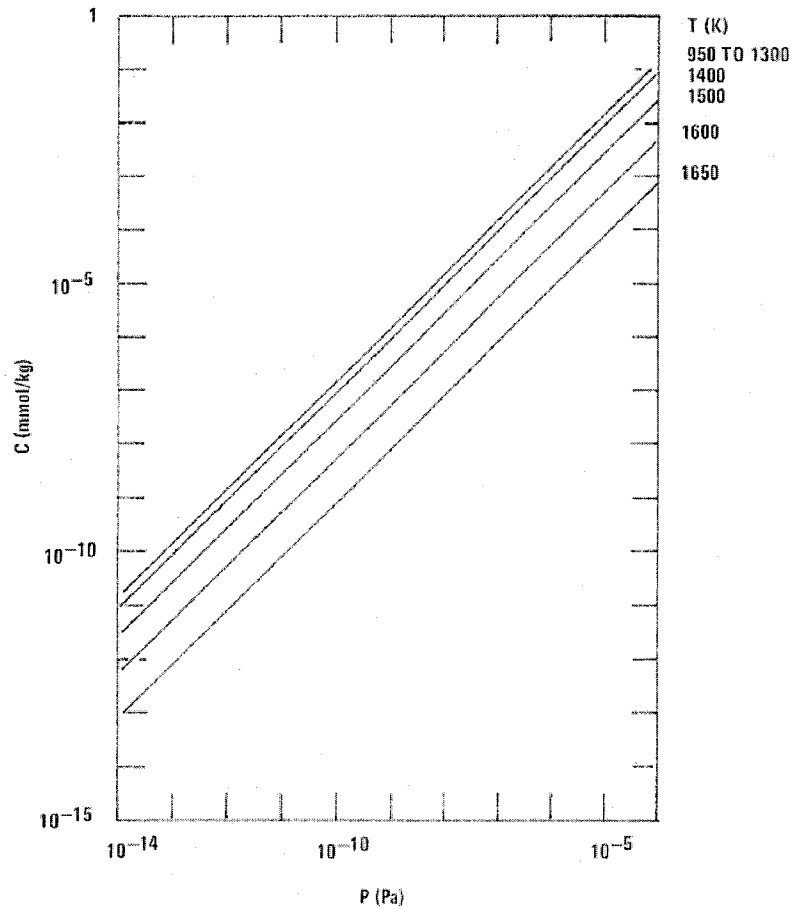
$C_H = \text{annealing factor},$

$T = \text{graphite temperature (K)},$

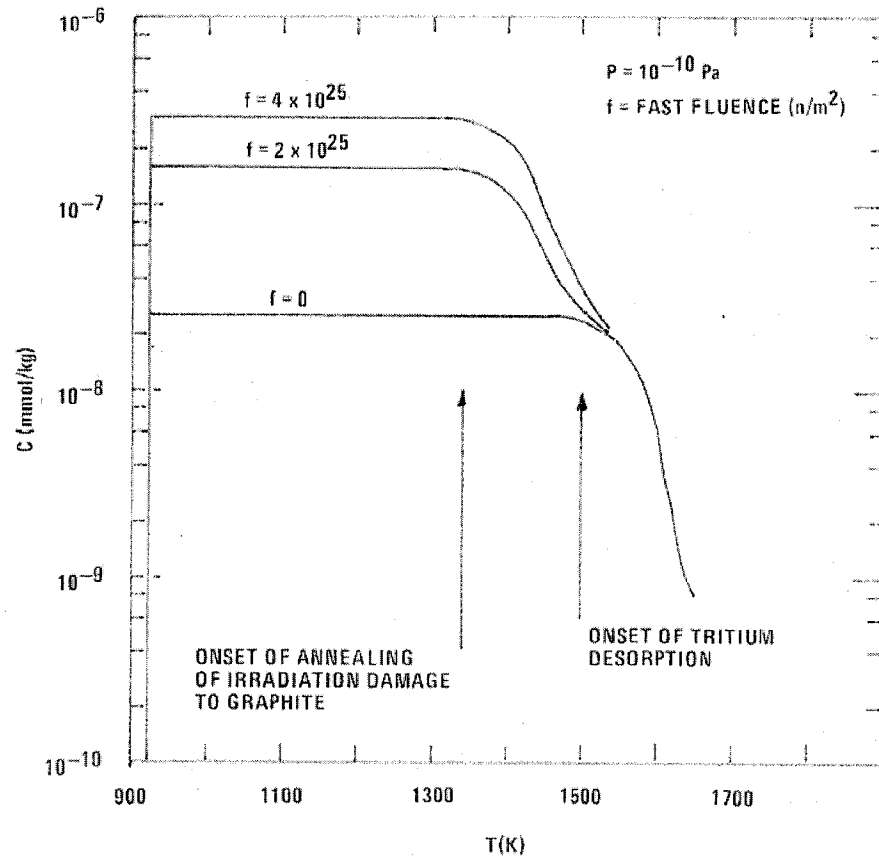
$T_o = \text{reference temperature (1523 K)}.$

The resulting isotherm is displayed in Figure 4-4, which shows the H-3 loading as a function of partial pressure and temperature at a constant fast fluence and the H-3 loading as a function of temperature and fast fluence at a constant partial pressure. Presumably, the Myers isotherm is an improvement over the original isotherm in that it includes crude temperature dependence and a fast fluence dependence that the now available experimental data indicate; however, the uncertainties in the Myers isotherm are clearly quite large and unquantified.

¹⁷ At present, a fast fluence of $6 \times 10^{25} \text{ n/m}^2$ is hard wired into the TRITGO code (Hanson 2006); at minimum, the fast fluence should be made an input variable.



H-3 Loading as Function of Pressure and Temperature



H-3 Loading as Function of Temperature and Fast Fluence

Figure 4-4. Myers Isotherm for H-3 Sorption on Graphite

4.2.4 H-3 Permeation through Metals

Models for H-3 permeation through heat exchanger tubes were developed by Myers at GA in the late 1980s [Martin 1993]. At that time, the primary interest was in steam-cycle HTGRs, and the preferred materials of construction for steam generator tubes were typically Alloy 800H for the superheater section and T22 (2¼% Cr-1% Mo steel, SA-387) for evaporator/economizer sections. The following correlation was derived for H-3 permeation through Alloy 800H and T22:

$$P_r = P_o \left(\frac{C_T}{C_{T_o}} \right)^n \left(\frac{\Delta C_T}{\Delta \tau_w} \right) \exp(-Q / RT) \tag{4-8}$$

with $n = n_o \exp(Q_o / RT)$ (4-9)

where: P = permeation rate (µCi/m²-hr)

P_o = constant (m-mm/hr),

C_T = tritium concentration on coolant side of tube [µCi/m³(STP)],

C_{T_o} = reference tritium concentration on coolant side of tube [µCi/m³(STP)],

τ_w = wall thickness of the SG tube (mm),

$\frac{\Delta C_T}{\Delta \tau_w}$ = tritium concentration gradient across the tube wall (µCi/m³-mm),

Q/R, Q_o/R = temperature coefficients (K),

T = temperature (K),

n_o = constant (dimensionless).

The values of the parameters of Eqns. 4-8 and 4-9 are presented Table 4-3. In computing the concentration gradient, the concentration on the steam side of the steam generator tube is assumed to be zero. The tritium permeation rates are shown in Figure 4-5 as a function of temperature for selected H-3 concentrations and a SG wall thickness of 3.2 mm for Alloy 800H and T22.

Table 4-3. Coefficients for H-3 Permeation Correlations

Parameter	Alloy	
	Alloy 800H	T22 (SA-387)
P _o (m-mm/h)	9.10E+00	1.42E+00
C _{T_o} (µCi/cm ³)	6.00E+02	6.00E+02
Q (J/mol)	5.35E+04	4.20E+4
n _o	9.35E-01	9.35E-01
Q _o (J/mol)	2.29E+03	2.29E+03

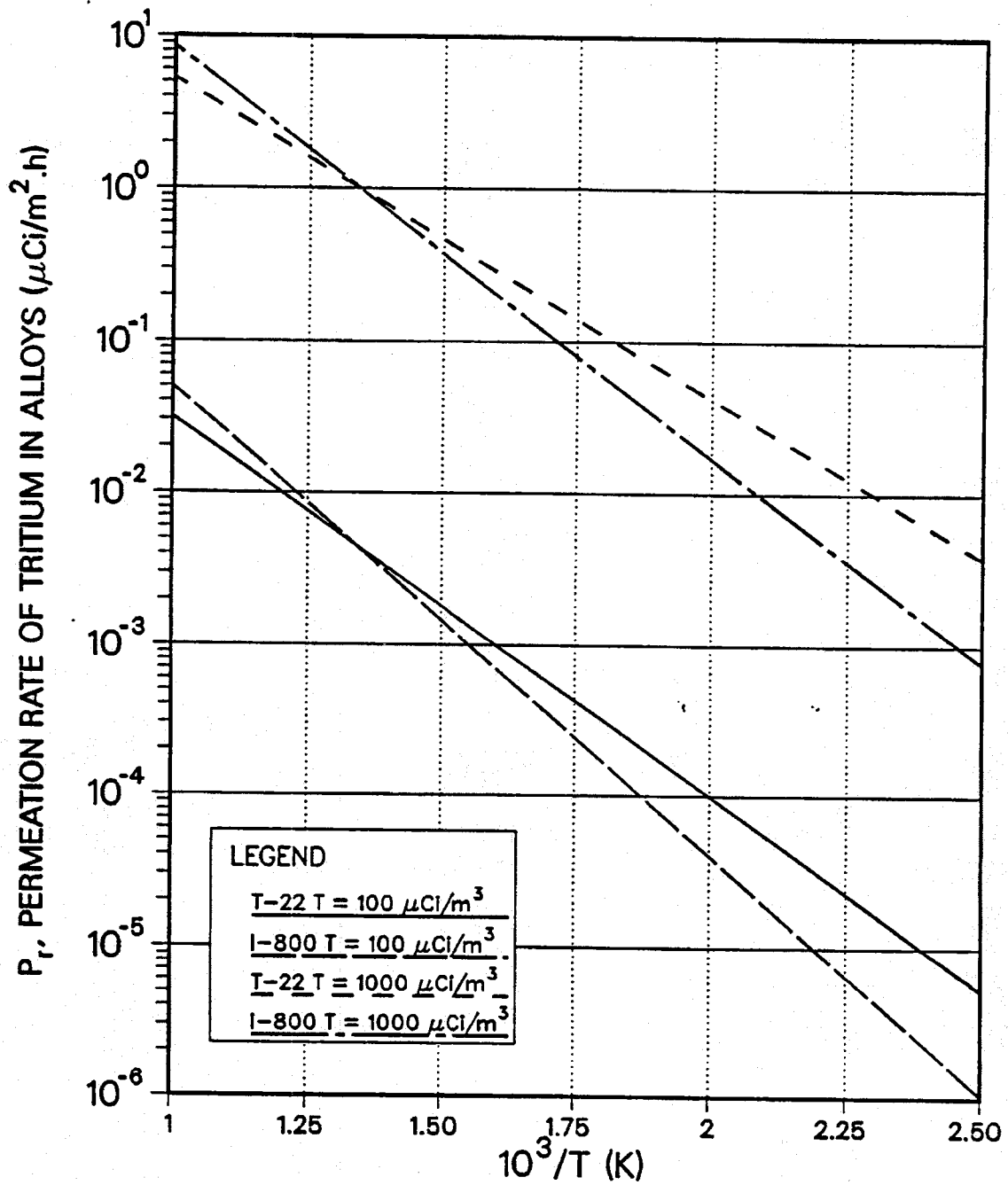


Figure 4-5. H-3 Permeation in Alloy 800H and T22

In 1991, the available data for H-3 permeation through Alloy 800 was reevaluated. The Myers correlation given above is based primarily upon the H-3 permeation rates measured for Incoloy 800 tube specimens removed from the Peach Bottom steam generator at end-of-life [Yang 1977]. These data were refit, and the following correlation was derived [Czechowicz 1991]:

$$R_{perm} = (R_o / \tau_w) C_T (P_{pri})^{1/2} (ppmv_{H_2})^{-1/2} \exp(B/T) \quad (4-10)$$

where: R_{perm} = permeation rate ($\mu\text{Ci}/\text{m}^2\text{-hr}$),

R_o = constant [$61.02 \text{ ppmv}^{1/2}\text{-m}^3(\text{STP})\text{-mm}/\text{atm}^{1/2}\text{-m}^2\text{-hr}$],

τ_w = wall thickness of the SG tube (mm),

C_T = tritium concentration on coolant side of tube [$\mu\text{Ci}/\text{m}^3(\text{STP})$],

P_{pri} = primary coolant pressure (atm),

ppmv_{H_2} = hydrogen concentration (ppmv),

B = constant (-6249 K)

T = absolute temperature (K).

This new correlation for H-3 permeation through Alloy 800 tubes is used in the TRITGO code (Hanson 2006a).

4.3 Material Property Data

Fundamental nuclear data, including microscopic cross sections, are obtained from standard nuclear industry sources, such as Evaluated Nuclear Data File B, Version 6 (ENDF/B-6) that are then modified as appropriate for application to graphite-moderated, gas-cooled reactor core design.

For reactor design and safety analysis, the H-3 producing impurities in the core components are assumed to be at the limits permitted by the fuel product specifications and graphite material specifications. These specifications for various HTGR applications limit the chemical impurities in core materials in several ways: (1) explicit limits on certain neutron poisons, especially boron, expressed in terms of total allowed boron equivalents; (2) explicit limits on certain chemical impurities, such as lithium, iron, and classes of chemical impurities, such as transition metals; and (3) nonspecific limits on "total ash."

5 TEST REQUIREMENTS

An experimental program shall be defined that is comprised of four elements: (1) measurement of H-3 release from irradiated TRISO particles, (2) measurement of the H-3 sorptivities of irradiated core graphites, (3) measurement of H-3 release from irradiated B₄C pellets, and (4) measurement of H-3 permeation rates through candidate IHX and SG metals. The test requirements are summarized in this section.

The test requirements given here are preliminary and intended to provide a technical basis for defining the scope, schedule and cost estimates of the planned tests. Detailed test specifications and test procedures shall be prepared to control the actual testing.

5.1 H-3 Release from TRISO Particles

The fractional releases of tritium from failed and intact, irradiated TRISO particles shall be measured as a function of temperature, time, burnup, irradiation temperature, and water partial pressure.

5.1.1 Test Articles

The primary test articles shall be irradiated, LEU UCO TRISO particles;¹⁸ however, some testing may be done with irradiated, LEU UO₂ particles if they become available earlier than irradiated UCO particles. The test articles shall meet the applicable fuel product specifications¹⁹ and have the following attributes:

<u>Parameter</u>	<u>Value</u>
Test articles	Irradiated, LEU UCO TRISO particles
Burnup	[10 – 22] % FIMA
Irradiation temperature	[800 – 1300] °C

5.1.2 Measurement Technique

Irradiated, intact TRISO-coated UCO particles shall be the primary test article. Intact TRISO particles shall be recovered from deconsolidated irradiated fuel compacts and/or from piggyback samples of loose particles from irradiation test capsules as available. The burnup of the test particles shall be determined by gamma analysis for suitable long-lived refractory radionuclide(s).

¹⁸ Consistent with [AGR Plan/1 2005], it is assumed here that the NGNP will have a prismatic core. If a pebble-bed core is selected, this test plan will be revised accordingly to emphasize LEU UO₂. In any case, it is highly likely that irradiated UCO particles (from AGR-1) become available before irradiated UO₂ particles.

¹⁹ The fuel product specification for the NGNP has not been issued at this writing since the core configuration has not yet been selected.

On a lower-priority basis, the coatings of selected intact TRISO particles shall be failed by mechanically cracking or by laser drilling. The test particles shall be heated in a high temperature furnace using a ramp-hold temperature history. The furnace shall be purged with a pure helium sweep gas, and the sweep gas shall be processed through a suitable sampling train that will quantitatively recover the tritium and separate it from other long-lived beta-emitting radionuclides that may be released from the fuel (in particular, 10.7-yr Kr-85, 2.1-yr Cs-134 and 30-yr Cs-137). The fractional release of tritium from intact and failed LEU UCO TRISO particles shall be determined.

5.1.3 Required Data

The fractional releases of tritium from failed and intact, irradiated TRISO particles shall be measured as a function of temperature, time, burnup, irradiation temperature, and water partial pressure. The primary test articles shall be irradiated, LEU UCO TRISO particles; however, some testing may be done with irradiated, LEU UO₂ particles if they become available earlier than irradiated UCO particles. The test matrix shall emphasize intact TRISO particles because the H-3 fractional release from failed is expected to approach 100% and the allowable, in-service failure fraction in a VHTR is expected to be $<1 \times 10^{-4}$ (Hanson 2004).

5.1.4 Instrumentation

Instrumentation shall be provided to measure the specified test parameters. The instrumentation shall include a high-sensitivity, high-precision, beta spectrometer for quantitative tritium analysis. All instrumentation shall be properly calibrated as required by the applicable quality assurance (QA) protocols (Section 6).

5.1.5 Pre-test Characterization

The test TRISO particles shall be subject to appropriate pre-test characterization to determine the burnup and to confirm that the SiC coatings are free of as-manufactured defects and/or irradiation-induced failures.

5.1.6 Test Conditions

The following steady-state conditions shall be established and maintained until an equilibrium surface loading is obtained:

<u>Parameter</u>	<u>Value</u>
Postirradiation heating temperature	[1000 – 1400] °C
Heating duration	Until H-3 fractional release >[1]% at each temperature
H ₂ O concentration	0 – [10,000] ppmv

5.1.7 Posttest Examination

The SiC coatings of the selected test particles shall be examined to determine if the coatings degraded during the post irradiation heating.

5.2 H-3 Sorption on Core Graphite

The H-3 sorptivities of reference fuel-compact matrix and core graphites shall be measured as a function of temperature, H-3 partial pressure, fast fluence, and coolant chemistry; these sorption data shall be obtained at representative reactor partial pressures.

5.2.1 Test Articles

The test articles shall be unirradiated and irradiated reference fuel-compact matrix and core graphites. The test articles shall meet the applicable product specifications.²⁰ It is anticipated that most of the graphite testing will be done with irradiated test articles since the H-3 sorptivity of irradiated graphites is much higher than that of unirradiated graphite.

5.2.2 Measurement Technique

The sorption measurements shall be performed using the measurement technique (or techniques) that is determined to be the most capable of measuring sorptivities at partial pressures representative of the primary circuit and capable of controlling and adjusting the coolant chemistry.

The measurements will be made in a laboratory environment. A promising technique at this writing appears to be a refined version of the experimental techniques developed at ORNL during the early 1980s when the iodine sorptivities of Alloy 800 and T22 were measured at partial pressures 10^{-10} atm [Osborne 1982].

5.2.3 Sorptivities to be Determined

The H-3 sorptivities of reference fuel-compact matrix and core graphites shall be measured as a function of temperature, partial pressure, surface state, and coolant chemistry; these sorption data shall be obtained at representative reactor partial pressures. At least two different grades of graphite are expected to be used in the NGNP core: one grade for the fuel elements and replaceable reflector elements, and another for the permanent graphite structures. Multiple grades may be used for the permanent graphite structures. See table below.

<u>Material</u>	<u>Primary Application</u>	<u>Fast Fluence (n/m²)</u>	<u>Temperature Range (°C)</u>
Matrix	Fuel compact	5×10^{25}	[800 – 1300]

²⁰ The reference core graphites have not been selected at this writing since the NGNP core configuration has not yet been selected.

Reference replaceable graphite	Fuel block, replaceable reflectors	$<8 \times 10^{25}$	[450 – 950]
Reference permanent graphite	Permanent reflectors, core support structure	$<8 \times 10^{25}$	[600 – 1000]

5.2.4 Instrumentation

Instrumentation shall be provided to measure specified test parameters. The instrumentation shall include devices for the measurement of the helium impurity levels (e.g., residual gas analyzer, RGA). The instrumentation shall also include a high-sensitivity, high-precision, beta spectrometer for quantitative tritium analysis. All instrumentation shall be properly calibrated as required by the applicable QA protocols (Section 6).

5.2.5 Pre-test Characterization

The test specimens shall be subject to detailed characterization to confirm that they meet the applicable, NGNP material and product specifications, including chemical impurities (since certain impurities may serve as H-3 sorption sites). Characterization shall include measurements of the BET surface area.

5.2.6 Test Conditions

The following steady-state conditions shall be established and maintained until an equilibrium loading is obtained:

<u>Parameter</u>	<u>Value</u>
Test articles	Fuel compact matrix, reference replaceable core graphite, reference permanent core graphite
Coolant	Helium
Duration of steady-state operation	Until equilibrium (1 – 10 days)
Tritium concentration range ²¹	$[10^{-6} - 10^{-3}] \mu\text{Ci}/\text{cm}^3$
Temperature range	Ranges specified in Section 5.2.3 in 100 C increments
Coolant impurities	Total oxidants $<[700] \mu\text{atm}$ $<[700] \mu\text{atm H}_2$
H ₂ O concentration	0 – [10,000] ppmv
Matrix/graphite burnoff	0 – [10]%

5.2.7 Posttest Examination

The fractional matrix/graphite burnoff shall be measured. The BET surface area shall be measured for test specimens where the burnoff $>[1]\%$ as determined by weight loss.

²¹ Based upon Fort St. Vrain operating experience.

5.3 H-3 Release from B₄C Pellets

The fractional releases of tritium from B₄C granules shall be measured as a function of temperature, time, fast fluence, irradiation temperature, and water partial pressure.

5.3.1 Test Articles

The primary test articles shall be irradiated, bare and PyC- and PyC+SiC-coated B₄C granules. The test articles shall meet the applicable product specifications for control materials²² and have the following attributes:

<u>Parameter</u>	<u>Value</u>
Test articles	Irradiated, bare and PyC- and PyC+SiC-coated B ₄ C granules
Fast fluence	0 - 5 x 10 ²⁵ n/m ²
Irradiation temperature	[800 – 1200] °C

5.3.2 Measurement Technique

The test specimens shall be heated in a high temperature furnace using a ramp-hold temperature history. The furnace shall be purged with a pure helium sweep gas, and the sweep gas shall be processed through a suitable sampling train that will quantitatively recover the tritium and separate it from other long-lived beta-emitting radionuclides that may be released from the fuel. The fractional release of tritium from bare and PyC- and SiC-coated B₄C granules embedded in a graphitic matrix shall be determined.

5.3.3 Required Test Data

The fractional releases of tritium from irradiated, from bare and PyC- and PyC+SiC-coated B₄C granules shall be measured as a function of temperature, time, fast fluence, irradiation temperature, and water partial pressure.

5.3.4 Instrumentation

Instrumentation shall be provided to measure the specified test parameters. The instrumentation shall include a high-sensitivity, high-precision, beta spectrometer for quantitative tritium analysis. All instrumentation shall be properly calibrated as required by the applicable QA protocols (Section 6).

²² The reference designs for the control materials have not been selected at this writing since the NGNP core configuration has not yet been selected. The inclusion of a steam generator in the primary circuit will increase the importance of coating the B₄C to minimize hydrolysis and boron migration.

5.3.5 Pre-test Characterization

The test articles shall be subject to pre-test characterization to determine the extent of hydrolysis of the B₄C granules in the uncoated test specimens and to determine the PyC-coating or SiC-coating failure fraction in the coated test specimens (test specimens should be free of failed coatings).

5.3.6 Test Conditions

The following steady-state conditions shall be established and maintained:

<u>Parameter</u>	<u>Value</u>
Postirradiation heating temperature	[1000 – 1400] °C
Heating duration	Until H-3 fractional release >[1]% at each temperature
H ₂ O concentration	0 – [10,000] ppmv

5.3.7 Posttest Examination

The test articles shall be subject to appropriate characterization to determine the extent of hydrolysis of the B₄C granules in the uncoated test specimens and to determine the PyC- or SiC-coating failure fraction in the coated test specimens as a result of the postirradiation heating.

5.4 H-3 Permeation through Heat Exchanger Metals

The H-3 permeabilities of candidate heat exchanger metals shall be measured as a function of tritium concentration, metal temperature, hydrogen partial pressure, and surface oxidation state; these permeation data shall be obtained with representative reactor coolant chemistry to the extent practical.

5.4.1 Measurement Technique

The permeation measurements shall be performed using the measurement technique (or techniques) that is determined to be the most capable of controlling and systematically varying the surface oxidation state on both sides of the test specimens (e.g., a cylindrical tube, a section of a PCHE plate, etc.).

The measurements will be made in a laboratory environment. The most promising technique at this writing appears to be a refined version of the experimental techniques developed at ORNL during the mid-1970s [Strehlow 1974, Bell 1975].

5.4.2 Permeabilities to be Determined

Candidate materials of construction have been identified for the NGNP [NGNP Materials R&D Plan 2005, NHI Plan 2005] and for the GT-MHR [Shenoy 1996], but the final selections have not been made; consequently, the metals to be investigated are subject to change as the design of the NGNP becomes better defined. It would be impractical to attempt to characterize the H-3

permeabilities of all the candidates; four metals were selected that are judged to be leading candidates and to be broadly representative of the candidates. The following systems shall be characterized; the temperature ranges were chosen to accommodate both an NGNP with a 950 °C core outlet temperature with an IHX and with IHX and a steam generator in the primary circuit.

<u>Metal</u>	<u>Primary Application</u>	<u>Temperature Range (°C)</u>	<u>Service Environment (primary/secondary side)</u>
Inconel 617	Hot duct, IHX H ₂ SO ₄ decomposer	[450 – 950] [800 – 950]	Primary He/secondary He Secondary He/H ₂ SO ₄
Hastelloy XR	Hot duct, IHX	[450 – 950]	Primary He/secondary He
Alloy 800H	SG superheater H ₂ SO ₄ decomposer	[400 – 800] [800 – 900]	Primary He/secondary steam Secondary He/H ₂ SO ₄
T22	SG evaporator/economizer	[200 – 400]	Primary He/secondary H ₂ O

5.4.3 Instrumentation

Instrumentation shall be provided to measure specified test parameters. The instrumentation shall also include devices for the measurement of the helium impurity levels (e.g., RGA).

5.4.4 Pre-test Characterization

The test specimens shall be subject to detailed characterization, including chemical composition and surface condition. Characterization shall include measurements of surface oxidation state, surface roughness and cleanliness with special attention to the effects of surface films to determine conformance with test specifications.

5.4.5 Test Conditions

The following preliminary steady-state conditions shall be established and maintained until an equilibrium surface loading is obtained. A detailed test matrix will be included in the test specification which will be prepared after the NGNP conceptual design is completed.

<u>Parameter</u>	<u>Value</u>
Test specimen configuration	All: tubes; IN617: section of PCHE plate
Primary coolant/secondary coolant	He/He
Duration of steady-state operation	Until equilibrium (1 – 10 days)
Tritium concentration range ²³	[10 ⁻⁶ – 10 ⁻³] μCi/cm ³
Temperature range	Ranges specified in Section 5.4.2 in 100 C increments
Primary coolant impurities	[<10] ppmv total oxidants (normal operation) [1 – 10] ppmv H ₂ [<1 – 10,000] ppmv H ₂ O (accidents)

²³ Based upon Fort St. Vrain operating experience.

<u>Parameter</u>	<u>Value</u>
Surface oxidation state	[equilibrium with reference He impurities; oxidized]

5.4.6 Posttest Examination

The surface state of the test specimens shall be determined, in particular the amount and nature of surface films or deposits, shall be characterized.

6 QUALITY ASSURANCE REQUIREMENTS

All activities carried out as part of the technology development workscope for the NGNP should be conducted in accordance with the DOE QA requirement specified in 10CFR830, "Nuclear Safety Management," including Subpart A, "Quality Assurance Requirements," and in DOE Order 414.1C, "Quality Assurance." All activities that have direct input to irradiation test specimen fabrication and irradiation will be conducted in accordance with the national consensus standard NQA-1, "Quality Assurance Requirements for Nuclear Facility Applications," published by the American Society of Mechanical Engineers (ASME).

7 DESCRIPTION OF PLANNED TESTS

In response to the H-3 transport DDNs presented in Table 2-1 and the test requirements given in Section 5, a series of single-effects tests will be performed to provide the experimental bases for deriving improved component models and material property correlations to describe H-3 transport behavior in VHTRs. The program is comprised of four elements: (1) measurement of H-3 release from irradiated TRISO particles, (2) measurement of the H-3 sorptivities of irradiated core graphites, (3) measurement of H-3 release from irradiated B₄C pellets, and (4) measurement of H-3 permeation rates through candidate IHX and SG metals.

Neither the initial issue nor Revision 1 of the AGR fuel plan addresses tritium transport [AGR Plan/0 and AGR Plan/1, respectively]. It is intended that the H-3 transport characterization workscope described in this test plan be incorporated into the next revision of AGR Plan (which is not currently scheduled); consequently, a task numbering system is proposed herein that is consistent with the AGR Plan. Using the next available number in the fission product transport subtasks in the AGR Plan, the H-3 transport tasks are identified as R&D Tasks 3.5.14.1 through 3.5.14.4 corresponding to the four H-3 transport characterization tasks identified in the preceding paragraph.

The schedule and estimated costs for each of these tasks are presented in Section 8, and the deliverables are given in Section 9.

Table 7-1. Experimental Tasks to Satisfy H-3 Transport DDNs

Subtask No.	Subtask Title	Applicable Ddns	Comments
3.5.14.1 3.5.14.1.1 3.5.14.1.2 3.5.14.1.3 3.5.14.1.4	H-3 Release from TRISO Particles Prepare test specification Select measurement technique Construct/commission test facility Perform H-3 release measurements	N.07.03.23. Tritium Release from TRISO Particles	Testing cannot begin until suitable test specimens become available.
3.5.14.2 3.5.14.2.1 3.5.14.2.2 3.5.14.2.3 3.5.14.2.4 3.5.14.2.5 3.5.14.2.6	H-3 Sorptivities of Core Graphites Prepare test specification Select measurement technique Construct/commission test facility Measure H-3 sorptivity of replaceable core graphite Measure H-3 sorptivity of permanent core graphite Measure H-3 sorptivity of compact matrix	C.07.03.06. Tritium Transport in Core Materials	Commissioning tests will include scoping measurements with H-451 to check consistency with previous data that are the bases for the current reference isotherms.
3.5.14.3 3.5.14.3.1 3.5.14.3.2 3.5.14.3.3 3.5.14.3.4 3.5.14.3.5	H-3 Release from B ₄ C Granules Prepare test specification Fabricate test articles Select measurement technique Construct/commission test facility Perform H-3 release measurements	N.07.03.24. Tritium Release from Control Materials	Testing cannot begin until suitable test specimens become available.
3.5.14.4 3.5.14.4.1 3.5.14.4.2 3.5.14.4.3 3.5.14.4.4 3.5.14.4.5 3.5.14.4.6 3.5.14.4.7	H-3 Permeabilities of HX Metals Prepare test specification Select measurement technique(s) Construct/commission test facility Measure H-3 permeability of IN 617 Measure H-3 permeability of Hastelloy XR Measure H-3 permeability of Alloy 800H Measure H-3 permeability of T22	C.07.03.05. Tritium Permeation in Heat Exchanger Tubes	Commissioning tests will include scoping measurements with Alloy 800H to check consistency with previous data that are the bases for the current reference isotherms.

7.1 H-3 Release from TRISO Particles

Task 3.5.14.1. The fractional releases of tritium from failed and intact, irradiated TRISO particles will be measured as a function of temperature, time, burnup, irradiation temperature, and water partial pressure. The required test articles are irradiated, LEU UCO TRISO particles; however, some testing may be done with irradiated, LEU UO₂ particles if they were to become available earlier than irradiated UCO particles.

Unfortunately, all irradiated LEU UCO TRISO particles in inventory at ORNL were disposed of as waste when the commercial MHTGR program was closed out in FY1996 and are evidently not recoverable [Morris 2007]. Consequently, these H-3 release tests cannot practically be performed until irradiated UCO particles become available from PIE of AGR-1 fuel which is currently scheduled to begin in April 2009 [AGR Plan/1 2005].

The only alternative would be to design and construct a simple, non-instrumented drop-in capsule containing loose LEU UCO TRISO particles (unirradiated UCO particles are available at ORNL and BWXT) and irradiate it in ATR or HFIR. Although drop-in capsules are conceptually much simpler than the multi-capsule test rigs being used for the AGR fuel irradiations in ATR [Maki 2005], the time and effort required to plan and conduct such tests are still considerable; consequently, it is highly unlikely that such an approach could produce high-burnup, irradiated LEU UCO particles earlier than April 2009, and consideration of such an approach is not recommended.

7.1.1 Subtask 3.5.14.1.1. Prepare Test Specification

A test specification for the H-3 release measurements will be prepared defining in detail the required test conditions. The contents of this test specification will be in compliance with the applicable QA protocols (Section 6).

7.1.2 Subtask 3.5.14.1.2. Select Measurement Technique

The various experimental techniques used previously to measure H-3 release from irradiated TRISO fuel particles (Section 3.2.1.1) will be reviewed and will provide the point of departure for selecting the measurement techniques most suitable for meeting the test requirements defined in Section 5.1.

Special attention will be given to the design of the furnace sweep gas system and the sampling train that will quantitatively recover the tritium and separate it from other long-lived beta-emitting radionuclides that may be released from the fuel. Alternatively, it may be possible to modify the sampling train and measure tritium release during the planned AGR-1 postirradiation heating tests [AGR Plan/1 2005].

7.1.3 Subtask 3.5.14.1.3. Construct/Commission Test Facility

Upon selection of the measurement techniques to be utilized, the requisite test facilities will be assembled in a standard radiochemistry laboratory capable of accommodating postirradiation heating of small quantities of high-burnup, irradiated TRISO particles (the particles will have cooled for 4-6 months prior to heating).

It is possible that these heating tests could be performed in the Core Conduction Cooldown Test Facility (CCCTF) at ORNL [Morris 1992], but the sampling train would likely need to be redesigned and replaced for quantitative trapping and analysis of tritium release rather than fission product release. Since it is anticipated that a relatively small number of irradiated particles will be heated in an individual test, it may prove simpler to utilize a small high-temperature furnace equipped with purge gas system and sampling train that are designed specifically for tritium analysis.

7.1.4 Subtask 3.5.14.1.4. Perform H-3 Release Measurements

The fractional releases of tritium from failed and intact, irradiated TRISO particles will be measured as a function of temperature, time, burnup, irradiation temperature, and water partial pressure for the test conditions given in Section 5.1.6. The test matrix will emphasize H-3 release from intact TRISO particles at temperatures >1000 oC. Early scoping tests with failed particles will determine whether there is sufficient kernel retention to justify characterizing H-3 release from failed particles (e.g., if the fractional release is >50% at core average temperatures, it is probably appropriate to simply assume 100% release from failed particles). The importance of testing with high water partial pressure will be determined when the NGNP conceptual design is finalized. The test procedures will comply with all applicable QA requirements (Section 6).

7.2 H-3 Sorptivities of Core Graphites

Task 3.5.14.2. The H-3 sorptivities of reference fuel-compact matrix and core graphites will be measured as a function of temperature, H-3 partial pressure, fast fluence, and coolant chemistry; these sorption data shall be obtained at representative reactor partial pressures.

The NGNP program has not yet made final selections of the reference core materials which is a significant complication for the measurements called for in this test plan. A resin-based, fuel-compact matrix material is being used by the AGR program; it has the same formulation as German A3 matrix and is intended to have the same prosperities. However, the raw materials (e.g., graphite powder) are somewhat different. Several grades of graphite, supplied by Graftech and SGL, are under consideration for use as the fuel-element graphite and replaceable reflector graphite [NGNP Materials R&D Plan 2005]. GA recommends that Toyo Tanso graphites (e.g., grade IG 110) be considered as well [NGNP TDP 2007].

Once the reference fuel-compact matrix and core graphites have been selected, there will be a further complication regarding the acquisition of irradiated samples of the reference materials for

the subject H-3 sorptivity measurements.²⁴ Depending upon the graphites selected, irradiated specimens of the reference replaceable and permanent core graphites might become available from the AGC-1 graphite irradiation capsule [NGNP Materials R&D Plan 2005] which is scheduled to begin irradiation in the ATR in March 2009. Small matrix samples will also be irradiated as piggyback samples in AGC-1. Conceptually, matrix material could also be obtained from fuel compacts irradiated in AGR-1; however, recovering matrix from irradiated fuel compacts has proven to be extremely difficult and is not recommended here.

There are several apparent alternatives for acquiring the required test articles. Piggyback samples could be prepared and irradiated in a future AGR fuel or fission product transport test rig (e.g., AGR-2 and/or AGR-3/-4, respectively). However, the graphite sleeves in the AGR-2 test capsules have extremely thin webs between the fuel holes [Maki 2005]; hence, they are not well suited for accommodating piggyback samples. The design of the test capsules for the AGR-3/-4 fission product release tests has not been finalized, but the proposed concentric-ring design [Hanson 2004] may be more suitable for accommodating piggyback samples. If the concentric-ring design proves feasible for AGR-3/-4, matrix and graphite samples could also be obtained from the matrix rings and graphite rings planned for inclusion in the capsule assembly [Hanson 2004]. However, these matrix and graphite rings are expected to be quite radioactive (high concentrations of Cs-134, Cs-137, and Sr-90), and using contaminated samples from them would complicate the sorption measurements.

Another alternative would be to design and construct a simple, non-instrumented drop-in capsule containing matrix and graphite samples and irradiate it in ATR or HFIR. Such a capsule would rely upon gamma heating to provide elevated temperatures. Given these circumstances, an HT capsule in HFIR would probably provide the highest irradiation temperature because of its significantly higher neutron flux compared to a HRB capsule in HFIR or a drop-in capsule in ATR.

7.2.1 Subtask 3.5.14.2.1. Prepare Test Specification

A test specification for the measurement of the H-3 sorptivities of reference matrix and graphite will be prepared defining in detail the required test program. In conjunction with preparing the test specification, a trade study will be performed to determine the optimal approach for obtaining the requisite test articles. The contents of this test specification will be in compliance with the applicable QA protocols (Section 6).

7.2.2 Subtask 3.5.14.2.2. Select Measurement Technique

The various experimental techniques available for measuring the H-3 sorptivities of matrix and graphite (Section 3.2.2.2) will be reviewed, and the method judged most capable of producing reliable data will be selected; in particular, the experimental technique will permit the H-3

²⁴ As discussed in Section 3.2.2.2, the H-3 sorptivities of nuclear graphites increase dramatically upon irradiation; consequently, most of the sorptivity measurements will be made with irradiated test specimens.

concentration to be varied over a wide range and the coolant chemistry to be controlled. At this writing, it is anticipated that the measurements will be made using refinements of the experimental techniques developed at ORNL during the early 1980s when the iodine sorptivities of Alloy 800 and T22 at partial pressures $<10^{-10}$ atm were measured [Osborne 1982].

7.2.3 Subtask 3.5.14.2.3. Construct/Commission Test Facility

Upon selection of an experimental technique, the requisite test facilities will be constructed at ORNL and/or INL in a standard radiochemistry laboratory. As part of the commissioning of the test facility, limited scoping measurements will be made on a graphite previously examined (e.g., POCO) to provide some indication of reproducibility.

7.2.4 Subtask 3.5.14.2.4. Measure H-3 Sorptivity of Replaceable Core Graphite

The H-3 sorptivities of reference replaceable core graphite will be measured as a function of temperature, H-3 concentration, fast fluence, H₂ partial pressure, and coolant chemistry; these sorption data will be obtained for the test conditions given in Section 5.2.6. The test matrix will emphasize H-3 sorption at temperatures >1000 °C. Measurements at selected conditions will be repeated periodically to check for possible hysteresis effects. The test procedures will comply with all applicable QA requirements (Section 6).

7.2.5 Subtask 3.5.14.2.5. Measure H-3 sorptivity of Permanent Core Graphite

The H-3 sorptivities of reference permanent core graphite will be measured as a function of temperature, H-3 concentration, fast fluence, H₂ partial pressure, and coolant chemistry; these sorption data will be obtained for the test conditions given in Section 5.2.6. The test matrix will emphasize H-3 sorption at temperatures $>[800]$ °C. Measurements at selected conditions will be repeated periodically to check for possible hysteresis effects. The test procedures will comply with all applicable QA requirements (Section 6).

7.2.6 Subtask 3.5.14.2.6. Measure H-3 Sorptivity of Compact Matrix

The H-3 sorptivities of reference fuel-compact matrix will be measured as a function of temperature, H-3 concentration, fast fluence, H₂ partial pressure, and coolant chemistry; these sorption data will be obtained for the test conditions given in Section 5.2.6. The test matrix will emphasize H-3 sorption at temperatures >1000 °C. Measurements at selected conditions will be repeated periodically to check for possible hysteresis effects. The test procedures will comply with all applicable QA requirements (Section 6)

7.3 H-3 Release from B₄C Pellets

Task 3.5.14.3. The fractional releases of tritium from B₄C granules will be measured as a function of temperature, time, fast fluence, irradiation temperature, and water partial pressure. The need for

applying a PyC- and/or SiC coating to the B₄C granules to improve oxidation resistance and tritium retention will be determined.

There are no irradiated B₄C pellets currently available to the AGR program. As discussed previously, specimens of B₄C granules coated with PyC and other specimens coated with PyC+SiC were prepared and irradiated as piggyback samples in fuel irradiation capsule HRB-21 [Heffernan 1991]. Unfortunately, only the structural integrity of the coated B₄C particles was examined visually during the PIE [Acharya 1995], and these test specimens were subsequently disposed of as radioactive waste [Morris 2007].

Given the present circumstances, the B₄C test articles will have to be purchased or fabricated. GA has in the past purchased extruded, lumped burnable poison (LBP) compacts and hot-pressed, reserve shutdown system (RSS) spheres for use in Fort St. Vrain. GA also coated B₄C granules with PyC and with PyC+SiC for irradiation in HRB-21 as indicated above. Presumably, suitable uncoated B₄C granules could be again purchased. However, B₄C granules coated with PyC and/or SiC will have to be fabricated at ORNL or BWXT.

As discussed in Section 7.2 for matrix and graphite test articles, there are again two alternatives for irradiating the test articles required here. Piggyback samples could again be prepared and irradiated in a future AGR fuel or fission product transport test rig (e.g., AGR-2 and/or AGR-3/-4, respectively). As discussed above, the design of the AGR-2 test rig is not well suited for accommodating piggyback samples. The proposed concentric-ring design of the test capsules for the AGR-3/-4 FP release tests may be suitable for accommodating piggyback samples.²⁵

The other alternative would be to design and construct a drop-in capsule containing B₄C pellets and/or loose B₄C granules (uncoated and coated) and irradiate it in ATR or HFIR. Such a capsule would rely upon gamma heating to provide elevated temperatures. Given these circumstances, an HT capsule in HFIR would probably provide the highest irradiation temperature because of its significantly higher neutron flux.

7.3.1 Subtask 3.5.14.3.1. Prepare Test Specification

A test specification for the measurement of H-3 release from B₄C control materials will be prepared defining in detail the required test conditions. In conjunction with preparing the test specification, a trade study will be performed to determine the optimal approach for fabricating and irradiating the requisite B₄C test articles. The contents of this test specification will be in compliance with the applicable QA protocols (Section 6).

²⁵ It is assumed here that the quantity of B₄C in the piggyback samples would not impact the neutronic performance of the test capsules to the extent that the main test objectives were compromised.

7.3.2 Subtask 3.5.14.3.2. Fabricate Test Articles

The uncoated B₄C test articles will be purchased if a suitable supplier can be identified; if not, B₄C granules (~300 μm effective diameter) will be fabricated. B₄C granules from the same batch will be coated with PyC and PyC+SiC at ORNL or BWXT and qualified to the QC protocols called out in the test specification.

7.3.3 Subtask 3.5.14.3.3. Select Measurement Technique

The various experimental techniques used previously to measure H-3 release from irradiated B₄C (Section 3.2.1.3) will be reviewed and will provide the point of departure for selecting the measurement techniques most suitable for meeting the test requirements defined in Section 5.3. In principle, these measurements of H-3 release from B₄C should be considerably simpler than those for H-3 release from irradiated TRISO particles because (1) the test specimens will not be nearly as radioactive and (2) there will be much less interference from other beta-emitting radionuclides.

7.3.4 Subtask 3.5.14.3.4. Construct/commission Test Facility

Upon selection of the measurement techniques to be utilized, the requisite test facilities will be assembled in a standard radiochemistry laboratory capable of accommodating postirradiation heating of small quantities of irradiated B₄C and of tritium handling.

It is possible that these heating tests could be performed in the CCCTF at ORNL [Morris 1992], but the sampling train would likely need to be redesigned and replaced for quantitative trapping and analysis of tritium release rather than fission product release. Since it is anticipated that a relatively small quantities of irradiated B₄C will be heated in an individual test, it will likely prove simpler to utilize a dedicated, small high-temperature furnace equipped with purge gas system and sampling train that are designed specifically for tritium analysis. In principle, the same test apparatus as used for measuring H-3 release from TRISO particles could be used for these B₄C measurements if it can be sufficiently decontaminated.

7.3.5 Subtask 3.5.14.3.5. Perform H-3 Release Measurements

The fractional releases of tritium from irradiated, uncoated and coated B₄C granules will be measured as a function of temperature, time, fast fluence, irradiation temperature, and water partial pressure for the test conditions given in Section 5.3.6. The test matrix will emphasize H-3 release from at temperatures >1000 °C and the effect of water vapor to determine the need and efficacy of coatings on the B₄C granules. The test procedures will comply with all applicable QA requirements (Section 6).

7.4 H-3 Permeabilities of HX Metals

Task 3.5.14.4. The H-3 permeabilities of candidate heat exchanger metals will be measured as a function of tritium concentration, metal temperature, hydrogen partial pressure, and surface

oxidation state; these permeation data shall be obtained with representative reactor coolant chemistry to the extent practical.

A large number of metals are under consideration for use in the NGNP [[NGNP Materials R&D Plan 2005, NHI Plan 2005]. It would clearly be impractical to measure the H-3 permeabilities of all of them. Consequently, engineering judgment was exercised to narrow the number of metals to be tested. There is a general consensus that Inconel 617 is the leading candidate for the IHX [e.g., NGNP TDP 2007]. Hastelloy XR (a low Co variant of Hastelloy X) appears to be a good backup because of its material properties and the fact that it was selected for the HTTR IHX. Based upon past experience with the FSV HTGR and with fossil-fired power plants, the leading materials for a steam generator are Alloy 800H (an improved version of Alloy 800 with greater creep resistance) for the superheater tube bundle and T22 (2¼% Cr-1% Mo chromalloy steel) for the evaporator/economizer tube bundles. Inconel 617 and Alloy 800H are also the leading candidates for the sulfuric acid decomposer. Once the reference materials for the NGNP are better defined during conceptual design, these materials selections will be reviewed and modified as appropriate.

7.4.1 Subtask 3.5.14.4.1. Prepare Test Specification

A test specification for the measurement of the H-3 permeabilities of selected candidate metals will be prepared defining in detail the required test program. The contents of this test specification will be in compliance with the applicable QA protocols (Section 6).

7.4.2 Subtask 3.5.14.4.2. Select Measurement Technique(s)

The various experimental techniques used previously to measure H-3 permeabilities of metals (Section 3.2.2.5) will be reviewed and will provide the point of departure for selecting the measurement techniques most suitable for meeting the test requirements defined in Section 5.4. The permeation measurements will be performed using the technique (or techniques) that is determined to be the most capable of controlling and systematically varying the surface oxidation state on both sides of the test specimens (e.g., a cylindrical tube, a section of a PCHE plate, etc.).

The most promising technique at this writing appears to be a refined version of the experimental techniques developed at ORNL during the mid-1970s [Strehlow 1974, Bell 1975].

7.4.3 Subtask 3.5.14.4.3. Construct/Commission Test Facility

Upon selection of an experimental technique, the requisite test facilities will be constructed at ORNL and/or INL in a standard radiochemistry laboratory capable of handling tritium. These measurements could be performed in the tritium laboratory at the INL where the tritium permeabilities of other metals have been measured. As part of the commissioning of the test facility, limited scoping measurements will be made with Alloy 800H for comparison with previous permeation measurements.

7.4.4 Subtask 3.5.14.4.4. Measure H-3 Permeability of IN 617

The H-3 permeability of Inconel 617 will be measured as a function of temperature, H-3 concentration, surface oxidation state, and coolant chemistry; these permeation data will be obtained for the test conditions given in Section 5.4.5. The test matrix will emphasize H-3 permeation near the peak service temperature. Measurements at selected conditions will be repeated periodically to check for possible hysteresis effects. The test procedures will comply with all applicable QA requirements (Section 6).

7.4.5 Subtask 3.5.14.4.5. Measure H-3 Permeability of Hastelloy XR

The H-3 permeability of Hastelloy XR will be measured as a function of temperature, H-3 concentration, surface oxidation state, and coolant chemistry; these permeation data will be obtained for the test conditions given in Section 5.4.5. The test matrix will emphasize H-3 permeation near the peak service temperature. Measurements at selected conditions will be repeated periodically to check for possible hysteresis effects. The test procedures will comply with all applicable QA requirements (Section 6).

7.4.6 Subtask 3.5.14.4.6. Measure H-3 Permeability of Alloy 800H

The H-3 permeability of Alloy 800H will be measured as a function of temperature, H-3 concentration, surface oxidation state, and coolant chemistry; these permeation data will be obtained for the test conditions given in Section 5.4.5. The test matrix will emphasize H-3 permeation near the peak service temperature. Measurements at selected conditions will be repeated periodically to check for possible hysteresis effects. The test procedures will comply with all applicable QA requirements (Section 6).

7.4.7 Subtask 3.5.14.4.7. Measure H-3 Permeability of T22

The H-3 permeability of T22 will be measured as a function of temperature, H-3 concentration, surface oxidation state, and coolant chemistry; these permeation data will be obtained for the test conditions given in Section 5.4.5. The test matrix will emphasize H-3 permeation near the peak service temperature. Measurements at selected conditions will be repeated periodically to check for possible hysteresis effects. The test procedures will comply with all applicable QA requirements (Section 6).

8 COST AND SCHEDULE

The estimated cost and schedule for the program are arranged in a work breakdown structure (WBS) consistent with the AGR Fuel Program Plan. The estimated costs in constant FY2007 dollars are given for each fiscal year beginning in FY2009.

8.1 Schedule Estimate

The preliminary schedule for the proposed H-3 characterization program is shown in Figure 8-1. This schedule assumes that funding will be available to initiate the H-3 program at the beginning of FY2009 (October 2008). The current NGNP design schedule is included since the H-3 test program is intended to support NGNP design and licensing. The schedules for fuel tests AGR-1 and for AGR-3/-4 and for graphite test AGC-1 are also included since these irradiation tests are assumed to provide test articles for some of the H-3 characterization tests.

The NGNP schedule was taken from [PPMP 2006]. That schedule is already somewhat outdated since, according to it, the conceptual design phase should have begun in October 2007; at this writing it appears that the conceptual design will probably begin in approximately July 2008. When the NGNP design schedule is officially updated, the H-3 characterization test schedule should be updated as well. As currently envisioned, the proposed H-3 test programs would take six years to complete with unconstrained funding.

The greatest challenge for the H-3 test programs is to obtain suitable test articles in a timely fashion. The various options were discussed in the major subsections of Section 7 describing the four H-3 characterization programs. Procurement of the metal test articles for the H-3 permeation measurements (Task 3.5.14.4) should be straightforward, and that task can proceed as soon as funds are available. Obtaining test articles for the other three H-3 tasks will be more problematic, especially for the B₄C tests. Since constrained funding appears to be inevitable for the foreseeable future, assumptions were made that should minimize program cost, but sometimes at the expense of schedule delays, as described below.

It was assumed that irradiated UCO TRISO particles from deconsolidation of fuel compacts would become available six months into the PIE of AGR-1 (October 2010) for Task 3.5.14.1. It is highly unlikely that a drop-in capsule could provide high-burnup irradiated TRISO particles much sooner, and the incremental cost would be considerable.

It was assumed that irradiated matrix and core graphite specimens for Task 3.5.14.2 would come from the AGC-1 graphite creep capsule by July 2011 (additional matrix samples will be available from AGR-3/-4). An HT drop-in capsule in HFIR or a drop-in capsule in an ATR flux trap position could probably produce test articles earlier but again at a large incremental cost.

Assuming that both uncoated and coated B₄C specimens need to be tested, B₄C granules would need to be procured and coated at ORNL or BWXT. It was further assumed that the bare and coated B₄C specimens would be irradiated as piggyback samples in AGR-3/-4. The schedule for AGR-3/-4 is uncertain at this writing; these irradiations are obviously delayed beyond the schedule given in [AGR Plan/1 2005]. It was assumed here that the AGR-3/-4 irradiations would begin in October 2009 and end in May 2012 and that the piggybacks would be recovered and the B₄C specimens would be available for postirradiation heating three months from the start of the AGR-3/-4 PIEs (November 2012). It is all but certain that irradiated B₄C test articles could be generated much earlier using a drop-in capsule in HFIR or ATR. However, the incremental cost is probably not justified, especially given that the priority of this task is judged to be lowest of the four H-3 characterization tasks.

8.2 Cost Estimate

The cost of the program was estimated from the worksopes and previous experience. The estimated costs are summarized in Table 8-1; assuming an average labor rate of \$30K/man-month, the total cost is \$3.9M. At this writing, the cost estimate relies heavily on engineering judgment and past experience.

Table 8-1. Cost Estimate for H-3 Characterization Program

	2009	2010	2011	2012	2013	2014	Total
H-3 Release from TRISO Particles							
Prepare Test Specification	\$60,000						\$60,000
Select measurement technique	\$90,000						\$90,000
Construct/commission test facility	\$155,000	\$85,000					\$240,000
Perform H-3 release measurements		\$560,000	\$170,000				\$730,000
H-3 Sorptivities of Core Graphites							
Prepare Test Specification			\$45,000				\$45,000
Select measurement technique			\$90,000				\$90,000
Construct/commission test facility			\$90,000				\$90,000
Measurement: replaceable graphite			\$142,500	\$127,500			\$270,000
Measurement: permanent graphite				\$270,000			\$270,000
Measurement: fuel compact matrix				\$151,500	\$118,500		\$270,000
H-3 Release from B4C Pellets							
Prepare Test Specification	\$45,000						\$45,000
Fabricate test articles	\$268,500	\$1,500					\$270,000
Select measurement technique				\$90,000			\$90,000
Construct/commission test facility				\$60,000	\$30,000		\$90,000
Perform H-3 release measurements					\$335,000	\$30,000	\$365,000
H-3 Permeabilities of HX Metals							
Prepare Test Specification	\$45,000						\$45,000
Select measurement technique	\$90,000						\$90,000
Construct/commission test facility	\$90,000						\$90,000
Measurement: IN 617	\$95,000	\$85,000					\$180,000
Measurement: Hastelloy XR		\$180,000					\$180,000
Measurement: Alloy 800H		\$100,000	\$80,000				\$180,000
Measurement: T22			\$180,000				\$180,000
Total	\$938,500	\$1,011,500	\$797,500	\$699,000	\$483,500	\$30,000	\$3,960,000

9 DELIVERABLES

Table 9-1 details the deliverables identified to date. They are organized in accordance with the WBS. Calendar dates will be added when the program start is determined and will be updated periodically.

The reports will satisfy the formal program management procedures and QA protocols for the preparation of specific documents to control the planning, execution and evaluation of experimental test programs. Examples of such reports are: test specifications, test plans/procedures, data compilation reports, and test evaluation reports. In simplified (and idealized) terms, the following sequence applies: (1) the cognizant design organization issues a Test Specification; (2) the testing organization prepares Test Plans/Test Procedures that are responsive to the Test Specification; (3) the testing organization performs the subject tests and documents the results in a Data Compilation Report; and (4) the design organization evaluates the test data, including the design implications, and documents the results in a Test Evaluation Report. In reality, the process is iterative, and the roles of the design and testing organizations often overlap significantly (e.g., both the design and testing organizations typically participate in the data evaluation and interpretation during collection of data and during preparation of Data Compilation Reports and Test Evaluation Reports).

Table 9-1. Major Deliverables

WBS	Task Name	Deliverable	Date ²⁶
	H-3 Release from TRISO Particles	<ol style="list-style-type: none"> 1. Test Facility <ol style="list-style-type: none"> a. Test specification b. Drawings c. Test procedures d. Report on facility construction commissioning 2. H-3 Release Measurements from TRISO particles <ol style="list-style-type: none"> a. Test specification b. Test plans/procedures c. Data compilation report d. Test evaluation report 	TBD
	H-3 Sorption on Core Graphites	<ol style="list-style-type: none"> 1. Sorption Test Facility <ol style="list-style-type: none"> a. Test specification b. Drawings c. Test procedures d. Report on facility construction commissioning 2. H-3 Sorption Measurements on Core Graphites <ol style="list-style-type: none"> a. Test specification b. Test plans/procedures c. Data compilation reports d. Test evaluation reports 	TBD
	H-3 Release from B ₄ C Granules	<ol style="list-style-type: none"> 1. Sorption Test Facility <ol style="list-style-type: none"> a. Test specification b. Drawings c. Test procedures d. Report on facility construction commissioning 2. H-3 Release Measurements <ol style="list-style-type: none"> a. Test specification b. Test plans/procedures c. Data compilation report d. Test evaluation report 	TBD

²⁶ Dates to be determined when a start date established.

WBS	Task Name	Deliverable	Date ²⁶
	H-3 Permeation through Metals	<ol style="list-style-type: none"> 1. Permeation test facility <ol style="list-style-type: none"> a. Test specification b. Drawings c. Test procedures d. Report on construction commissioning 3. Permeation tests with IN 617 <ol style="list-style-type: none"> a. Test specification b. Test plans/procedures c. Data compilation report d. Test evaluation report 4. Permeation tests with Hastelloy XR²⁷ <ol style="list-style-type: none"> a. Test specification b. Test plans/procedures c. Data compilation report d. Test evaluation report 5. Permeation tests with Alloy 800H <ol style="list-style-type: none"> a. Test specification b. Test plans/procedures c. Data compilation report d. Test evaluation report 6. Permeation tests with T22 <ol style="list-style-type: none"> a. Test specification b. Test plans/procedures c. Data compilation report d. Test evaluation report 	TBD

²⁷ Test specifications and test plans/procedures for tasks 4 – 6 are likely to be successive revisions of the test control documents prepared for task 3.

10 REFERENCES

- Acharya, R., et al., "Fuel Capsule HRB-21 Postirradiation Examination Data Report," DOE-HTGR-100229 (ORNL-6836), Oak Ridge National Laboratory, April 1995.
- [AGR Plan/0] "Technical Program Plan for the Advanced Gas Reactor Fuel Development and Qualification Program" ORNL/TM-2002/262, Oak Ridge National Laboratory, April 2003.
- [AGR Plan/1] "Technical Program Plan for the Advanced Gas Reactor Fuel Development and Qualification Program" INL/EXT-05-00465, Rev. 1, Idaho National Laboratory, August 2005.
- Andrew, P. L., and A. A. Haasz, "Models for Hydrogen Permeation in Metals," J. Appl. Phys. **72(7)**, October 1992, p. 2749.
- Bansal, R. C., F. J. Vastola, and P. L. Walker, Jr., Carbon, **9**, 1971, p. 185.
- Bell, J. T., et al., paper presented at the American Nuclear Society Conference on Remote Systems Technology, San Francisco, CA, October 1975.
- Causey, R. A., "The Interaction of Tritium with Graphite and its Impact on Tokamak Operations," J. Nucl. Mat., **162-164**, 1989, pp. 151-161.
- Compere, E. L., et al., "Distribution and Release of H-3 in High-Temperature Gas-Cooled Reactors as a Function of Design, Operational and Material Parameters," ORNL-TM-4303, Oak Ridge National Laboratory, June 1974.
- Cordewiner, H. J., "Numerische Berechnung des Tritium-Verhaltens von Kugelhaufenreaktoren am Beispiel des AVR-Reaktors," Juel-1607, Kernforschungsanlage, Juelich, July 1979 (*in German*).
- Czechowicz, D., and L. Brown, "New Correlation for Tritium Permeation through NP-MHTGR Steam Generator Tubes," CEQA Internal Memorandum, CEQA-M-91-3066, November 18, 1991.
- [DDN Procedure], "DOE Projects Division Program Directive #16: HTGR Programs - Design Data Needs (DDNs) Interim Procedure," PD#16, Rev. 1, Plant Design Control Office, February 1986.
- [DOE-GT-MHR-100217] "600 MW(t) Gas Turbine Modular Helium Reactor Design Data Needs," Rev. 0, General Atomics, July 1996 (*Draft*).
- [DOE-HTGR-86025] "Design Data Needs: Modular High-Temperature Gas-Cooled Reactor," Rev. 4, General Atomics, October 1989.
- Dyer, F. F., et al., "Distribution of Radionuclides in the Peach Bottom Primary Circuit during Core 2 Operation," ORNL-5188, Oak Ridge National Laboratory, March 1977.
- Fischer, et al., "Contributions to the Transport Characteristics of Fission Products and Tritium in HTRs," in Reaktortagung, Proceedings of the Reactor Conference, Berlin, 1974, p. 420.
- Fujimoto, N., et al., "Present status of HTTR Project, Achievement of 950 °C of Reactor Outlet Coolant Temperature," Proceedings of 2nd International Topical Meeting on High Temperature Reactor Technology, Beijing, China, September 22-24, 2004.
- [GA] "HTGR Base Program Quarterly Progress Report for the Period Ending August 31, 1972," GA-A12222, Gulf General Atomic, September 30, 1972.
- [GA PCDSR] "NGNP and Hydrogen Production Preconceptual Design Studies Report," 911107, Rev. 0, General Atomics, July 2007.
- Gainey, G. W., "A Review of Tritium Behavior in HTGR Systems," GA-A13461, General Atomic, April 1976.
- Hanson, D., and J. Saurwein, "Development Plan for Advanced High Temperature Coated-Particle Fuels," PC-000513, Rev. 0, General Atomics, November 2004.

Hanson, D. L., "Recommendations for Fission Product Transport Irradiation Tests," PC-000527, Rev. 0, General Atomics, September 2005.

Hanson, D. L., "TRITGO Code Description and User's Manual," GA Document 911081, Rev. 0, General Atomics, February 2006a.

Hanson, D. L., "Review of Tritium Behavior in High Temperature Gas-Cooled Reactors," PC-000535, Rev. 0, General Atomics, May 2006b.

Heffernan, T. F., "Capsule HRB-21 Preirradiation Report," DOE-HTGR-88357, Rev. C, General Atomics, April 1991.

[ISU] "Tritium Information Section," <http://www.physics.isu.edu/radinf/tritium.htm>, Idaho State University, April 2006.

Lederer, C. M., and V. S. Shirley, *Table of Isotopes*, 7th ed., Lawrence Berkeley Laboratory, John Wiley & Sons, Inc., New York, 1978.

Maki, J., "AGR-1 Irradiation Experiment Test Plan," INL/EXT-05-00593, Idaho National Laboratory, August 2005.

Martin, R. C., "Compilation of Fuel Performance and Fission Product Transport Models and Database for MHTGR Design," ORNL/NPR-91/6, Oak Ridge National Laboratory, October 1993.

Morris, R.N., "Current Status of the CCCTF - Summer 1992," ORNL/NPR-92/33, Oak Ridge National Laboratory, October 1992.

Morris, R. N., Oak Ridge National Laboratory, personal communication, November 7, 2007.

Myers, B. F., "Update of Fuel Performance Data and Models," 908721, Rev. 0, GA Technologies, February 1986 (*GA Proprietary Information*).

[NGNP PCD] "Next Generation Nuclear Plant Pre-Conceptual Design Report," INL/EXT-07-12967, Idaho National Laboratory, September 2007.

[NGNP TDP] Hanson, D. L., "NGNP Umbrella Technology Development Plan," PC-000543, Rev. 0, General Atomics, July 2007.

[NGNP Materials R&D Plan] Hayner, G. O., et al., "Next Generation Nuclear Plant Materials Research and Development Program Plan," INEEL/EXT-05-00758, Rev. 2, Idaho National Laboratory, September 2005.

[NHI Plan] "Nuclear Hydrogen Initiative Ten Year Program Plan," US Department of Energy, March 2005.

Perdijk, H. J. R., "Thermochemical Equilibria of Residual Gases in Vacuum Devices," *Vacuum*, **21**, 1971, p. 211.

Pitner, A. L., and J. A. Basmajian, "Tritium Production and Retention," W/FFTF-7311159, Westinghouse Hanford, December 1973.

[PPMP] Weaver, K., et al., "Next Generation Nuclear Plant Project Preliminary Project Management Plan," INL/EXT-05-00952, Rev. 1, Idaho National Laboratory, March 2006.

[PSID] "Preliminary Safety Information Document for the Standard MHTGR," Volumes 1-6, HTGR-84-024, Amendment B, General Atomics, August 1992.

Richards, M., and A. Shenoy, "Hydrogen Generation using the Modular Helium Reactor," Proceedings of ICONE12: 12th International Conference on Nuclear Engineering, April 25-29, 2004, Arlington, Virginia USA, ICONE12-49228, American Society of Mechanical Engineers, 2004.

Richards, M., et al., "H2-MHR Conceptual Design Report: SI-Based Plant," GA-A25401, General Atomics, April 2006a.

Richards, M., et al., "H₂-MHR Conceptual Design Report: HTE-Based Plant," GA-A25402, General Atomics, April 2006b.

Shenoy, A., "GT-MHR Conceptual Design Description Report," 910720, Rev. 1, General Atomics, July 1996.

Strehlow, R. A., and H. C. Savage, "The Permeation of Hydrogen Isotopes through Structural Metals at low Pressures and through Metals with Oxide Film Barriers," Nucl. Tech., **22**, April 1974, p. 127.

Steward, K. P., "Final Summary Report on the Peach Bottom End-of-Life Program," GA-A14404, General Atomic, July 1978.

Takeda, T., et al., "Study on Tritium/Hydrogen Permeation in the HTTR Hydrogen Production System," 7th International Conference on Nuclear Engineering, Tokyo, Japan, April 19-23, 1999, ICONE-7102, American Society of Mechanical Engineers.

[TECDOC] "Fuel Performance and Fission Product Behavior in Gas Cooled Reactors," IAEA-TECDOC-978, International Atomic Energy Agency, November 1997.

Thomas, R., et al., "NPR-MHTGR Tritium Target Performance Demonstration and Qualification Program Plan," EGG-NPRD-8797, Idaho National Engineering Laboratory, December 1989 (*UCNI*).

Tzung, F., "TRAFIC-FD, A Finite Difference Program to Compute Release of Metallic Fission Products from an HTGR Core: Code Theory and Users Manual," CEQA-001904, Rev. N/C, CEQA Corporation, September 1992.

Walter, K. H., G. Lange, and K. H. Kienberger, J. Nucl. Mater., **48**, 1973, p. 287.

Wichner, R. P., and F. F. Dyer, "Distribution and Transport of Tritium in the Peach Bottom HTGR," ORNL-5497, Oak Ridge National Laboratory, August 1979.

Yang, L., W. A. Baugh, and N. L. Baldwin, "Study of Tritium Permeation through Peach Bottom Steam Generator Tubes," GA-A14376, General Atomic, June 1977.